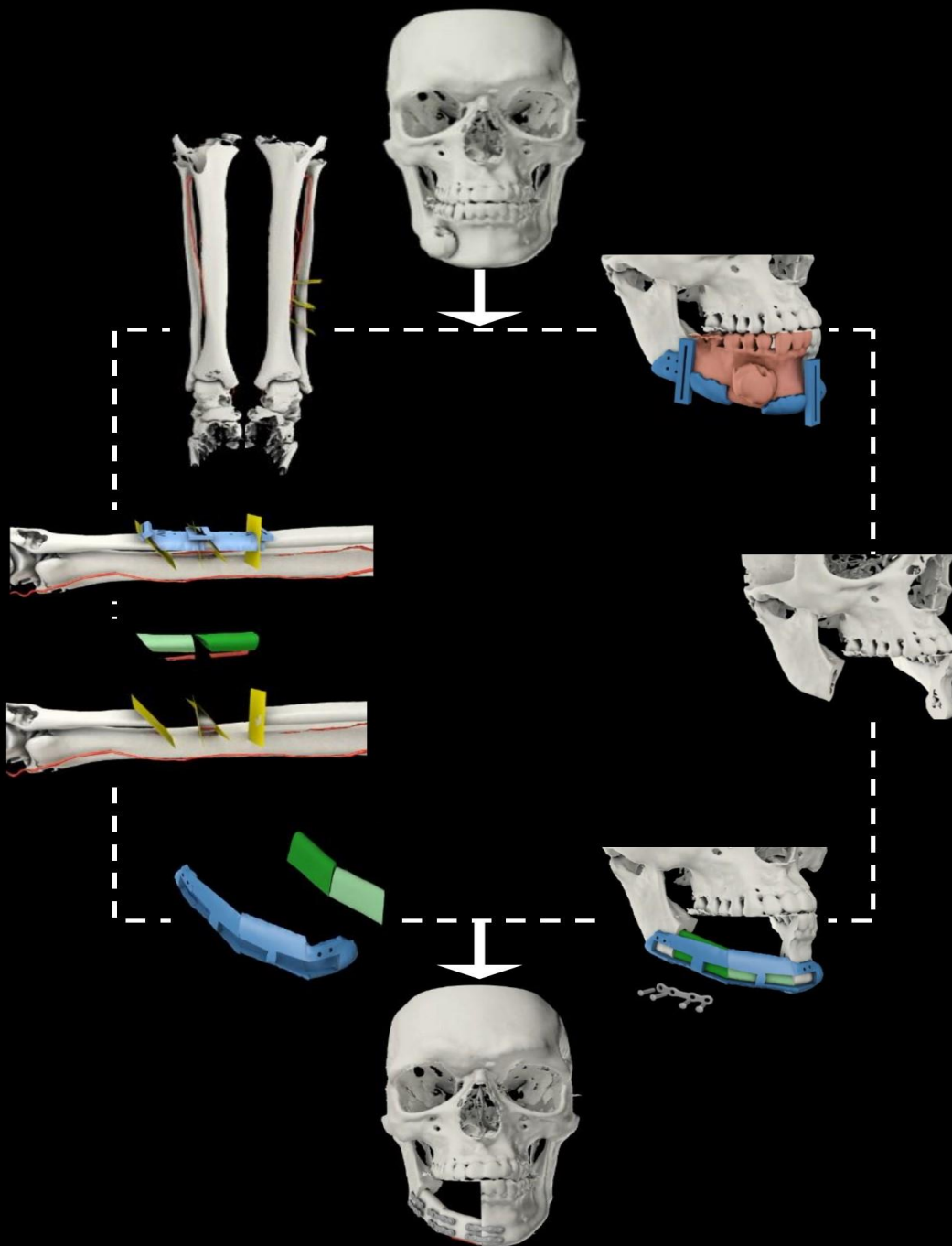


Improvement of patient-specific resection templates in mandible reconstruction using a fibula graft



Masterthesis S.L. Boukes
4340620

Supervisors:
Prof. Dr. J. Dankelman
Ir. L. Verhamme (RadboudUMC)

Contents

Introduction.....	5
Scope and aim	5
Outline	6
Improvement of patient-specific resection templates in mandible reconstruction using a fibula graft. .	7
Abstract	7
Introduction.....	8
Mandible defects.....	8
Mandibulectomy	8
Mandible reconstruction	9
Methods	10
Problem analysis.....	10
Design requirements	10
Concept generation	11
Exploring test and concept evaluation	11
Design evaluation	13
Results	14
Problem analysis.....	14
Design requirements	15
Concept generation	17
Exploring test and concept evaluation	18
Design generation and evaluation.....	18
Discussion	19
Problem analysis.....	19
Design requirements	20
Exploring test and concept evaluation	20
Design generation and evaluation.....	20
Conclusion	21
Recommendations.....	21
Bibliography.....	21
Appendix A: Background	28
A.1. Anatomical background	28
A.2. Clinical background	28
A.3. Mandibulectomy	29
A.4. Reconstruction	29
A.4.I. Step 1. Preoperative scanning.....	32
A.4.II. Step 2. Virtual surgery	32

A.4.III. Step 3. Manufacturing.....	33
A.4.IV. Step 4. Real surgery	34
A.4.V. Step 5. Postoperative scanning	36
A.4.VI. Step 6. Assessment of surgical outcome.....	36
Appendix B: Problem analysis	37
B.1 Current treatment	37
B.2 Current devices.....	38
B.3 Visualization of a deviated formation of the neomandible.....	41
B.4 Stress distributions on the (neo-) mandible	45
Appendix C: Design requirements	47
C.1. Boundary conditions	47
C.2. Clinical requirements.....	48
C.2.I. Mandible	48
C.2.II. Fibula	50
C.2.III. Conclusion	51
C.2.IV. Haptic feedback.....	51
C.2.V. Sterilization	52
C.3 Technical requirements.....	53
Appendix D. Concept generation	55
D.1 Ideas and idea selection	55
D.2. Concepts.....	57
D.2.I. Concept B – Reduced sleeve width	57
D.2.II. Concept C – Contact-fitted.....	57
D.2.III. Concept D – Top guidance	58
D.2.IV. Concept E – Metal insert.....	58
D.2.V. Concept F – Bone-contouring guidance.....	59
Appendix E. Concept evaluation: Exploring test.....	60
E.1. Materials.....	61
E.1.I. 3D-printed concepts	61
E.1.II. Bone block	61
E.1.III. Reciprocating saw.....	61
E.2. Methods	61
E.2.I. Dimensions bone blocks	61
E.2.II. Laser surface scanner	63
E.2.III. Performing the test	64
E.2.IV. Evaluation of the concepts.....	65
E.3. Results	65

E.4. Discussion	69
E.5. Conclusion: Concept selection.....	70
Appendix F. Design choices	71
F.1. Design 1 – Backguidance 1.....	71
F.2. Design 2 – Backguidance 2.....	72
F.3. Design 3 – Smaller top guidance.....	72
F.4. Design 4 – Current model	73
F.5 Design 5 – Titanium insert	73
Appendix G. Evaluation of the design choices.....	74
G.1. Materials	74
G.2. Methods	74
G.2.I. Dimensions bone blocks	74
G.2.II. Performing the test	75
G.2.III Design evaluation.....	76
G.3. Results.....	77
G.3.I. Usability and adaptability	78
G.3.II. Biocompatibility, clean ability and sterilization	78
G.3.III. Simplicity, production method and costs	79
G.3.IV. Ischemia time.....	79
G.3.V. Safety and strength.....	79
G.3.VI. Accuracy trajectory (statistics).....	80
G.3.VII. Discussion	81
G.3.VIII. Recommendations	83
Abbreviations	84
Glossary of terms.....	84
Bibliography.....	86

Introduction

On a yearly basis in the Netherlands, 400 patients are diagnosed with throat cancer, 700 patients with cancer of the oral cavity, and 200 patients with cancer of the lip.¹ These tumors may involve the mandible, referred to as the lower jaw. The mandible is a u-shaped bone that serves as a base for the attachment of dentition, ligaments, and muscles. The muscles can initiate mouth movements, while the ligaments are responsible for restricting mouth movements. The synchronization between muscles and ligaments is important for smooth and coordinated mouth movements.² When the mandible is affected by tumor growth, this synchronization may be compromised and the patient may experience difficulties in speech, swallowing, breathing and mastication.³

Besides functional problems, patients can encounter severe facial aesthetic deformities.^{4,5} The mandible defect can be treated by segmental mandibulectomy. With this treatment, the affected segment of the mandible will be resected (taken out) by osteotomy. Thereby, a gap in the mandible is obtained, which should be reconstructed to recover mandible functioning.

Mandible reconstruction can be performed using an autogenous bone graft, for which the fibular free graft is the most suitable donor site.^{5,6,7,8,9,10,11} The fibula graft will be cut into several segments that can be combined in such a way that a perfect fit is obtained between the graft and the mandible gap. The newly formed mandible that is formed, is shaped similar to the original mandible, known as the neomandible. All processes, such as determining the extent of resection to remove all affected tissue, reshaping of the fibula, and placement of the segments, was conventionally performed without aiding instruments. The process was solely based on the experience and skills of the surgeon, and intraoperative decisions. There was no guidance available during surgery to check if the shape of the neomandible is sufficient in restoring the functioning and facial contours. Complications of bad surgical outcome will not be known until after surgery and the only measure to enhance mandible functioning is second surgery.¹²

Currently, mandibulectomy and fibula segmentation is supported by 3D techniques such as computer-aided simulation, computer-aided design, and computer-aided manufacturing techniques (CAS/CAD/CAM techniques). In short, these techniques introduce virtual surgery to design a virtual mandibular resection plan to remove the mandible defect and a segmentation plan of the fibula to allow an appropriate reconstruction. To transfer the virtual situation to the operation theatre, the virtual plans can be realized into patient-specific devices by CAM techniques. The realized plan consists of three-dimensionally printed resection templates that will serve as intraoperative guiding molds during osteotomy. Virtual planning can accelerate mandibulectomy, fibula harvesting, fibula segmentation and fixation of the fibula segments to decrease time of ischemia and operation time.¹² Thereby, 3D techniques improve surgical outcomes such as mandible functioning and facial aesthetics through provision of intraoperative guidance, while operation time is decreased.

Scope and aim

Surgical experiences and a literature study have pointed out that discrepancies between the virtual planning and the real surgery are present, despite the intraoperative guidance of patient-specific manufactured templates.^{13,14,15,16,17} These differences will result in a less optimal surgical outcome and will affect patient functioning and aesthetics. Resulting from a literature study, attendance of surgeries, examination of the currently applied instruments, and some simulations it was found that the interaction of instruments may contribute highly to this discrepancy by introducing deviations from the planned osteotomy trajectory.^{18,19}

Therefore, this thesis aims at enhancing the transfer between the virtual situation and operating theatre by adjusting the design of the resection templates, to reduce the difference between the planned and the obtained osteotomy trajectory. A precise and predictable resection will minimize the chance on collateral damage and improve the match between the virtual plan and surgical outcome with regard to mandible functioning and facial aesthetics. Thereby, the quality of life of the patient will be improved.

Outline

Because the whole treatment is very broad, and multiple factors come into play with the design process, it was decided to write a paper that summarizes the design process, while the more expanded rationale is dealt with in the appendices. The anatomical and clinical background of mandible defects and the treatment are described in Appendix A. A more extensive problem analysis of the current treatment, the discrepancies, the currently applied instruments and their interactions and visualizations of the problem(s) are given in Appendix B. Furthermore, design requirements that need to be aimed at according to clinical and technical restrictions are discussed in Appendix C. In appendix D, there will be a description of the process of generating ideas to the sub-problems of appendix B, and the resulting concept creation phase. Additionally, an exploring test was performed to evaluate the concepts with regard to the design requirements, as explained in Appendix E. The resulting design choices are given in Appendix F. Finally, the methodology of design evaluation, discussion and recommendations are described in Appendix G.

To facilitate understanding of the clinical terms that are applied in these reports, some abbreviations and a glossary of terms is given at the end of the Appendix G.

Improvement of patient-specific resection templates in mandible reconstruction using a fibula graft.

Abstract

Background: The mandible can be affected by tumor invasion or osteoradionecrosis, leading to severe esthetic deformities, problems in speech, swallowing, and mastication. To restore the mandible, the defect is resected, after which the mandible is reconstructed with a segmented autogenous fibula graft. Using supportive CAS/CAD/CAM methods, an optimal virtual resection, segmentation and reconstruction plan can be obtained that can be transferred to the real surgery using 3D-printed resection templates. However, differences were detected between the planned and the obtained mandible reconstruction, which may affect patient aesthetics and mandible functioning. The aim of this study is to enhance the transfer between the virtual and the real surgery by reducing the difference between the planned and the obtained osteotomy trajectory.

Methods: A problem analysis was performed by a literature study, attendance of surgeries, examination of the currently applied instruments and by performing simulations of these findings in SolidWorks to visualize the problem. According to this analysis, design requirements were generated from a clinical perspective to improve the current design. Several ideas were realized and evaluated according to an exploring test. To allow a more extensive testing, most promising prototypes were developed further. The osteotomy trajectory was assessed by calculating distances and angulations between the planned and obtained resection trajectories.

Results: Deviations between the planned and obtained resection trajectories may be introduced within CAS/CAD/CAM methods. As a result, it was experienced by the surgeon that the designed templates may render obsolete during surgery and the surgeon should to switch back to unguided surgery. Furthermore, no true safety measure was applied during surgery to protect the peroneal artery during resection, while the artery is of major importance for survival of the reconstructive fibula graft. Five different designs were generated that all fulfill all the design requirements that were set.

Conclusions: There are multiple perspectives from which advances can be made to improve the treatment of mandibulectomy and mandible reconstruction using CAS/CAD/CAM methods. This study focused on improving control and reliability of the osteotomy trajectory, by adjusting the design of the resection templates. Multiple designs significantly reduced the deviation of the obtained osteotomy trajectory with regard to the planned trajectory. Additional to improving control over the osteotomy trajectory, one design provides protection to the peroneal artery. Therefore, it is recommended to develop this design further to allow clinical adaption, since it will improve the surgical outcome and resulting patient aesthetics and mandible functioning.

Introduction

Mandible defects

The maxillofacial region consists of the face, the neck, the mouth, the tongue and both jaws.

The upper-jaw is also known as maxilla, the lower-jaw is also known as mandible. (Fig. 1)

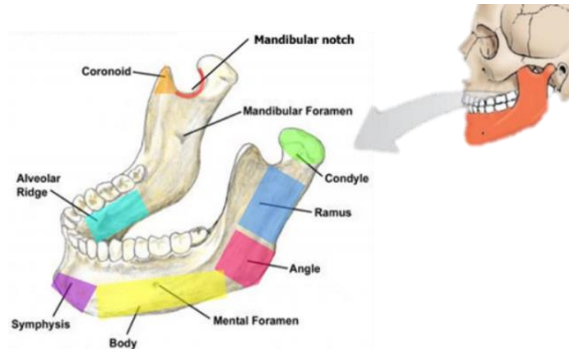


Figure 1. Basic anatomy of the mandible, with eight different regions indicated by eight different colors.²⁰

Mandible functioning can be affected by multiple factors. However, this study focusses only on issues related to cancer. This includes both the presence of tumors and mandibular osteoradionecrotic (ORN) tissue. ORN tissue is defined as tissue that lacks vitality during three months after a treatment using radiotherapy, when no recurring tumor is present and a response of impaired bone healing is detectable.^{21,22} These factors can cause large mandible defects, resulting in loss of support to external facial features, severe esthetic deformities, and functional problems in speech, swallowing and mastication. (Fig.2)^{4,5}



Figure 2. Visualization of a mandible that is severely affected by cancer-related factors such as ORN (A,B) and mandibular tumor growth (C,D)

Mandibulectomy

To treat these patients, the affected part of the mandible can be resected (taken out) during surgery by osteotomy (bone cutting), a treatment that is known as mandibulectomy. The amount of affected mandible tissue determines the extent and type of resection. When bone marrow is affected, osteotomy with a reciprocating saw will be performed to resect a complete segment, known as segmental mandibulectomy.²³ During resection of the defect, it is of major importance to take a safety margin of 10 to 15 mm into account to ensure a sufficient removal of affected tissue.^{24–26} The safety margin contains a desired minimal distance from the affected tissue, to ensure that small deviations during osteotomy will not lead to insufficient removal. An insufficient removal increases chance on developing metastasis, wound complications and local recurrence of tumor tissue.^{27,28} To enhance control on the trajectory of resection during osteotomy, 3D techniques were introduced. Preoperative three-dimensional available data of the patient is loaded into computer-aided simulation (CAS) software.²⁹ Within this software, the extent of affected tissue can be determined and an optimal osteotomy trajectory with a sufficient safety margin is planned. (Fig 3a)^{30,31} Furthermore, when the affected side is severely distorted due to late treatment and no anatomical landmarks are present, the healthy side of the mandible can be mirrored towards the affected side to create a reconstruction plan within this software.³²

The optimal osteotomy trajectory is summarized into designed resection templates that can be realized using computer-aided design and computer-aided manufacturing (CAD/CAM) techniques such as 3D-printing.²⁹

These templates contain resection sleeves that will guide the reciprocating saw in achieving the planned osteotomy trajectory during osteotomy. (Fig. 3B)³³

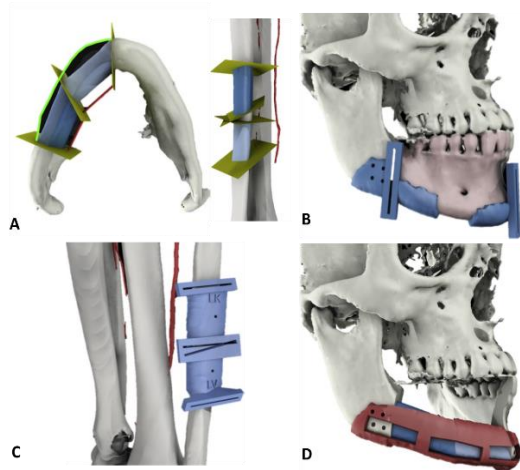


Figure 3. A) The planned resection trajectories for removal of the mandible defect (left), and the planned resection trajectories of the fibula to achieve an optimal reconstruction of the mandible (right) B) the corresponding mandibular resection template to obtain the planned osteotomy trajectory. C) The corresponding fibular resection template to obtain the planned segmentation. D) The positioning template to achieve a correct order and orientation of the fibula segments.³³

Mandible reconstruction

To restore both occlusal functionality and facial aesthetics, as well as to improve the quality of life of the patient, the mandible is reconstructed using a vascularized, autogenous bone graft with a skin flap. The graft is usually harvested from the fibula of the same patient, after which the vascularized graft is resected into segments, known as segmentation. It is of major importance to handle the peroneal vessel of the fibula with care, since it is needed for survival of the fibula graft and skin flap. Segmentation of the fibula is supported by CAS/CAD/CAM techniques. A segmentation plan of the fibula is generated using CAS, to obtain an optimal inner fit between the fibula segments and an optimal external fit to the mandibular residue. (Fig. 3a) This segmentation plan is simultaneously realized into a resection template plan using computer-aided design (CAD) and 3D-printing. (Fig 3c) To allow translocation of the segmented donor graft to the recipient mandible, the peroneal vessel is clipped off, whereby ischemia time (disrupted blood supply) is initiated.²⁹ Quick performance during this situation is recommended, to increase the chance of survival of both the segmented graft and the skin flap.²⁹ Correct placement of the segmented fibula into the mandibular residue can also be supported by CAS/CAD/CAM techniques, by

means of a positioning template. (Fig 3d) This template enforces the segments into the planned order and orientation, to obtain an optimal fit and a shape of the graft that mimics the native mandible (original mandible).³³ When the fibula segments are positioned correctly, titanium plates and screws are applied to allow mechanical fixation. The segments are internally fixated to one another, after which the edge segments are externally fixated to the mandibular residue. Finally, the peroneal vessel of the graft is reconnected to the mandibular blood supply, known as anastomosis.³² After surgery, three-dimensional data is retrieved and the match between the reconstructed mandible, the virtually planned mandible and the original mandible can be evaluated. This newly formed, reconstructed mandible that mimics the shape of the native mandible is further referred to as neomandible in this article.

The implementation of 3D techniques within mandibulectomy and mandible reconstruction has improved this treatment with regard to an enhanced control of the osteotomy trajectory. Furthermore, an improved surgical efficiency is obtained since a reduced amount of time is occupied for intraoperative trial and error during mandible resection and fibula segmentation. This will result in a decrease of both ischemia as well as operation time, leading to a reduced chance on complications, and an increased chance on fibula graft survival.¹² In the end, the quality of life of the patient will be improved.^{29,34}

However, according to both surgeons from Radboud University Nijmegen Medical Centre as well as from a literature study, still a lot of improvements can be made to this treatment regarding to the transfer from virtual surgery to the intraoperative situation.^{17,18,35,36} There are problems encountered with the inner and outer fit of the fibula segments within the mandibular residue. A bad fit compromises mandible functioning and aesthetics. Therefore, an extensive problem analysis was performed to determine aspects that can be handled from both a clinical and a design perspective to enhance this transfer.

An enhanced transfer will make the treatment more reliable, and improves the surgical outcome in terms of neomandible functioning, patient aesthetics and the quality of life of the patient.

Methods

To perform an extensive problem analysis, four different methods were applied to detect and visualize the problem(s). A literature study was performed, the instruments that are applied during surgery were examined, surgery was attended, and simulations were performed.

Problem analysis

Errors may be introduced during patient scanning, and during the virtually planned surgery. Additionally, errors may occur during realization of the resection templates with CAS/CAD/CAM techniques, during placement of all templates, and during the resections. Because the treatment is extensive and complex, it may be difficult to identify and localize factors that directly introduce errors.

Literature study

First, a literature study was performed according to a six-step approach that divides the treatment process into six regions: 1) preoperative scanning, 2) virtual surgery, 3) manufacturing, 4) real surgery, 5) postoperative scanning, 6) accuracy measurements. The aim of this approach is to detect a region where biggest advances can be made.

Instrument examination

Second, the currently applied surgical devices, including the patient-specific resection templates were examined during and after surgery. Special attention was given to the dimensions, curvatures and materials of the currently applied surgical devices.

Attendance of surgery

Third, three surgeries were attended to clarify surgical conditions and consider events that may compromise surgical outcome. Therefore, special attention was given to events such as placement of the resection template, guidance of the template during osteotomy with a reciprocating saw, and positional feedback of the positioning template.

Simulations

Finally, to visualize the problems with a bad fit of fibula segments, a simulation of possible surgical outcomes was performed using SolidWorks (SolidWorks Corp. 2015).

Design requirements

Since it concerns a clinical driven problem that partly will be handled from a design perspective, there are requirements from both clinical and technical disciplines that have to be accounted for. The clinical design requirements include usability and amount of feedback provided towards the surgeon, safety during use and biocompatibility of the materials towards the patient. Furthermore, the sterilization department requires measures according to the sterilization and clean ability of the design.

Literature study

Sterilization requirements were set according to the Guideline for Disinfection and Sterilization in Healthcare Facilities,³⁷ the DSMH (Dutch Association for Experts Sterile Medical Devices),³⁷ and ISO 13485 and the standards this document refers to. The resection templates contain small gaps and lumens, and are into direct contact with patient inner structures. Therefore, all forms of microbial life should be destructed and the sterilization documents should be explored according to methods that are applicable to achieve a sufficient sterilization.

Furthermore, information required for establishing clinical requirements with regard to the anatomies involved can be retrieved from literature.

Instrument examination

Technical requirements are linked to the osteotomy trajectory, the geometries of the anatomies that are involved, and strength of the materials applied. Moreover, according to manufacturing methods, there will be geometric requirements to the design.

To obtain this information, instruments were examined, photographed and measured using a digital caliper (Powerfix Profi+).

Simulations

Since anatomical shapes and dimensions are specific to patients, mean values will be processed using SolidWorks to set a minimum and maximum dimension that could be implemented in the design requirements.

Moreover, the interaction between current instruments and the resection templates were simulated (SolidWorks), to detect possible discrepancies that may compromise their performance.

Attendance of surgery

Additionally, the available working space of the instruments, mandible and fibula shape, and possible other discrepancies of the instruments that may compromise the treatment can be detected during attendance of surgery.

Concept generation

Because rationale towards the improvement of the treatment comes from a design perspective, concepts were generated according to a morphologic analysis. Within this analysis, options were created to four functions the design should occupy and which should be included in the design. It was decided not to change the base of the design to allow a quick and easy clinical adaption. The four functions included: 1) connection between the bone and template, 2) the fit of the template, 3) the strength of the template, 4) the guiding perspective. The options were combined into concepts, thereby, concepts were generated that fulfill one or multiple design requirements. A scoring system was generated to select the concept that is most promising in improving the treatment and should be developed further into a prototype. The scores of the scoring system are based on the extent of fulfilling a design requirement.

Exploring test and concept evaluation

It was noticed that the scoring system could not be completed purely based on CAD models, theoretical knowledge and considerations. To retrieve practical feedback, an exploring test was performed.

Different concepts were manufactured, and their practical performance towards the design

requirements were assessed during an exploring test. Design requirements that could be scored according to this test were accuracy, safety, disassembly time, usability, strength of the concept to withstand forces of the saw blade and the amount of feedback that was provided to the user.

A synthesized bone block (Sawbone, Pacific Research Laboratories Inc.) was introduced as mechanical model during the test, to evaluate the performance of the concepts with regard to accuracy and strength of the design. The blocks consist of two layers with relevant mechanical properties of human bone. An epoxy sheet mimics human cortical bone, while the thickest layer that is made of solid polyurethane foam mimics human cancellous bone. This makes them suitable for biomechanical testing. A large block was processed into smaller blocks to create dimensions similar to both the mandible and the fibula. (Fig.4)

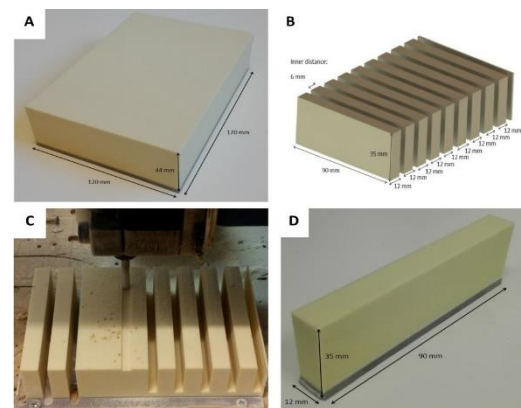


Figure 4. The synthesized bone blocks applied during the exploring test.

To perform the resection, a reciprocating handpiece with a saw blade (Braunn Aesculap) was used, equal to the one applied currently during surgery.³⁸ Additionally, a vise was applied to fixate the bone blocks and minimize potential user errors. Each concept contained two straight resection sleeves, and two angulated resection sleeves. Photographs were taken before and after the resections to evaluate hardness and strength of the concept towards withstanding the vibrations of the saw blade. Remarks regarding to safety, such as visual feedback, were noted during the experiment. The experimental set-up is presented in figure 5.

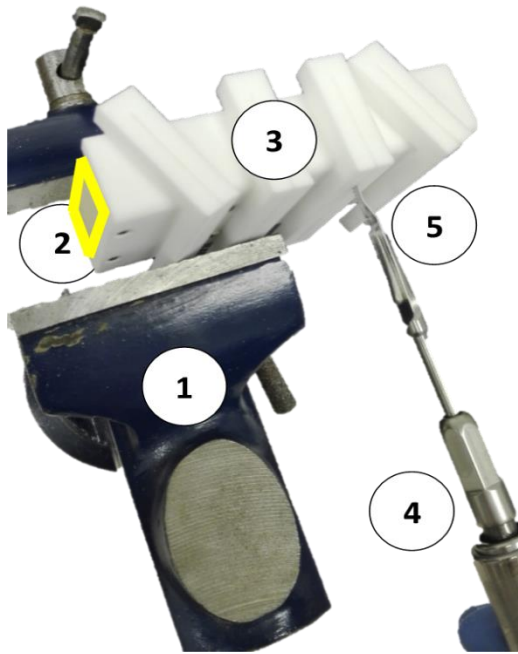


Figure 5. The experimental set-up as applied during the exploring test. 1) The vise, 2) a bone block, 3) a resection template with resection sleeves, 4) a reciprocating saw with a saw blade, 5) the saw blade guided by the resection sleeve, ready to perform a resection

Then, the correspondence between the planned osteotomy trajectory and the obtained osteotomy trajectory was evaluated to assess the accuracy and performance of the concepts. The planned osteotomy trajectory was retrieved by simulating the trajectory into the CAD model in SolidWorks. This trajectory was projected onto a virtual bone block, and the bone block was virtually segmented. The segments were saved into a stereolithographic (stl) format. The dimensions of a bone block represent the planned osteotomy trajectory and will act as reference surface. (Fig. 6b)

To evaluate differences between the obtained and planned segmented bone blocks, the obtained blocks were converted into a stl format using a 3D laser surface scanner. (D500 3D scanner, 3Shape, Copenhagen, Denmark) This type of laser scanner uses two 1.3 MP cameras and a red laser to scan objects with a very high resolution, accuracies of 10 μm are claimed.³⁹ To obtain 3D models of the real segments that can be used in software, the obtained segmented bone blocks were scanned. The dimensions of these scanned blocks represent the obtained osteotomy trajectory and will be compared to

the reference surface of the planned trajectory. (Fig. 6a)

The stl files of the planned segmented bone blocks and the stl files of the obtained segmented bone blocks were loaded into medical image computing software (Maxilim V2.3.0.3, Medicim NV, Mechelen, Belgium). This software applies a surface-based registration algorithm to align surfaces. To align these models, the unaffected surfaces of the obtained block, front surface and back surface can be matched to the corresponding surfaces of the planned block. The result is presented in figure 5c. The surfaces of interest, along which the resection was performed, were selected to create a distance map. (Fig. 7) Distances are displayed by a color map to retrieve an overview of the quality of the alignment. A large distance represents a bad correspondence between the planned and obtained surface, and vice versa. This is a quick, simple method through which performances of the concepts with regard to the accuracy of the osteotomy trajectory can be obtained. However, it is hard to compare the concepts solely based on a visual representation. Therefore, the distances of the distance map were transported as a distance kit to allow calculation of the mean distance, the standard deviation and the 95 percentile of each map. Based on these values, concepts could be scored at their guiding performances in terms of keeping the distance between the planned an obtained osteotomy trajectory within boundaries.

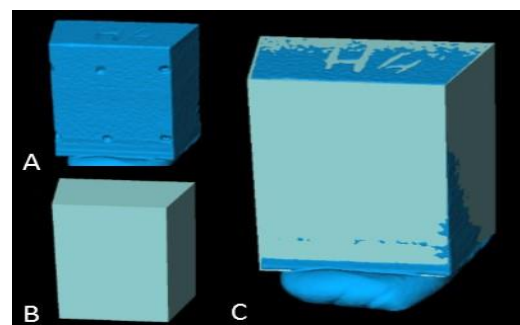


Figure 6. a) An obtained segmented bone block, b) A virtually segmented bone block, representing the planned resection surfaces and inherent trajectories. C) An aligned set of a planned and obtained bone block using Maxilim.

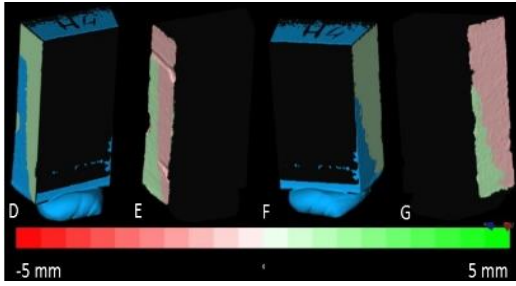


Figure 7. Distance maps between two aligned surfaces, in a range of -5 to 5 mm. d) registration of the left resected surface, e) the resulting distance map of this surface, f) registration of the right resected surface, g) the resulting distance map of this surface.

Design evaluation

The designs were evaluated on a synthesized bone block, simultaneously to the method applied for evaluating the concepts during the exploring test. However, to increase the sample size, the bone block was divided into twenty pieces instead of nine. Both distance maps and distance kits were generated simultaneously to the method applied during the exploring test.

Additionally, to refer back to deviations found in literature, another area of interest is the angulation over the surface of resection. The insertion of the device may be well-guided, while the deviation of the osteotomy trajectory increases over the distance of the osteotomy. Therefore, the stl-files of the planned and obtained bone blocks were loaded into 3D-modeling software (3ds Max 2016, Autodesk). With this software, normal vectors of the obtained resection surface could be calculated. All normal vectors were averaged into one normal vector. Perpendicular to this averaged normal vector, a plane was created. Simultaneously, a plane was created perpendicular to the planned resection surface of the planned bone block. (Fig 8.) To determine the angulation of the osteotomy trajectory, angles between both planes could be calculated.

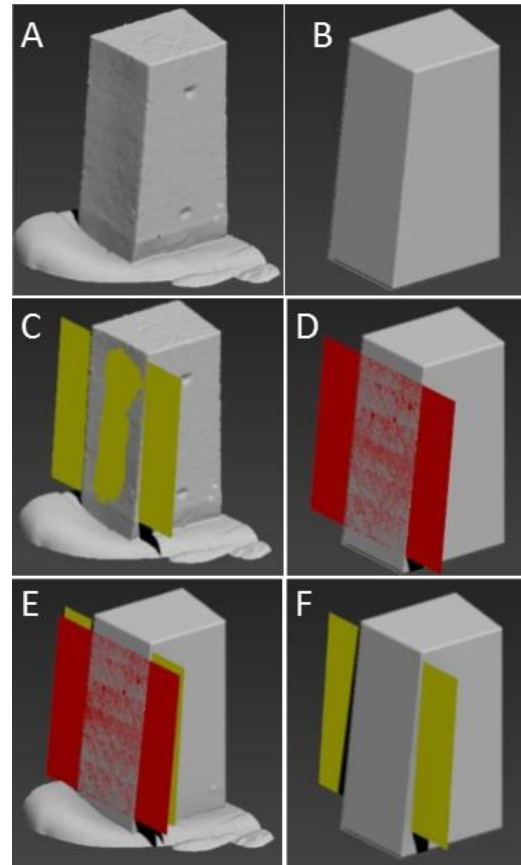


Figure 8. The method of calculating the angulation of the osteotomy trajectory. A) The obtained bone block. B) The planned bone block. C) The obtained resection plane perpendicular to the calculated averaged normal vector of the resected surface. D) The planned resection plane perpendicular to the calculated averaged normal vector of the planned surface. E) Both planes are superimposed to calculate differences. F) The planned bone block with the obtained resection plane in place, a discrepancy can be noticed.

The angulation of the osteotomy trajectory was represented using the deviation in yaw, pitch, and roll. (Fig. 9) The yaw provides information according to the trajectory from the top to the bottom. The roll deviation represents the extent to which the osteotomy trajectory is followed from the front to the back of the bone block. Finally, the pitch describes the performance of following the trajectory regarding to horizontal deviations.

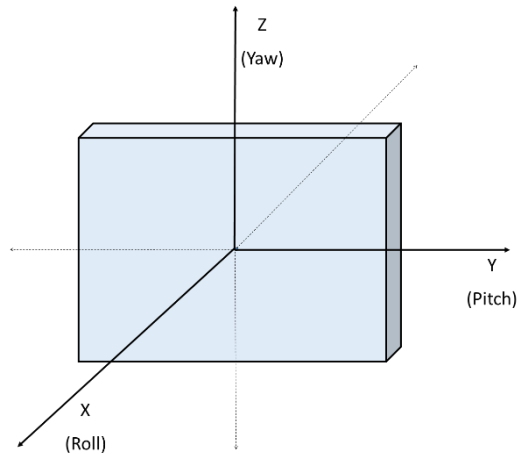


Figure 9. The yaw, pitch and roll of the planes used to determine the angulations of the obtained osteotomy trajectory in comparison with the planned trajectory during osteotomy.

Results

Problem analysis

Literature study

Different accuracy measurement methods were found in literature with regard to studies that assessed the accuracy of the osteotomy trajectory. It was noticed that positioning of parts of the neomandible can severely deviate from the preoperative situation. A condylar shift of 10.0 ± 6.0 mm (mean \pm SD) and angulations of $9.1 \pm 9.9^\circ$ of mandibular angle were found (mean \pm SD).⁴⁰ This deviation can be introduced during each of the five distinct steps mentioned before. For step 1 and step 5, in which a CBCT scan is obtained from the patient, an error up to 2.00 mm was found.¹³ According to step 2 and step 3 of the process, the CAS/CAD/CAM transfer, an error of 0.13 ± 0.11 mm (mean \pm SD) was found with a maximum error of 0.97 mm.¹⁶ According to step 4 of the process, an error of 2.06 ± 0.86 mm (mean \pm SD) was found with a maximum deviation of 3.7 mm.¹⁸ Furthermore, during the real osteotomy, a depth angle of 5.43° occurred.⁴¹ This was referred to as the difference between the planned trajectory and the obtained trajectory with respect to the depth of the cut and can be experienced as a roll deviation.

Additionally to the mandible resection and fibula segmentation, there were discrepancies found during placement of the segments into

the mandibular residue. There were angulations found up to $4.3^\circ \pm 3.2^\circ$ (mean \pm SD).¹⁷

Instrument examination

The examination of the currently applied surgical devices and resection templates ended up in detecting a discrepancy between the thin and flexible saw blade and the relatively wide resection sleeve. The thickness of the sawblade is 0.25 mm, while the width of the resection sleeve is designed at 0.70 mm. To find the corresponding depth angle that could be caused by this discrepancy, a simulation was performed using SolidWorks. It was found that solely the interaction between the saw blade and the resection sleeve can already lead to a depth angle of 5.13° . (Fig. 10)

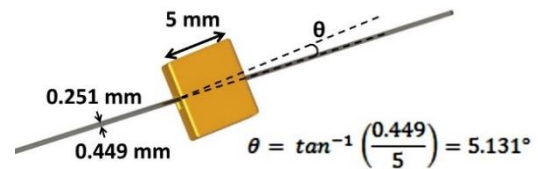


Figure 10. Calculation of the depth angle that can be caused by the discrepancy between the resection sleeve and reciprocating saw blade.

Attendance of surgery

During the attendance of surgeries, four different events were noticed. First, there was no true professional safety measure to protect the peroneal vessel during segmentation of the fibula, while it is of major importance that no damage is caused to the vessel for survival of the graft and the resulting success of this treatment. Second, it was detected that the reciprocating saw went through the resection template, and a part of the template broke off. (Fig 11a) Third, the positioning template could not be applied during surgery, because there was a gap between the mandibular residue and the fibula segments that could not be bridged by the template. (Fig. 11b) Therefore, this template rendered obsolete and surgeon needed to switch back to the conventional method of manual positioning and placement.

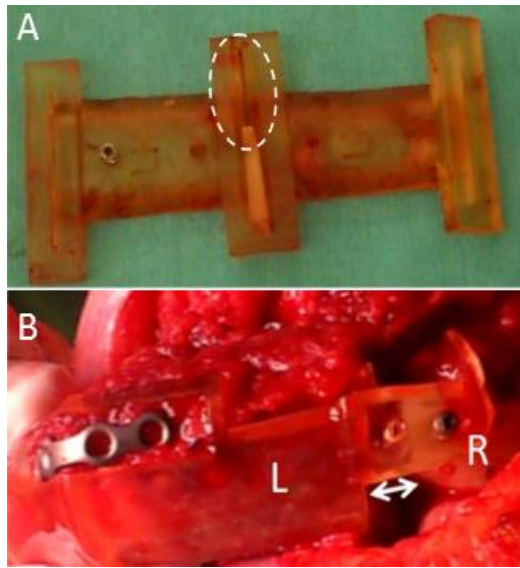


Figure 11. A) A fibular resection template that was cut through and parts broke off. B) A bad fit of the positioning template

Fourth, the available space for placement of the mandibular resection template was limited due to soft tissue obstructions, and parts of the template had to be cut off to achieve a sufficient fit on the bone. This included the top of a resection sleeve, which is suspected to compromise the strength of the resection sleeve. Thereby, a contact point is eliminated, such that horizontal movements of the saw blade are allowed. This may lead to an increased angulation of the saw blade within the sleeve.

Simulations

According to a simulation in SolidWorks using a maximal mandible height of 51.50 mm that was found in literature, this depth angle may lead to a deviation of 4.90 mm at the end of the osteotomy trajectory. (Fig. 12)

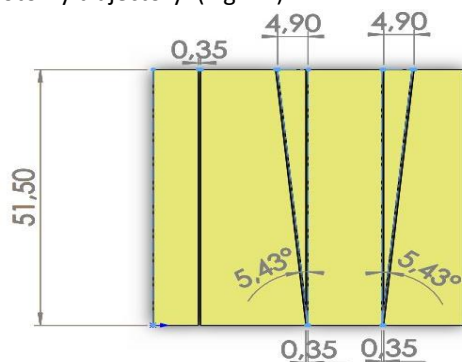


Figure 12. Calculation of the deviation at the end of the osteotomy trajectory when the depth angle is 5.43°.

A simulation was performed in SolidWorks to visualize the impact on the neomandibular shape, when a deviated osteotomy trajectory and angulation of fibula segments within the mandibular residue occurred. The initial conditions differed in the direction of rotation, and the amount of rotation. The deviation of the osteotomy trajectory was fixated at 5.43°. The segments could rotate both clockwise and anti-clockwise, and both a mean rotation of 4.3° and a maximum rotation of 10.9° were simulated. (Fig. 13) From this simulation, it was suggested that the front angle of the neomandibular body is more prone to clockwise rotations (Fig. 13a) than counterclockwise rotations (Fig. 13b).

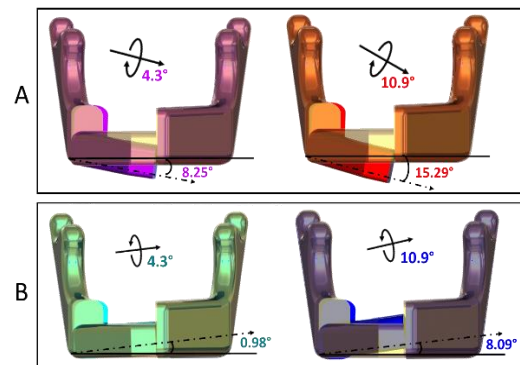


Figure 13. Simulation of a deviated osteotomy trajectory of 5.43° and different rotations of the fibula segments.

Design requirements

First, to obtain a feasible design, three boundary conditions have to be met: a) the deviation of the achieved osteotomy trajectory in comparison with the planned osteotomy trajectory should not exceed $\pm 2^\circ$, while b) the production costs of the patient-specific devices do not exceed 350 euro's and c) the ischemia time does not exceed 100 minutes.

Literature study

Second, mandible thicknesses and heights were explored using literature. Thereby, it had to be taken into account that this treatment is usually performed on edentulous patients. Therefore, the impact of an altered force transmission on the jaw had to be studied as well. Other studies found in literature showed that a jaw without teeth causes severe bone resorption. (Fig. 14)

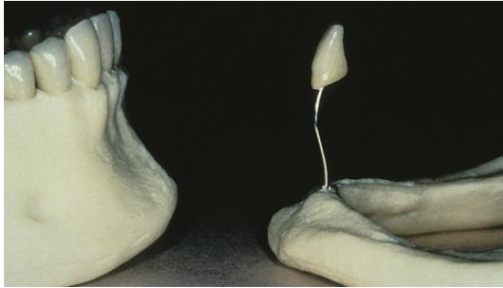


Figure 14. The impact of loss of teeth from the perspective of mandible resorption.⁴²

To include this in the design requirements, minimum height and thickness was based on edentulous jaws, while maximum height and thickness was retrieved from dentate patients. This resulted in a range of 8.00 mm to 51.50 mm for the mandible height, and a range of 3.02 mm to 14.03 mm for the mandible thickness.^{43,44,45}

What should be accounted for setting up dimensional requirements according to the fibula bone, is that roughly three different shape types are commonly found. (Fig. 15)

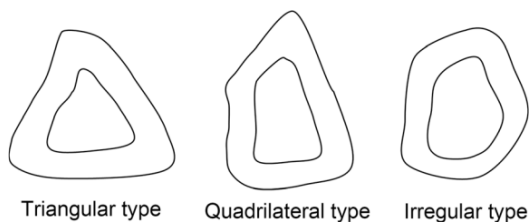


Figure 15. The three types of shape that are commonly found for the fibula.⁴⁶

Furthermore, the shape and the material(s) of the design should be conform to available sterilization methods. According to the Guideline for Disinfection and Sterilization in Healthcare Facilities, the DSMH and ISO 13485 and the standards this document refers to, it was supported to use autoclave steam.³⁷ Therefore, the material should withstand temperatures between 121° - 148°C for a duration of 10 to 60 minutes.³⁷

Simulations

To determine which shape set the dimensional boundaries of bone should be bridged during osteotomy, the values for fibula height and thickness as found in literature were simultaneously processed in SolidWorks. (Fig. 16)⁴⁶

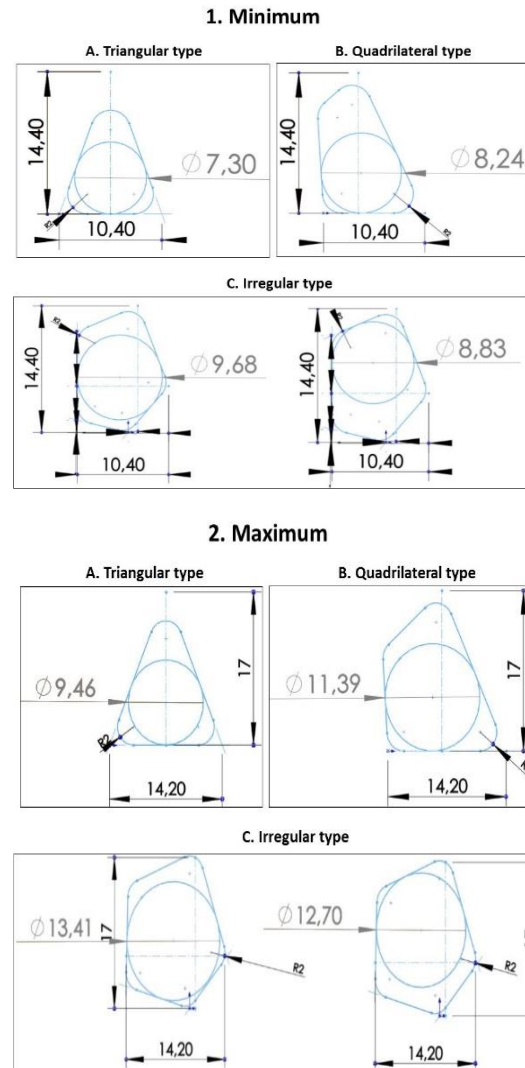


Figure 16. The calculation method of minimum and maximum fibula bone as performed in SolidWorks, based on the three different shapes commonly found.

From this simulation it was retrieved that the minimum diameter of fibula bone that should be bridged was 7.30 mm and the maximum diameter was 13.41 mm.

According to requirement to improve the amount of haptic feedback provided to the surgeon, it is suggested that the design could protect the peroneal artery or allow increased visual feedback.

Secondly, technical requirements were introduced to control production time and production costs, while a sufficiently performing design is obtained. As diagnosed during the problem analysis, the currently applied combination of instruments allow osteotomy deviations up to 5.13°, which corresponds to a

deviation of 4.62 mm at the end of the trajectory. With regard to improving the accuracy and reliability of the osteotomy trajectory, a maximum deviation of 2.0° was set.

Thereby, at the end of the osteotomy trajectory, a maximum deviation of 1.8 mm will be caused. (Fig. 17)

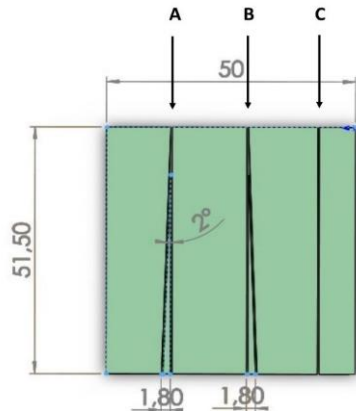


Figure 17. The calculation of the deviation at the end of the osteotomy trajectory when an angulation of 2.0° of the saw blade is set as initial condition.

An overview of the generated clinical and technical design requirements and the approach of assessment is given in table 1.

Table 1. The clinical and technical requirements resulting from the different analysis methods described in the methodology section.

#	Clinical requirement	Value
1	Usability	Amount of required training time
2	Adjustable to anatomy shapes	(x-,y-,z-plane)
3	Haptic feedback	Availability of interacting forces to the surgeon
4	Ischemia/disassembly time	≤100 min. ¹⁰
5	Clean ability	Shape, gap sizes
6	Sterilization	121°C - 148°C
7	Biocompatible	Risk of injury, toxicity or rejection by the immune system
8	Safety	Amount of collateral damage
#	Technical requirement	Value
1	Accuracy osteotomy	≤2° or ≤ 5 mm
2	Simple production method	≤ 500 euro's
3	Angulation graft placement	≤2°
4	Bone thickness that should be bridged during osteotomy	3.02 mm - 51.50 mm
5	Resistant material / design	Young's modulus, tensile strength
6	Simple construction	Amount of parts

Concept generation

To create a low threshold of clinical implementation and since it is suspected that remarkable progress can be made by adjusting the current design of the resection template, the concept choices were based on adjustments to the current design of the resection template. (Fig. 18) Additionally, because the surgeon is experienced with using the reciprocating saw, it was chosen to make no adjustments to the device applied for osteotomies. Adjustments were made according to the four functions mentioned during the generation of concepts.

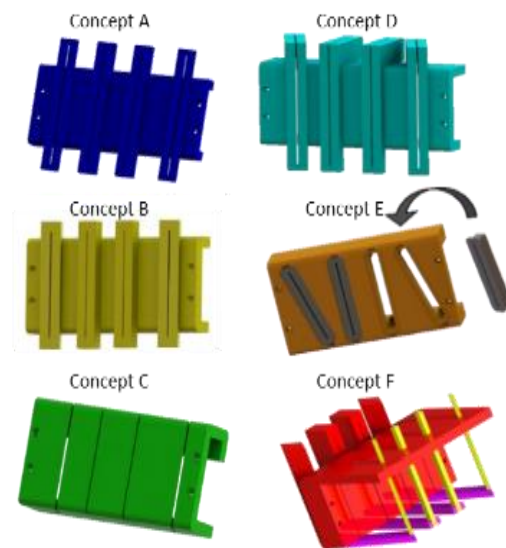


Figure 18. The CAD models of the created concepts.

First, the connection between the bone and the resection template was maintained by a screw connection. Second, the concepts were manufactured by 3D-printing using PA 2200, since this material is biocompatible and it is suitable for medical applications according to ISO 13485.⁴⁷ Additionally by the application of PA 2200, the models can be processed to relatively low cost, because this material has a melting temperature of 176 °C, which makes it suitable for autoclave steam sterilization.⁴⁷ Furthermore, a metal part was introduced within one concept for local enforcement of the template. Third, the fitting problem of the current design was attempted to be tackled by a shape-fitted increased contact area.

Fourth, to handle the occurring deviation of the osteotomy trajectory, the interaction between the reciprocating saw and the resection

template was adjusted. This was attempted by either reducing the width of the resection sleeve, or the amount of directions through which guidance was provided, or both.

Exploring test and concept evaluation

The current design as reference model, and five created concepts were manufactured and tested on the synthesized bone blocks, to retrieve practical feedback. The models were mechanically fixated using titanium screws, after which osteotomy was performed. The obtained bone segments were scanned using the laser scanner to convert them into stl models that can be matched to the virtually planned segments.

The main aim of the exploring test was to fill in the scoring table as presented in table 2. All concepts improved the current design, except concept C. Concept C was based on an increased contact area. However, the design of this concept took away all sight, which compromises the placement of the template, and the safety towards soft tissues during osteotomy. Additionally, concept C scored worst on accuracy of the osteotomy trajectory.

Design generation and evaluation

Concept B and concept D obtained a considerably higher total score according to the scoring table. Therefore, these concepts were selected for the next phase of design generation. Additionally, it was decided to develop concept E and concept F as well, based on their inventiveness and additional measures regarding to safety.

Based on concept B, D, E and F, five designs were generated. (Fig. 19) Remarks of the exploring test were taken into account for the designs to improve their performance. Two types of connection systems of multipart concept F were designed, concept B and D were combined and small adjustments were made to concept E. Thereby, five designs were obtained. Their performances were tested using the same experimental set-up, and were evaluated simultaneously to the methods applied for the concepts.

Table 2. The scoring table, completed using scores given according to the experiences retrieved from the exploring test.

Requirement	Weighing factor	Score Concept A: Current	Score Concept B: Smaller	Score Concept C: Contact	Score Concept D: Top guidance	Score Concept E: Titanium	Score Concept F: Contouring
Usability	8	8	8	7	8	7	5
Adjustable to anatomy shapes	6	5	5	5	5	5	5
Haptic feedback	8	4	5	3	5	5	9
Ischemia time / disassembly time	8	8	8	8	8	7	5
Sterilization	6	8	8	8	8	7	8
Biocompatible	8	9	9	9	9	9	9
Safety	9	5	5	3	5	5	9
Accuracy	10	5	7	6	9	9	8
Simple production method	7	9	9	9	9	6	7
Simple construction	6	10	10	7	9	8	5
Resistant material	9	6	6	6	6	9	6
Total score (%)	850	582 (68,5%)	610 (71,8%)	540 (63,5%)	624 (73,4%)	602 (70,8%)	596 (70,1%)

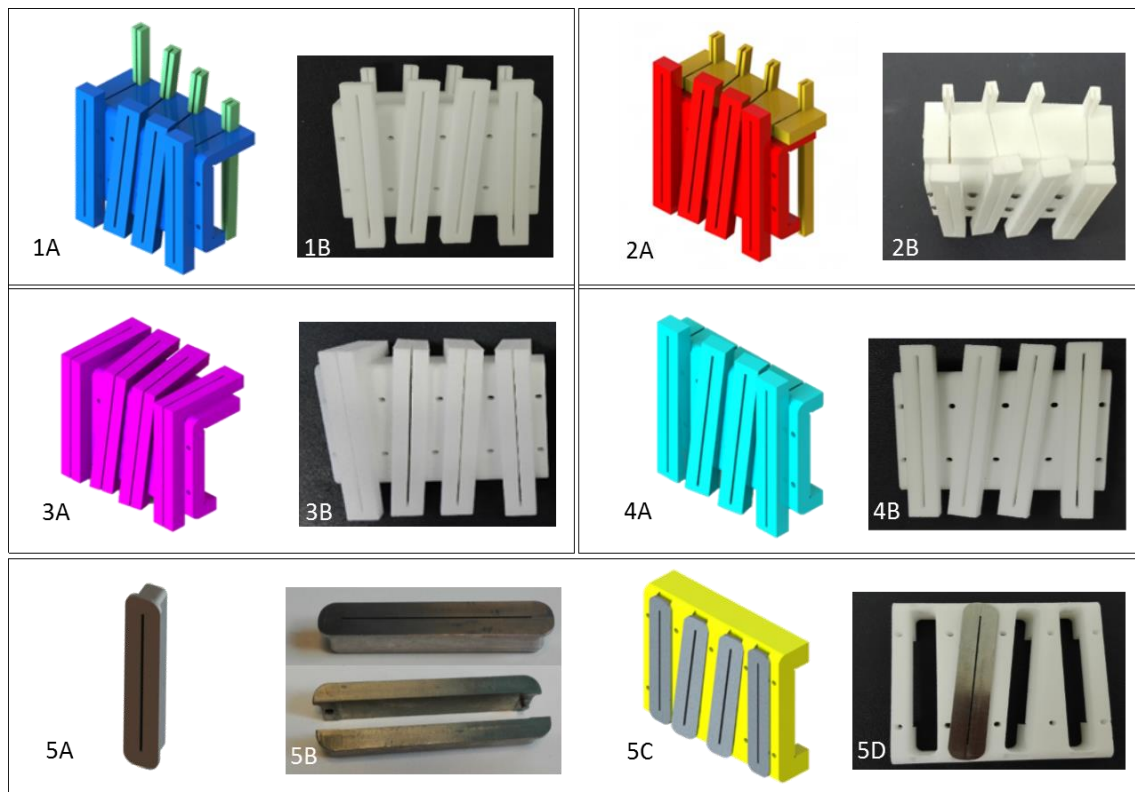


Figure 19. The 5 selected designs that were evaluated during the final experiment. A) The CAD models of the design. B) The corresponding 3D-printed models.

During the experiment, the five designs were used to perform eight straight osteotomies and eight equally angulated osteotomies. The straight and angulated osteotomies were analyzed separately.

Using evaluation method 1, calculation of the distances between the obtained and the planned straight trajectory, there were no significant differences found between the designs. With regard to the angulated trajectory, design 3, “smaller topguidance”, showed a significantly improved accuracy in comparison with the current design ($p=0.042$). The mean distance of the obtained trajectory to the planned trajectory was 0.18 ± 0.11 mm (mean \pm SD) for this design, while the current design caused a deviated trajectory of 0.30 ± 0.09 mm (mean \pm SD).

Using evaluation method 2, calculation of the angle between the obtained and the planned straight osteotomy plane, a significant difference was found with regard to the roll of the trajectory. The current design caused a roll deviation of $1.24 \pm 0.19^\circ$ (mean \pm SD), while

design 5, “titanium insert” kept the roll within $0.32 \pm 0.07^\circ$ ($p=0.001$). According to the yaw of the angulated trajectory, three designs showed a significantly improved control. The yaw deviation of the current design was $0.25 \pm 0.32^\circ$ (mean \pm SD). Design 1, “backguidance 1” reduced this deviation to $0.07 \pm 0.16^\circ$ (mean \pm SD), ($p=0.05$). Design 3, “smaller topguidance” reduced this deviation to a deviation of $0.05 \pm 0.06^\circ$ (mean \pm SD), ($p=0.016$). Design 5, “titanium insert”, reduced this to a deviation of $0.07 \pm 0.08^\circ$ (mean \pm SD) ($p=0.045$). Furthermore, design 1, “backguidance 1” showed a significantly improved control of the pitch of the osteotomy trajectory. This design reduced the pitch from $2.14 \pm 1.81^\circ$ (mean \pm SD) to $0.85 \pm 0.84^\circ$ (mean \pm SD), ($p=0.017$).

Discussion

Problem analysis

Discrepancies between the virtual surgery and real operation were detected by the surgeons at Radboud University Nijmegen Medical Centre. This was confirmed during attendance of

surgery. Even though it was personally experienced, the interaction between the reciprocating saw and the resection templates is just one part of the broad process of this treatment. There are multiple other factors that may contribute to a bad reconstruction. However, the vast majority of literature does not confirm problems the surgeons of this hospital encounter, most studies conclude that the treatment was already dramatically improved by the introduction of assisting 3D techniques. Moreover, no assessment methods of neither the treatment nor the accuracy of the osteotomy trajectory were clearly described in literature.^{17,41,48}

Design requirements

According to the interaction of the instruments that are applied, advances can be made within both the osteotomy devices and the templates to improve the resection and reconstruction within this treatment. During this study it was attempted to reduce this discrepancy by adjusting the design of the resection template to improve the interaction between the saw and the resection template. Within this field, it was decided to focus on adjusting the design of the template, while it is suspected that also the osteotomy device contributes highly to the interaction and resulting deviation of the osteotomy trajectory. Alternatives to this instrument were not extensively studied, while in the literature search other osteotomy devices seemed promising, such as the Er:YAG laser and the piezoelectric device. These devices showed smoother cuts and increased bone healing abilities. However, it was concluded that the piezoelectric device is not sufficient to achieve deep osteotomies as required in this treatment, and the laser requires robot assistance to benefit from the advantages this device offers.^{49,50,51} Those devices require further development before they can be applied within this treatment and therefore it was decided to use the reciprocating saw as osteotomy device. Additionally, alternative perspectives to the design could be selected to adjust the resection template, such as the fitting principle or the choice of material. However, in such short time span towards a process this broad, choices had to be made and focusing on enhancing the

control of the osteotomy trajectory by making adjustments to the design of the resection templates seemed most promising.

Exploring test and concept evaluation

Multiple issues concerning the strength and connection of different parts of the design were noticed. The angulated resection sleeve of concept D created a bad fixation in the vise. The titanium insert of concept E received a loose fit in the template, and the different parts of concept F did not contain a sufficient connection. This could compromise the outcome of this test with regard to the score of accuracy within the scoring table. However, since it was an exploring test and not only the accuracy of the trajectory was assessed but also other requirements were evaluated by these 3D-printed models, it can be concluded that the exploring test did achieve its main purpose.

Design generation and evaluation

Two evaluation methods were applied to assess the performance of the designs according to a straight and an angulated resection trajectory. Small differences were calculated between the models, and most significant differences were found for the angulated trajectory. However, results from the angulated trajectory are of major importance, since most planned resection trajectories are angulated to obtain segments that can be constructed into a neomandible that is shaped similar to the native mandible. Therefore, it can be concluded that major advances were made by design “backguidance 1”, because both the yaw as well as the pitch of the trajectory were better controlled by this design. The yaw was reduced from $0.25 \pm 0.32^\circ$ to $0.07 \pm 0.16^\circ$ (mean \pm SD), ($p=0.05$). The pitch was most improved of all angulations, by reducing the angulation from $2.14 \pm 1.81^\circ$ of the current design to an angulation $0.85 \pm 0.84^\circ$ (mean \pm SD), ($p=0.017$) for design “backguidance 1”.

A limitation to this study was the small sample size. Because both straight and angulated resections were performed, the amount of available synthesized bone blocks for testing was restricted. As a result, the sample size may be not sufficient to draw appropriate conclusions about the accuracy and reliability of

the design. Furthermore, a vise was used to keep contributing cofactors within boundaries. However, this measure could add excessive control over the resection trajectory by limiting the synthesized bone block in all movements and rotations, while these are not restricted during real surgery. Furthermore, it could not be avoided that the template was fixated within the vise as well. Therefore, it is suspected that the differences in performance of the models would be larger when no vise was applied during the practical testing because the impact of this fixation was not equally for each design. Especially design 1 and 2 suffered from the fixation, because the back sleeves compromised the fixation within the vise.

Conclusion

From literature search, surgical findings, examination of the currently applied surgical devices and simulations in SolidWorks to visualize and retrieve insight in interactions of current instruments, it was concluded that there are multiple perspectives from which advances can be made to improve this treatment.

An increased control of the osteotomy trajectory will decrease the chance on insufficient removal of affected tissue and reduce the chance of a bad fit between the fibula segments and the mandibular residue due to an osteotomy deviation. Therefore, this study mainly focused on improving the interaction between the instruments and templates that are applied, to enhance the control and reliability of the osteotomy trajectory. The main approach for achieving this was by adjusting the design of the resection template.

The aim of this study was to enhance the transfer between the virtual and the real surgery by adjusting the design of the resection templates, to reduce the difference between the planned and the obtained resection trajectory. Several designs within this study showed a significantly improved control of the osteotomy trajectory, even though the differences are small. Therefore, it may be concluded that this aim is achieved, and adjusting the design of the resection templates

is a promising area to enhance the transfer between virtual surgery and the real surgery.

Recommendations

Besides enhancing the accuracy and reliability of the osteotomy trajectory, design 1, "backguidance 1" protects the peroneal artery at the back of the fibula during the osteotomy. Therefore, this design increases the safety of the treatment in two way. This makes design 1, "Backguidance 1" promising to improve the current treatment with regard to critical soft tissue structures and subsequent skin flap survival, the fit of the fibula segments and the resulting patient aesthetics and mandible functioning. Therefore, it is recommended to develop this design in the future. One perspective of further development that is recommended is the adaption of an angle into the design of the back sleeve. This will facilitate placement of the sleeve behind the triangular-shaped fibula.

Furthermore, additional appliance of the navigation system may provide a more accurate and forcing guidance during the transfer from the virtual planning towards the real surgery, especially during localization and orientation of the resection templates.

Bibliography

1. Antoni van Leeuwenhoek. Mondkanker en tongkanker. Antoni van Leeuwenhoek - Nederlands Kanker Instituut. <http://www.avl.nl/kankersoorten/mondkanker/>.
2. Chim H, Salgado C, Mardini S, Chen H-C. Reconstruction of Mandibular Defects. *Semin Plast Surg.* 2010;24(2):188-197. doi:10.1055/s-0030-1255336.
3. Guven Y, Zorlu S, Cankaya AB, Aktoren O, Gencay K. A Complex Facial Trauma Case with Multiple Mandibular Fractures and Dentoalveolar Injuries. *Case Rep Dent.* 2015;2015:1-6. doi:10.1155/2015/301013.
4. Lonie S, Herle P, Paddle A, Pradhan N, Birch T, Shayan R. Mandibular reconstruction: meta-analysis of iliac-versus fibula-free flaps. *ANZ J Surg.*

- 2015;n/a-n/a. doi:10.1111/ans.13274.
5. Rana M, Warraich R, Kokemüller H, et al. Reconstruction of mandibular defects - Clinical retrospective research over a 10-year period - Clinical r. *Head Neck Oncol.* 2011;3(1):23. doi:10.1186/1758-3284-3-23.
 6. Zavatiero E, Fasolis M, Garzino-Demo P, Berrone S, Ramieri G a. Evaluation of plate-related complications and efficacy in fibula free flap mandibular reconstruction. *J Craniofac Surg.* 2014;25(2):397-399. doi:10.1097/SCS.0000000000000656.
 7. Kalra GS, Goel P, Singh PK. Reconstruction of post-traumatic long bone defect with vascularised free fibula: A series of 28 cases. *Indian J Plast Surg.* 2013;46(3):543. doi:10.4103/0970-0358.122013.
 8. Minami A, Kasashima T, Iwasaki N, Kato H, Kaneda K. Vascularised fibular grafts. *J Bone Jt Surg - Ser B.* 2000;82(7):1022-1025. <http://ovidsp.ovid.com/ovidweb.cgi?T=JS&PAGE=reference&D=emed5&NEWS=N&AN=2000335393>.
 9. Cordeiro PG, Disa JJ, Hidalgo D a, Hu QY. Reconstruction of the mandible with osseous free flaps: a 10-year experience with 150 consecutive patients. *Plast Reconstr Surg.* 1999;104(5):1314-1320. <http://www.ncbi.nlm.nih.gov/pubmed/10513911>.
 10. Kääriäinen M, Kuuskeri M, Gremoutis G. Utilization of Three-Dimensional Computer- Aided Preoperative Virtual Planning and Manufacturing in Maxillary and Mandibular Reconstruction with a Microvascular Fibula Flap. 2015.
 11. Hidalgo D a. Fibula free flap: a new method of mandible reconstruction. *Plast Reconstr Surg.* 1989;84(1):71-79. doi:10.1016/S0901-5027(05)80583-1.
 12. Antony AK, Chen WF, Kolokythas A, Weimer K a., Cohen MN. Use of Virtual Surgery and Stereolithography-Guided Osteotomy for Mandibular Reconstruction with the Free Fibula. *Plast Reconstr Surg.* 2011;128(5):1080-1084. doi:10.1097/PRS.0b013e31822b6723.
 13. Leong J-L, Batra PS, Citardi MJ. CT-MR image fusion for the management of skull base lesions. *Otolaryngol Head Neck Surg.* 2006;134(5):868-876. doi:10.1016/j.otohns.2005.11.015.
 14. Wong KC, Kumta SM, Antonio GE, Tse LF. Image fusion for computer-assisted bone tumor surgery. *Clin Orthop Relat Res.* 2008;466(10):2533-2541. doi:10.1007/s11999-008-0374-5.
 15. Zhang WB, Wang Y, Liu XJ, et al. Reconstruction of maxillary defects with free fibula flap assisted by computer techniques. *J Cranio-Maxillofacial Surg.* 2015;43(5):630-636. doi:10.1016/j.jcms.2015.03.007.
 16. Tsai MJ, Wu CT. Study of mandible reconstruction using a fibula flap with application of additive manufacturing technology. *Biomed Eng Online.* 2014;13(1):57. doi:10.1186/1475-925x-13-57.
 17. Schepers RH, Raghoobar GM, Vissink A, et al. Accuracy of fibula reconstruction using patient-specific CAD/CAM reconstruction plates and dental implants: A new modality for functional reconstruction of mandibular defects. *J Craniomaxillofac Surg.* 2015;43(5):649-657. doi:10.1016/j.jcms.2015.03.015.
 18. Shu D, Liu X, Guo B, Ran W, Liao X, Zhang Y. Accuracy of using computer-aided rapid prototyping templates for mandible reconstruction with an iliac crest graft. *World J Surg Oncol.* 2014;12(1):190. doi:10.1186/1477-7819-12-190.
 19. Ritacco LE, Milano FE, Farfalli GL, Ayerza M a., Muscolo DL, Aponte-Tinao L a. Accuracy of 3-D Planning and Navigation in Bone Tumor Resection. *Orthopedics.* 2013;36(7):e942-e950. doi:10.3928/01477447-20130624-27.
 20. Soule WC, Fisher LH. Mandibular Fracture Imaging. Medscape. <http://emedicine.medscape.com/articl>

- e/391549-overview. Published 2015.
21. Kim MG, Lee ST, Park JY, Choi SW. Reconstruction with fibular osteocutaneous free flap in patients with mandibular osteoradionecrosis. 2015. doi:10.1186/s40902-015-0007-3.
 22. Chronopoulos A, Zarra T, Tröltzsch M, Mahaini S, Ehrenfeld M, Otto S. Osteoradionecrosis of the mandible: A ten year single-center retrospective study. *J Cranio-Maxillofacial Surg.* 2015;43(6):837-846. doi:10.1016/j.jcms.2015.03.024.
 23. Lin C-H, Kang C-J, Tsao C-K, et al. Priority of Fibular Reconstruction in Patients with Oral Cavity Cancer Undergoing Segmental Mandibulectomy. *PLoS One.* 2014;9(4):e94315. doi:10.1371/journal.pone.0094315.
 24. Gardner DG, Pecak a M. The treatment of ameloblastoma based on pathologic and anatomic principles. *Cancer.* 1980;46(11):2514-2519. doi:10.1002/1097-0142(19801201)46:11<2514::AID-CNCR2820461133>3.0.CO;2-9.
 25. Matsushita Y, Yanamoto S, Yamada S, et al. Correlation between degree of bone invasion and prognosis in carcinoma of the mandibular gingiva: Soft tissue classification based on UICC classification. *J Oral Maxillofac Surgery, Med Pathol.* 2015;27(5):631-636. doi:10.1016/j.ajoms.2014.12.002.
 26. Lam KH, Lam LK, Ho CM, Wei WI. Mandibular invasion in carcinoma of the lower alveolus. *Am J Otolaryngol - Head Neck Med Surg.* 1999;20(5):267-272. doi:10.1016/S0196-0709(99)90026-1.
 27. Shan X-F, Li R-H, Lu X-G, Cai Z-G, Zhang J, Zhang J-G. Fibular Free Flap Reconstruction for the Management of Advanced Bilateral Mandibular Osteoradionecrosis. *J Craniofac Surg.* 2015;26(2):1. doi:10.1097/SCS.0000000000001391.
 28. Lee M, Chin RY, Eslick GD, Sritharan N, Paramaesvaran S. Outcomes of microvascular free flap reconstruction for mandibular osteoradionecrosis: A systematic review. *J Cranio-Maxillofacial Surg.* 2015. doi:10.1016/j.jcms.2015.03.006.
 29. Metzler P, Geiger EJ, Alcon A, Ma X, Steinbacher DM. Three-Dimensional Virtual Surgery Accuracy for Free Fibula Mandibular Reconstruction: Planned Versus Actual Results. *J Oral Maxillofac Surg.* 2014;72(12):2601-2612. doi:10.1016/j.joms.2014.07.024.
 30. Cornelius C-P, Smolka W, Giessler G a., Wilde F, Probst F a. Patient-specific reconstruction plates are the missing link in computer-assisted mandibular reconstruction: a showcase for technical description. *J Cranio-Maxillofacial Surg.* 2015;43(5):624-629. doi:10.1016/j.jcms.2015.02.016.
 31. So TYC, Lam Y-L, Mak K-L. Computer-assisted Navigation in Bone Tumor Surgery: Seamless Workflow Model and Evolution of Technique. *Clin Orthop Relat Res.* 2010;468(11):2985-2991. doi:10.1007/s11999-010-1465-7.
 32. Chan HHL, Siewerdsen JH, Vescan A, Daly MJ, Prisman E, Irish JC. 3D Rapid Prototyping for Otolaryngology — Head and Neck Surgery: Applications in Image-Guidance , Surgical Simulation and Patient-Specific Modeling. 2015:1-18. doi:10.1371/journal.pone.0136370.
 33. Coppen C, Weijs W, Bergé SJ, Maal TJJ. Oromandibular reconstruction using 3D planned triple template method. *J Oral Maxillofac Surg.* 2013;71(8):243-247. doi:10.1016/j.joms.2013.03.004.
 34. Hanasono MM, Skoracki RJ. Computer-assisted design and rapid prototype modeling in microvascular mandible reconstruction. *Laryngoscope.* 2013;123(3):597-604. doi:10.1002/lary.23717.
 35. Huang J-W, Shan X-F, Lu X-G, Cai Z-G. Preliminary clinic study on computer assisted mandibular reconstruction: the positive role of surgical navigation technique. *Maxillofac Plast Reconstr Surg.* 2015;37(1):20. doi:10.1186/s40902-015-0017-1.

36. Yu H, Wang X, Zhang S, Zhang L, Xin P, Shen SG. Navigation-guided en bloc resection and defect reconstruction of craniomaxillary bony tumours. *Int J Oral Maxillofac Surg.* 2013;42(11):1409-1413. doi:10.1016/j.ijom.2013.05.011.
37. Rutala WA, Ph D, Weber DJ. Guideline for Disinfection and Sterilization in Healthcare Facilities , 2008. *Centers Dis Control Prev.* 2008;1-158. doi:10.1086/423182.
38. Braunn. *Aesculap Power Systems Burrs & Blades Katalog.*; 2009. <http://webcache.googleusercontent.com/search?q=cache:43hpXzLDJSwJ:www.veterinary-instrumentation.co.uk/skin1/admin/UserFiles/File/JS-PDF/BRAESBUR.pdf+&cd=1&hl=nl&ct=link&gl=nl>.
39. Hollenbeck K, Allin T, Poel M Van Der. Dental Lab 3D Scanners – How they work and what works best. 2012;(January):1-5.
40. Leiggener CS, Krol Z, Gawelin P, Buitrago-Télez CH, Zeilhofer H-F, Hirsch J-M. A computer-based comparative quantitative analysis of surgical outcome of mandibular reconstructions with free fibula microvascular flaps. *J Plast Surg Hand Surg.* 2014;6764(April):1-7. doi:10.3109/2000656X.2014.920711.
41. Cartiaux O. Computer-Assisted and Robot-Assisted Technologies to Improve Bone-Cutting Accuracy When Integrated with a Freehand Process Using an Oscillating Saw. *J Bone Jt Surg.* 2010;92(11):2076. doi:10.2106/JBJS.I.00457.
42. Misch CE. *Rationale for Dental Implants.* Second Edi. Elsevier Inc.; 2014. doi:10.1016/B978-0-323-07845-0.00001-4.
43. Beaty NB, Le TT. Mandibular thickness measurements in young dentate adults. *Arch Otolaryngol Head Neck Surg.* 2009;135(9):920-923. doi:10.1001/archoto.2009.109.
44. Flanagan D. A Comparison of Facial and Lingual Cortical Thicknesses in Edentulous Maxillary and Mandibular Sites Measured on Computerized Tomograms. *J Oral Implantol.* 2008;34(5):256-258. doi:10.1563/0.915.1.
45. Sağlam AA. The vertical heights of maxillary and mandibular bones in panoramic radiographs of dentate and edentulous subjects. *Quintessence Int.* 2002;33(6):433-438. <http://www.ncbi.nlm.nih.gov/pubmed/12073723>.
46. Ide Y, Matsunaga S, Harris J, O 'connell D, Seikaly H, Wolfaardt J. Anatomical examination of the fibula: digital imaging study for osseointegrated implant installation. *J Otolaryngol - Head Neck Surg.* 2015:1-8. doi:10.1186/s40463-015-0055-9.
47. Oceanz your 3D printing professional. Medisch 3D printen. <http://www.oceanz.eu/branches/medisch>. Published 2016.
48. Cartiaux O, Paul L, Docquier PL, et al. Accuracy in planar cutting of bones: an ISO-based evaluation. *Int J Med Robot.* 2009;5(1):77-84. doi:10.1002/rcs.237.
49. Baek K-W, Deibel W, Marinov D, et al. Clinical applicability of robot-guided contact-free laser osteotomy in cranio-maxillo-facial surgery: in-vitro simulation and in-vivo surgery in minipig mandibles. *Br J Oral Maxillofac Surg.* 2015:1-6. doi:10.1016/j.bjoms.2015.07.019.
50. Stopp S, Deppe H, Lueth T. A new concept for navigated laser surgery. *Lasers Med Sci.* 2008;23(3):261-266. doi:10.1007/s10103-007-0476-4.
51. Stübinger S, Kober C, Zeilhofer H-F, Sader R. Er:YAG laser osteotomy based on refined computer-assisted presurgical planning: first clinical experience in oral surgery. *Photomed Laser Surg.* 2007;25(1):3-7. doi:10.1089/pho.2006.2005.
52. Horta R, Costa J, Valenc R, Amarante JM.

- ALT chimeric flap associated to a dura mater biomatrix substitute for severe desfigurative mandible osteoradionecrosis and deficient bone consolidation after a free fibula flap. 2014;52:3-5. doi:10.1016/j.bjoms.2014.01.024.
53. Mehra M, Somohano T, Choi M. Mandibular fibular graft reconstruction with CAD/CAM technology: A clinical report and literature review. *J Prosthet Dent*. 2015;1-6. doi:10.1016/j.prosdent.2015.05.012.
 54. Lyons A, Ghazali N. Osteoradionecrosis of the jaws: current understanding of its pathophysiology and treatment. *Br J Oral Maxillofac Surg*. 2008;46(8):653-660. doi:10.1016/j.bjoms.2008.04.006.
 55. Kildal M, Wei F-C, Chang Y-M, Huang W-C, Chang K-J. Reconstruction of bilateral extensive composite mandibular defects after osteoradionecrosis with two fibular osteoseptocutaneous free flaps. *Plast Reconstr Surg*. 2001;108(4):963-967. doi:10.1097/00006534-200109150-00022.
 56. Weitz J, Kreutzer K, Bauer FJM, Wolff K-D, Nobis C-P, Kesting MR. Sandwich flaps as a feasible solution for the management of huge mandibular composite tissue defects. *J Cranio-Maxillofacial Surg*. 2015;43(9):1769-1775. doi:10.1016/j.jcms.2015.07.038.
 57. Babu N. Unicystic Ameloblastoma of Mandible Treated with an Innovative Approach: A Clinical Case Report. *J Clin Diagnostic Res*. 2015;9(7):11-13. doi:10.7860/JCDR/2015/13908.6177.
 58. Knoll W-D, Gaida A, Maurer P. Analysis of mechanical stress in reconstruction plates for bridging mandibular angle defects. *J Cranio-Maxillofacial Surg*. 2006;34(4):201-209. doi:10.1016/j.jcms.2006.01.004.
 59. Yamaguchi S, Nagasawa H, Suzuki T, et al. Sarcomas of the oral and maxillofacial region: a review of 32 cases in 25 years. *Clin Oral Invest*. 2004;8(2):52-55. doi:10.1007/s00784-003-0233-4.
 60. Hawrot A, Alam M, Ratner D. Squamous cell carcinoma. *Curr Probl Dermatol*. 2003;15(3):91-133. doi:10.1016/S1040-0486(03)00039-5.
 61. Wong KC, Kumta SM, Sze KY, Wong CM. Use of a patient-specific CAD/CAM surgical jig in extremity bone tumor resection and custom prosthetic reconstruction. *Comput Aided Surg*. 2012;17(6):284-293. doi:10.3109/10929088.2012.725771.
 62. Markiewicz MR, Bell RB, Bui TG, et al. Survival of microvascular free flaps in mandibular reconstruction: A systematic review and meta-analysis. *Microsurgery*. 2015;30(3):242-248. doi:10.1002/micr.
 63. Mazzoni S, Bianchi A, Schiariti G, Badiali G, Marchetti C. Computer-Aided Design and Computer-Aided Manufacturing Cutting Guides and Customized Titanium Plates Are Useful in Upper Maxilla Waferless Repositioning. *J Oral Maxillofac Surg*. 2015;73(4):701-707. doi:10.1016/j.joms.2014.10.028.
 64. Tarsitano A, Ciocca L, Ciprani R, Scotti R MC. Mandibular reconstruction using fibula free flap harvested using a customised cutting guide : how we do it. *Clin Tech Technol*. 2015;35:198-201.
 65. Liu Y, Xu L, Zhu H, Liu SS-Y. Technical procedures for template-guided surgery for mandibular reconstruction based on digital design and manufacturing. *Biomed Eng Online*. 2014;13(1):63. doi:10.1186/1475-925X-13-63.
 66. Zheng G Sen, Su YX, Liao GQ, Liu HC, Zhang SE, Liang LZ. Mandibular reconstruction assisted by preoperative simulation and accurate transferring templates: Preliminary report of clinical application. *J Oral Maxillofac Surg*. 2013;71(9):1613-1618. doi:10.1016/j.joms.2013.02.018.
 67. Sternheim A, Daly M, Qiu J, et al. Navigated Pelvic Osteotomy and Tumor Resection. *J Bone Jt Surg*. 2015;97:40-46.
 68. Gouin F, Paul L, Odri GA, Cartiaux O.

- Computer-Assisted Planning and Patient-Specific Instruments for Bone Tumor Resection within the Pelvis: A Series of 11 Patients. *Sarcoma*. 2014;2014:842709. doi:10.1155/2014/842709.
69. Weijs W, Coppen C. Research subject. 2016.
 70. NextDent B.V. NextDent SG (Surgical Guide). <http://nextdent.com/products/sg-surgical-guide/>. Published 2016.
 71. Vertex Dental. NextDent 3D printing materials. 2014;23:1-6. <http://nextdent.com/wp-content/uploads/2014/10/Safety-Data-Sheet-NextDent-Materials.pdf>.
 72. Martin GmbH & Co. KG. Septumlevatorium Roger. <http://www.klsmartin.com/catalog/de/article/37/Periostelevatorien/>. Published 2015.
 73. Matros E, Santamaria E, Cordeiro PG, Cam CAD. Standardized Templates for Shaping the Fibula Free Flap in Mandible Reconstruction. 2013.
 74. Olayemi AB. Assessment and determination of human mandibular and dental arch profiles in subjects with lower third molar impaction in Port Harcourt, Nigeria. *Ann Maxillofac Surg*. 2011;1(2):126-130. doi:10.4103/2231-0746.92775.
 75. Tie Y, Wang DM, Ji T, Wang CT, Zhang CP. Three-dimensional finite-element analysis investigating the biomechanical effects of human mandibular reconstruction with autogenous bone grafts. *J Cranio-Maxillofacial Surg*. 2006;34(5):290-298. doi:10.1016/j.jcms.2006.03.004.
 76. Ma L, Zhou Y, Zhang Y, et al. Biomechanical Effects of Masticatory Muscles on Human Mandible After Reconstructed Mandibulectomy Tumor. *J Craniofac Surg*. 2015:1563-3732. doi:10.1097/SCS.0000000000000840.
 77. Ji T, Tie Y, Wang D, Zhang C. Three-dimensional finite element analysis of the mandible reconstruction with fibula. *West China J Stomatol*. 2009;27(2):7-10.
 78. Mertens C, Decker C, Engel M, Sander A, Hoffmann J, Freier K. Early bone resorption of free microvascular reanastomized bone grafts for mandibular reconstruction - A comparison of iliac crest and fibula grafts. *J Cranio-Maxillofacial Surg*. 2014;42(5):217-223. doi:10.1016/j.jcms.2013.08.010.
 79. Makiguchi T, Yokoo S, Hashikawa K, Miyazaki H, Terashi H. Evaluation of bone height of the free fibula flap in mandible reconstruction. *J Craniofac Surg*. 2015;26(3):673-676. doi:10.1097/SCS.0000000000001509.
 80. Elsevier, Netter FH. Teeth: Surfaces of a Tooth. Elsevier. <https://www.netterimages.com/teeth-surfaces-of-a-tooth-labeled-norton-1e-dentistry-dental-hygiene-frank-kip-11813.html>. Published 2016.
 81. Ural Ç, Bereket C, Şener I, Aktan AM, Akpınar YZ. Bone height measurement of maxillary and mandibular bones in panoramic radiographs of edentulous patients. *J Clin Exp Dent*. 2011;3(1):5-9. doi:10.4317/jced.3.e5.
 82. Klatzky RL, Lederman S, Reed C. Haptic Integration of Object Properties : Texture , Hardness , and Planar Contour. 1989;15:45-57.
 83. Bholat OS, Haluck RS, Murray WB, Gorman PJ, Krummel TM. Tactile feedback is present during minimally invasive surgery. *J Am Coll Surg*. 1999;189(4):349-355. doi:10.1016/S1072-7515(99)00184-2.
 84. Pinzon D, Byrns S, Zheng B. Prevailing Trends in Haptic Feedback Simulation for Minimally Invasive Surgery. *Surg Innov*. 2016. doi:10.1177/1553350616628680.
 85. Maxim integrated products inc. Sterilization Methods and Their Impact on Medical Devices Containing Electronics. <https://www.maximintegrated.com/en>

- /app-notes/index.mvp/id/5068.
Published 2011.
86. Patel M. *MEDICAL STERILIZATION METHODS*; 2003.
<https://www.digikey.com/WebExport/SupplierContent/lemo-1124/pdf/lemo-rf-medical-steril.pdf?redirected=1>.
 87. Wang K. The use of titanium for medical applications in the USA. *Mater Sci Eng A*. 1996;213(1-2):134-137.
doi:10.1016/0921-5093(96)10243-4.
 88. Pacific Research Laboratories. Sawbones.
[http://www.sawbones.com/Catalog/Biomechanical/Biomechanical Test Materials](http://www.sawbones.com/Catalog/Biomechanical/BiomechanicalTestMaterials). Published 2013.
 89. Sawbones. Catalogue biomechanical testmaterials. In: Pacific Research Laboratories, Inc; 2014.
http://www.sawbones.com/UserFiles/Docs/biomechanical_catalog.pdf.
 90. De Waard O, Baan F, Verhamme L, Breuning H, Kuijpers-Jagtman AM, Maal T. A novel method for fusion of intra-oral scans and cone-beam computed tomography scans for orthognathic surgery planning. *J Cranio-Maxillofacial Surg*. 2016;44(2):160-166.
doi:10.1016/j.jcms.2015.11.017.
 91. Field A, Hole G. *How to Design and Report Experiments*. London: SAGE Publications; 2003.
 92. Spinelli G, Lazzeri D, Conti M, Agostini T, Mannelli G. Comparison of piezosurgery and traditional saw in bimaxillary orthognathic surgery. *J Cranio-Maxillofacial Surg*. 2014;42(7):1211-1220. doi:10.1016/j.jcms.2014.02.011.
 93. Baek K, Deibel W, Marinov D, et al. A comparative investigation of bone surface after cutting with mechanical tools and Er:YAG laser. *Lasers Surg Med*. 2015;432(February):n/a-n/a.
doi:10.1002/lsm.22352.

Appendix A: Background

A.1. Anatomical background

The mandible, known as the lower jaw, is a u-shaped bone that can be divided into eight regions (Fig. 1) The condyle, coronoid process and mandibular notch are part of the temporomandibular joint (TMJ). The TMJ connects the mandible to the maxilla. The muscles and ligaments that are attached to both jaws help maintaining space within the oral cavity to allow smooth and coordinated mouth movements.² Muscles such as the masseter, temporalis and both lateral and medial pterygoid are responsible for opening and closing of the mouth, while the ligaments keep the movements between limits. A synchronous interaction between those muscles, saliva, and the TMJ enables speech, swallowing, breathing, tongue functioning and mastication.³

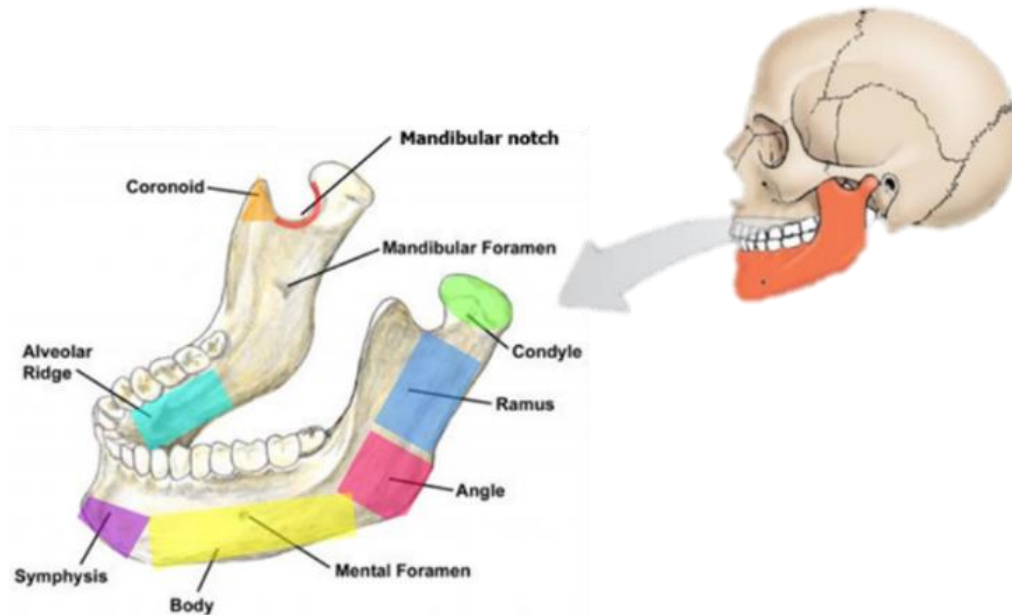


Figure 1. Basic anatomy of the mandible, with eight different regions indicated by eight different colors.²⁰

A.2. Clinical background

On a yearly basis in the Netherlands, 400 patients are diagnosed with throat cancer, 700 patients with cancer of the oral cavity, and 200 patients with cancer of the lip.¹ Most common pathologic indications for mandibulectomy are squamous cell carcinoma (SCC) and carcinoma. SCC is a type of skin cancer that can have multiple triggers and may invade into the mandibular gingiva. This pathology has an overall survival rate of 44% after 5 years, due to uncontrollable recurrence and distant metastasis. Mandibular carcinoma is the main cause of mandible tumor growth. It originates from the gingiva, and due to the proximity towards the mandible and only a thin layer as major obstacle, they can infiltrate rapidly into the periodontal membrane and destroy the mandible. Furthermore, as a complication of radiotherapy, osteoradionecrosis (ORN) may occur in mandible tissue. ORN tissue is defined as tissue that lacks vitality during three months when no recurring tumor is present and a response of impaired bone healing is detectable.²¹ However, the exact pathophysiology of developing ORN tissue is not known. ORN tissue is assigned to a reaction of acute inflammation, free radical damage and an increased amount of fibroblast activation. As a result, tissue suffers from ischemia and a reduced ability of repair and remodeling of the tissue is detected.^{52–54} Both tumor growth and ORN affected tissue can lead to severe aesthetic deformities and both intra- and extra-oral soft mandibular tissue loss that can lead to mandible exposure, as presented in figure 2.

Besides esthetical problems, mandible functioning will be affected when the mandible suffers from tumor growth or osteoradionecrotic tissue. The bony support is lost, and patients may suffer from airway reduction, speech impairment and mastication problems due to a failure in retaining saliva and having difficulties with swallowing.⁵⁵



Figure 2. Visualization of two types of mandible defects. A) Extra- and intra-oral tissue loss of a patient suffering from osteoradionecrosis.⁵⁶ B) A patient with severe esthetic deformities as a result of osteoradionecrosis.⁵⁵ C) A patient suffering from mandibular tumor growth.⁵⁷ D) A CBCT scan of the same patient as in C, presenting the severe mandibular bone loss as a result of tumor growth.⁵⁷

A.3. Mandibulectomy

In the end, the existing functional problems, esthetical problems, and psychosocial problems will lead to a severely reduced quality of life of the patient.⁵⁸ To treat these patients, mandibulectomy is performed. Within this treatment, the mandible defect is surgically resected (removed) by osteotomy. Tissue types involved within the pathologies are soft tissues, bone, skin, and oral lining. Usually, within this treatment an *en bloc* resection is performed since all types of tissue are affected.⁴

Besides the type of resection, the extent of resection should be adapted to both the amount as well as the type of tissue that is affected. If the defect is small and no bone marrow is affected, marginal mandibulectomy is performed. Thereby, solely a small part of bone, teeth, and adjacent soft tissues are removed, thus continuity of the mandible is maintained.²³ When the defect is larger or also bone marrow is affected, it is supported to perform segmental mandibulectomy.²³ The size of the segment that will be resected is determined by the location and the extent of the defect. Additionally, to provide a sufficient removal of all affected tissue, a safety margin of 10-15 mm around the affected tissue is supported.²⁴⁻²⁶ The safety margin is a measure of minimal distance to the affected tissue and acts as the actual border. It is introduced to allow small deviations of the resecting cut without unnecessarily harming healthy tissue. Without this margin, there will be increased chance on affected tissue residue, which will increase the chance on local recurrence, metastasis or wound complications.^{24-28,59-61}

A.4. Reconstruction

However, removal of a bony segment will not restore facial aesthetics or mandible functioning. To restore occlusal functionality and improve the quality of life of the patient, the existing mandible gap should be reconstructed. This is commonly performed using a vascularized, autogenous fibula graft, since this showed a sufficient reconstruction with a survival rate of 94.8%.⁶² Mandible reconstruction after segmental mandibulectomy consists of three phases. First, a part of the fibula bone, including a vessel and a skin island are harvested from the same patient, after which the fibula will be reshaped manually into a resemblance of the native mandible. Second, the vascularized reshaped graft is disconnected from the fibular blood supply, transferred, and mechanically fixated to the mandibular residue using titanium screws and titanium reconstruction plates. Third, the blood vessel of the fibula graft is reconnected to the mandibular blood supply.³²

Currently, the reconstruction of the mandible is supported by 3D techniques such as Computer Assisted Surgery (CAS), Computer Aided Design (CAD), and Computer Aided Manufacturing (CAM). These 3D techniques enable three-dimensional virtual planning with regard to mandibulectomy and mandible reconstruction prior to surgery. Thereby, there will be a reduced chance on insufficient resection. Moreover, fibula harvesting and segmentation will be accelerated, leading to a reduced operating time and ischemia time. Thereby, risk of infection is reduced and fibula graft and skin flap survival is increased. The whole reconstruction processes, including the 3D processes, is summarized in a six-step approach to provide a clear explanation of the process. The reduced six-step approach consists of:

- 1) Retrieve preoperative scans of the important structures of the patient.
- 2) Diagnose the amount of affected tissue and perform virtual surgery with CAS, including a safety margin.
- 3) Generate a concrete planning for the real surgery using CAM and resulting 3D-printed templates.
- 4) Execution of the real surgery.
- 5) Retrieve a postoperative CBCT scan of the neomandible (reconstructed mandible).
- 6) Assessment of the surgical outcome by an analysis of the correspondence between the virtual plan and the reconstructed situation, and eventually the preoperative situation.

An overview of the process is given in figure 3.

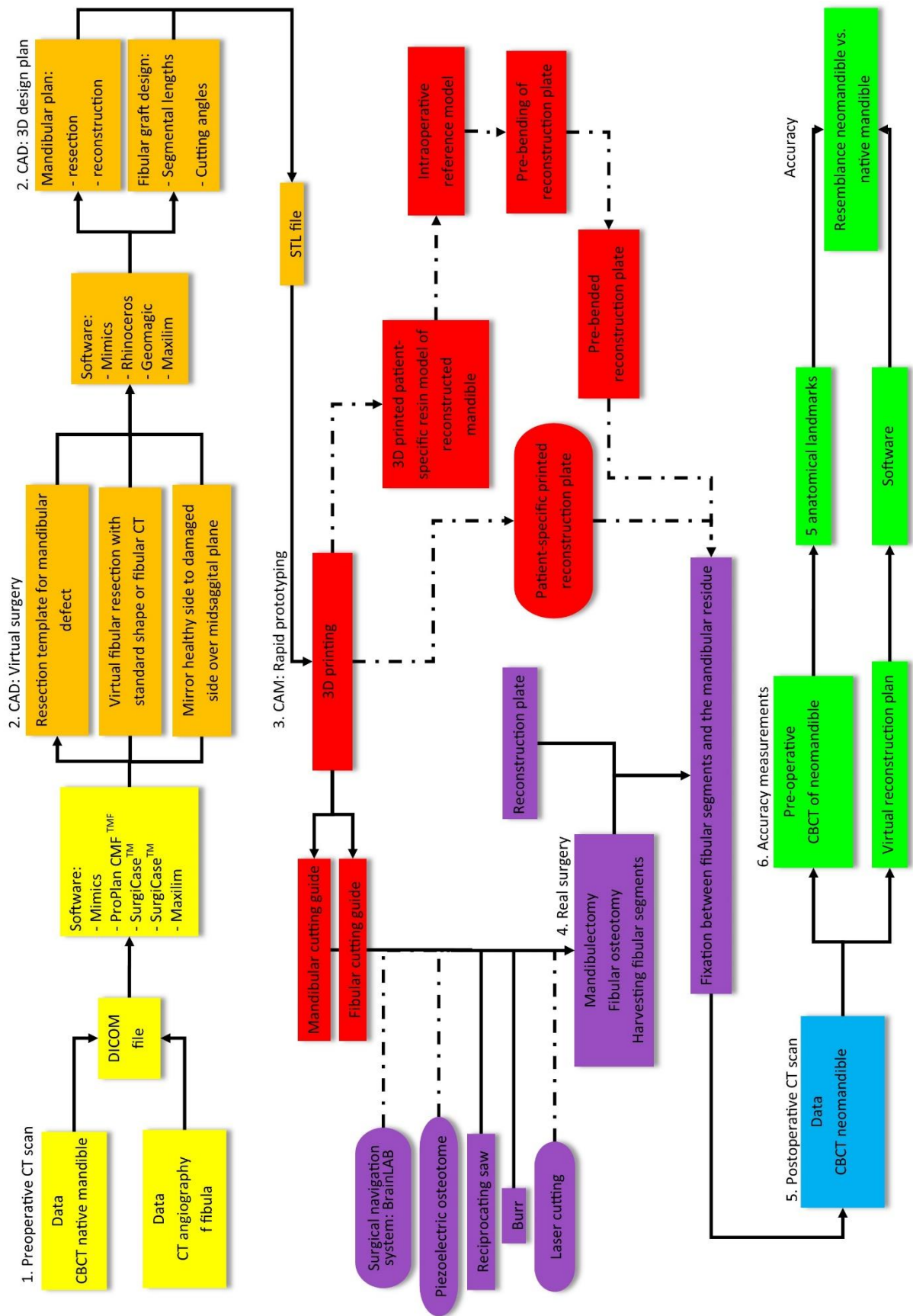


Figure 3. An overview of the steps included in the 3D planning process during mandibulectomy and mandible reconstruction.

A.4.I. Step 1. Preoperative scanning

The 3D-planning process is initiated by performing a high-resolution CBCT (cone-beam computed tomography) scan of the mandible. Additionally, a high-resolution CTA (computed tomography angiography) and an MRI (magnetic resonance imaging) scan of the fibula of the patient are required. The MRI scan image and CTA scan image from the fibula are fused, to obtain an image with both bony details and soft tissue details. The fused image contains information about both the bony structure and three-vessel supply as retrieved from the CTA, as well as soft tissue anatomies including differentiating inflammatory conditions, as retrieved from the MRI. Thereby the surgeon is able to distinguish between tissues such as tumor tissue and scar tissue.¹⁴ This differentiation can be used to determine the extent of tumor invasion, and assists in determining the recommended extent of resection. Additionally, the condition and location of the soft tissues can be detected, to allow an optimal surgical approach.^{30,31}

A.4.II. Step 2. Virtual surgery

The CT-MR fused images can be loaded into computer-aided simulation (CAS) software, to create a three-dimensional model. Simulations can be performed on this 3D model, such as mandible resection and fibular segmentation, to obtain an optimal resection and reconstruction plan. This planning process is known as virtual planning, which is presented in figure 3. Additionally, when the native mandible structure is dramatically distorted due to an invasive disease or late treatment, a mirroring technique is featured by CAS. Within this feature, the healthy side will be mirrored over the midsagittal plane (facial midline) and superimposed on the affected side. This mirrored model can act as base to reconstruct the distorted side.³²

The mandibular resection plan consists of the correct positioning of the osteotomy trajectory on the mandible, to resect the defect. Within the resection plan, a safety margin of 10 to 15 mm with regard to the tumor tissue should be taken into account. The reconstruction plan consists of both the planning for the fibular segmentation, as well as the location of the positioning template with fibula segments and the reconstruction plates.²⁹ Using CAS, fibular segmentation can be simulated. The fibula graft can be segmented virtually into segments with a sufficient size, angle, positioning and interferences between the segments. The segmented parts of the fibula should correspond to resected part of the mandible in terms of size and shape for a sufficient reconstruction. Usually, the number of segments applied ranges between one and three.^{6,10}

Within the same software, these virtual plans can be converted into a designed mandible resection template, a fibula resection template, and a positioning template. The resection templates contain cutting sleeves that match to the either planned segmental mandibulectomy or the planned fibula segmentation. By the positioning template, the fibula segments are forced into the correct order and orientation. Furthermore their fixation is guided by fixation holes in the template.³³

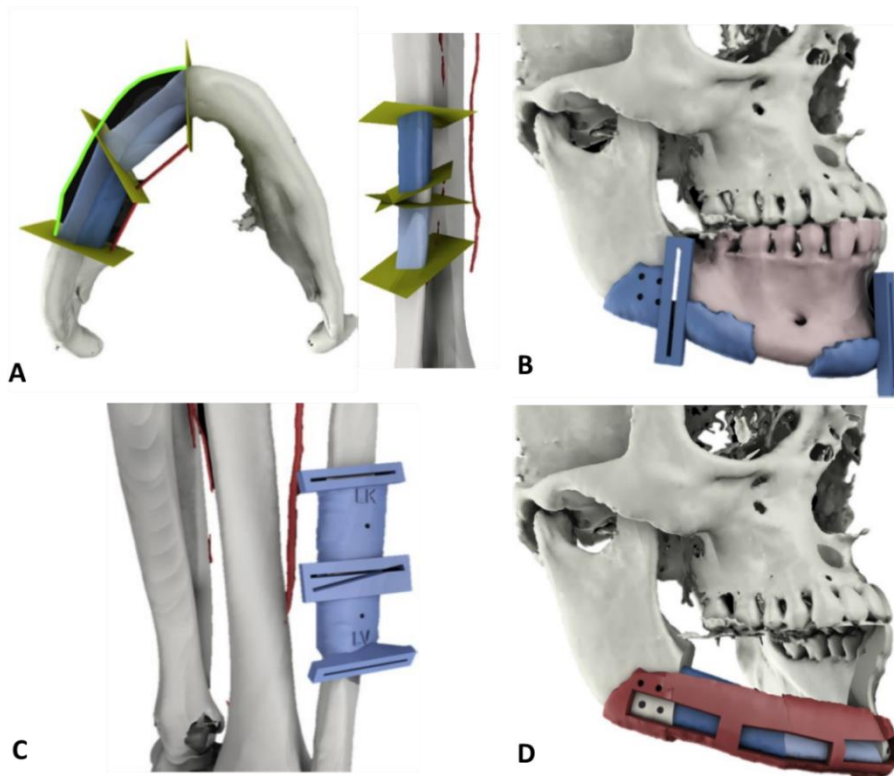


Figure 4. An overview of the virtual planning process for mandible resection and reconstruction. A) The planned mandible resection planes and fibula resection planes for a segmentation that will provide a perfect fit into the mandibular residue, while resembling the native mandible. Notice the presence of the periosteal artery that allows anastomosis with the mandibular residue. B) The resulting virtual mandibular resection template as planned in A. C) The resulting virtual fibular resection template to obtain a correct number of segments with correct sizes and inter angles. D) Virtually planned positioning template to force the correct orientation of the fibula segments and allow internal and external fixation of the fibular segments.³³

A.4.III. Step 3. Manufacturing

The virtually designed templates are saved as stereolithographic files (STL files) that can be loaded into computer-aided manufacturing (CAM) software. Using quick fabrication methods such as 3D-printing, polypropylene templates can be printed. The printed templates serve as transfer from virtual surgery to the operation theatre.^{63,64} (Fig. 4) Ideally, the resection templates are manufactured in such a way that their shape forces the template onto the planned location and orientation during surgery, to resect the bony parts as planned.⁶³ Additionally, a positioning template can be printed, and if requested, a true-to-size reconstructed mandible can be printed. This true-to-size printed reconstructed model can be applied as reference mandible during surgery, to check the correspondence between the planning and the obtained mandible gap, and the reconstructed shape.^{32,34}

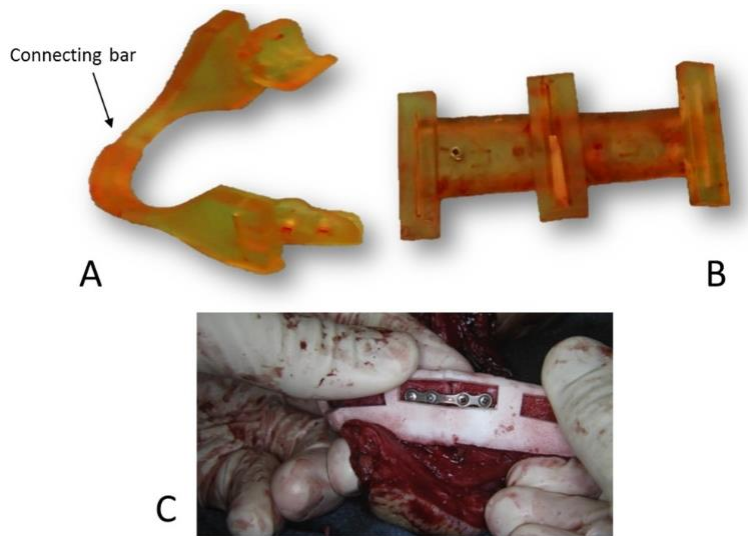


Figure 5. An overview of the different templates that can be manufactured using 3D-printing. A) The mandibular resection template, including a connection bar between the two resection sites, as indicated by the arrow. B) The fibular resection template, containing four resection sleeves, to obtain two fibula segments. C) The positioning template on which the fibula segments are placed. This template contains gaps to allow placement of the mini reconstruction plates and fixate the segments internally.

A.4.IV. Step 4. Real surgery

The real surgery is performed using a two-team approach. One team is responsible for the mandibulectomy, while the other team is responsible for the fibular segmentation. First, the mandible defect is exposed. Simultaneously, a surgical plan for the fibular skin flap is drawn on the patient, and the fibula is exposed. (Fig. 5) Thereby, a sufficient amount of fibula bone is harvested, while 8 cm fibular bone is left in situ on both the distal end as well as on the proximal end of the fibula, to secure a stable donor site.³³ Generally, an amount of fibula bone up to 19 cm is harvested.^{6,10,65}

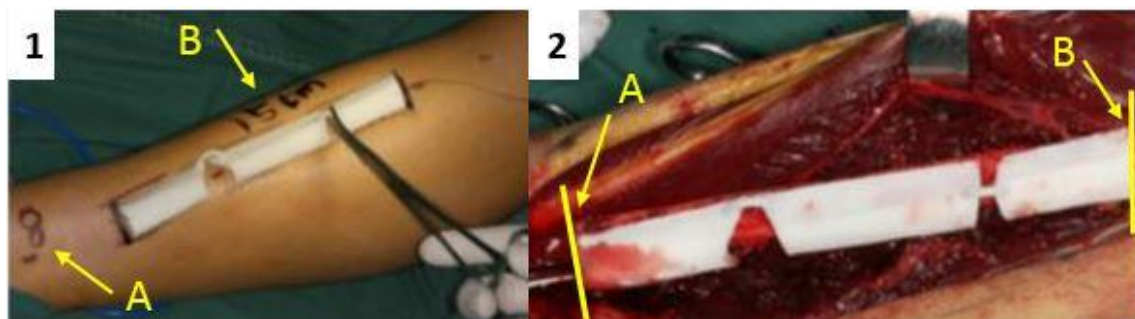


Figure 6. An overview of fibula harvesting during surgery. 1) The surgical plan is drawn on the skin of the patient. At the distal side (A), 8 cm fibular bone will be left in situ to secure a stable ankle joint, and (B) 15 cm donor bone of this patient will be harvested. 2) The fibular bone is exposed and the fibular resection template is in place to act as global cutting border for both the distal (A) and the proximal end(B).⁶⁵

Second, the mandibular resection template is placed on the planned location, where it will be fixated by screws. The location should ideally be secured by the shape of the template, since the shape is fitted to the planned location on the mandible. The mandible defect is resected using a reciprocating saw. The saw will be guided by the cutting sleeves of the resection template. (Fig. 6) The occurring mandibular gap can be matched with the reference mandible or positioning template, to check whether the planned amount is resected or possibly an under- or overresection occurred.

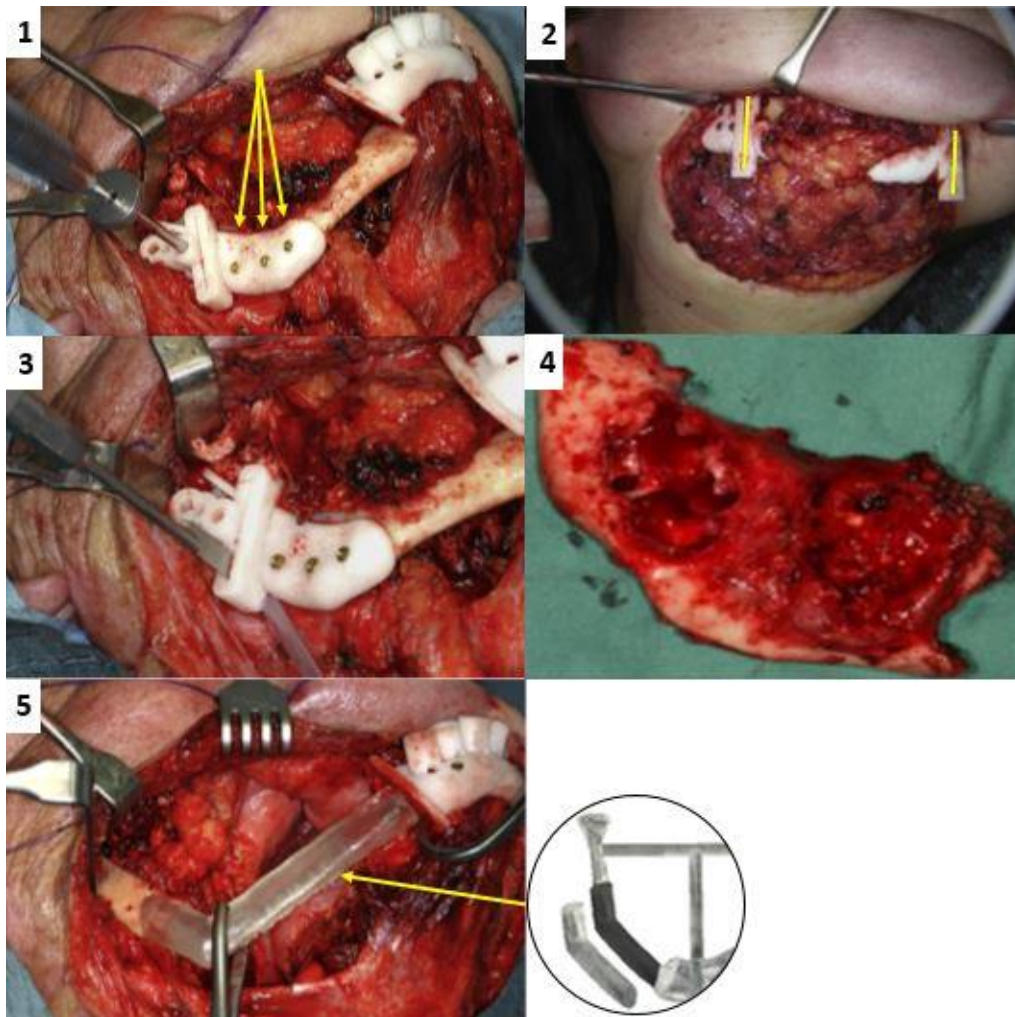


Figure 7. An overview of mandible resection during surgery. 1) The mandibular resection templates will be screwed into place on the exposed mandibular bone. The screws are indicated by yellow arrows. 2) The planned cutting sleeves are indicated by yellow lines. 3) The mandible is resected using an oscillating saw. The cutting sleeves act as guidance. 4) The mandibular resection template is removed, and the mandible defect is taken out. 5) The correspondence between the obtained mandible gap and planned size of the gap is checked by a STL reference model of the reconstructed part of the mandible.^{65,30,33}

When it is confirmed that there is a match between the planned and obtained size of resection, the fibular resection template is placed and fixated to the bone. Once more, segmentation is performed by the reciprocating saw that is guided by the cutting sleeves of the fibular resection template. (Fig. 7) The obtained fibula segments can be placed into the positioning template. The positioning template forces the fibula segments into an order and morphology with dimensions that should fit perfectly into the existing mandible gap.

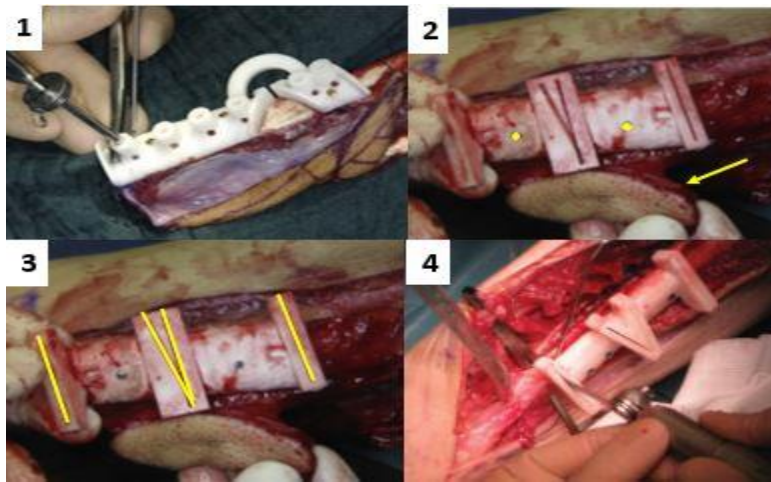


Figure 8. An overview of performing fibular segmentation. 1) A fibular resection template is screwed into place, 2) The prepared skin flap is indicated by the yellow arrow and screws by yellow dots. 3) The cutting sleeves of the resection template are indicated by yellow lines, these allow guidance of the cutting device to obtain the planned segment sizes and angles. 4) Osteotomy is performed by an oscillating saw, which is guided by a cutting sleeve of the resection template.^{10,30,33}

Then, the vascular pedicle of the fibular skin flap is clipped off to allow translocation of the segmented graft. The phenomena of clipping off a vessel through which tissue receives restricted blood supply is known as ischemia. Subsequently, the time between clipping off and connection to another blood supply is known as ischemia time. Quick performance during ischemia is recommended, since a longer ischemia time is associated with bad fibula graft and skin flap survival.²⁹ During ischemia, the positioning template with the fibula segments is translocated to the mandible site, and possible deviations from the planning can be detected. When the fit is sufficient, the fibula segments will be fixated to one another, after which the outer segments are fixated to the mandibular residue. To obtain an adequate mechanical fixation, titanium mini reconstruction plates and screws are used. After fixation of the fibula onto the mandible, anastomosis (connection) is performed between the vascular pedicle of the fibula graft with the mandibular blood supply. This is performed by microscopic surgery with the participation of both surgical teams. As a result, a neomandible is formed that mimics the shape of the native mandible and the functioning is restored.^{33,65,66}

A.4.V. Step 5. Postoperative scanning

After surgery, a new CBCT scan is performed, which can be processed once more by software into a 3D model. This postoperative 3D model of the reconstructed mandible can be registered on the original model of the mandible to check the correspondence between the newly created neomandible and the native mandible. The same methodology can be applied to analyze the match between the obtained neomandible the virtual planned model.

A.4.VI. Step 6. Assessment of surgical outcome

The conventional method to assess the quality of the reconstruction applied easily detectable points on the mandibular bone, known as anatomical landmarks. About five landmarks will be selected on both the preoperative and postoperative CBCT scans. By superimposing the preoperative and postoperative scans and measure horizontal distances between the selected landmarks, accuracy of the reconstruction is retrieved. However, according to the 3D planning method, a more extensive analysis was introduced to assess the surgical outcome. Additional to comparisons with the preoperative scan, the postoperative CBCT scan can be compared to the virtually planned reconstructed mandible within 3D software.^{17,18,34} A three-dimensional model can be converted into a point-cloud model, a surface is divided into an enormous amount of points. Using an iterative closest point (ICP) algorithm to calculate distances between two points of the point-clouds of two models, this software can assess the surgical outcome based on an enormous amount of points instead of just 5 anatomical landmarks.^{34,19}

Appendix B: Problem analysis

B.1 Current treatment

Mandibulectomy and mandible reconstruction are improved by the 3D planning process to guide osteotomy.³⁵ Virtually planned resection of the defect and virtually planned reconstruction will reduce the prevalence and amount of time that is required for trial and error during real surgery.^{29,34} Thereby, the surgical outcome is not solely dependent on intraoperative view, intraoperative decisions, or experience and skills of the surgeon. Using supportive 3D techniques, the quality of surgical outcome depends on the quality of virtual planning, the transfer of the planning to the operation theatre and the surgical skills. Therefore, optimal results can solely be achieved when the virtual process such as an adequate data acquisition (CBCT scanning), software processing and planning, and manufacturing of the templates is optimal.²⁹ To prevent or minimize the chance of introduction and accumulation of errors, leading to a less optimal surgical outcome and quality of life of the patient, it should be pursued that every step of the 3D planning process adds no or minimal bias to the treatment.

However, since the treatment with assisting 3D techniques appeared to be extensive and complex, identification of errors may be difficult. Therefore, to provide a stepwise analysis in the identification of potential errors, the 6-step approach as generated in appendix A was applied during a literature study

According to the registration of CT and MR images during step 1 and step 5 of this process, an error up to 2 mm was found in literature.^{14,13} Additionally, a mean error of 0.13 ± 0.11 mm was found for the transfer of CAS to CAM, as applied during step 2 and step 3.¹⁶

Furthermore, both a literature study and surgical findings have pointed out that during step 4 of the process also contributes to deviations from the planning. During resection and segmentation, small angular deviations occur in spite of guidance through resection templates. The most common applied device for performing osteotomies to resect the mandible defect and segment the fibula, is the reciprocating saw. However, this device perceived the highest cutting deviations. According to the literature study performed, this may be due to the flexibility of the saw blade.⁶⁷

The depth angle of the osteotomy plane, which is referred to as the difference between the planned and obtained trajectory of the saw with respect to the depth of the cut, was found to be $5.43 \pm 4.39^\circ$ (mean \pm SD).⁴¹ Additionally, a mean error of 2.06 ± 0.86 mm (mean \pm SD) between the planned and executed mandibulectomy plane was found, with a maximum deviation of 3.7 mm.¹⁸

These errors may have negative impact on achieving the safety margin, as well as affect the fit of fibular segments into the neomandible. The safety margin is the actual border of a resection. Within this border, a distance about 10 to 15 mm to the affected tissue is taken into account to ensure a sufficient resection towards all affected tissue.²⁵ The safety margin is introduced as safety measure, it allows small deviations in the bone cutting trajectory, without causing additional risks to surrounding tissue. However, the safety margin may still be exceeded when cutting deviations are too large, leading to extensive under- or over resections. Subsequently, this leads to either unnecessary removal of healthy tissue or non-radical removal of affected tissue. When affected tissue is not resected, the recurrence rate will increase.⁶⁸

Besides there will be a higher risk of occurrence, large deviations of the planned osteotomy trajectory may alter the segment length or the inter-angle between segments. Additionally, the fibula segments are placed and fixated manually into the positioning template, after which this is placed and fixed manually into the mandibular residue. Both manual events can easily introduce deviations from the planned orientation of the fibula segments. These deviations from the planned orientation are known as angulations.¹⁷ Angulations of the fibula segments and changes in inter-angles will have impact on the shape and subsequently the functioning of the neomandible.⁴⁰

This was also experienced by the surgeon, since it occurred that the positioning template rendered obsolete during surgery.⁶⁹ (Fig. 1) Surgeon's experience that the prepared fibula segments do not fit in the template, or the segments appear to fit in multiple orientations. Sometimes, the template does not provide a correct fit into the mandible gap. Therefore, the benefits of using CAD/CAM techniques during this treatment may be eliminated. As mentioned before, these benefits are found in an improved surgical outcome, time savings and an increased survival rate of the skin island.

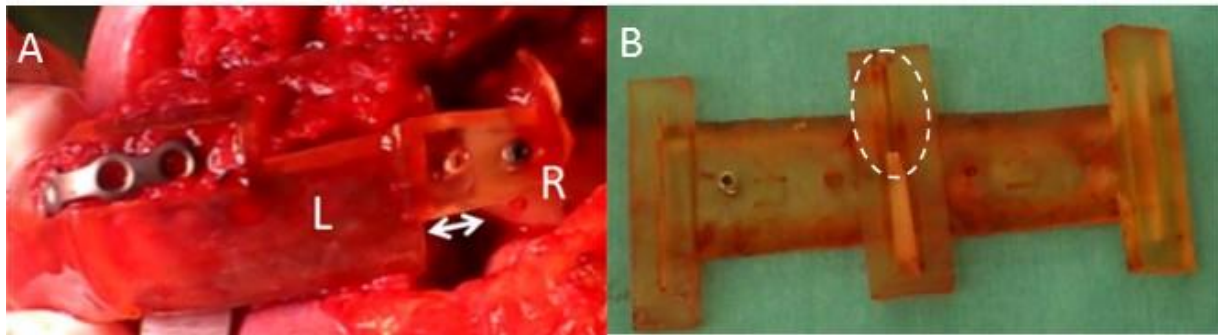


Figure 1. A) An example of a bad fit of a temporally fixated positioning template placed at the intended location. A gap exists between the mandibular residue (R) and the fibula segments (L), as indicated by the arrow. B) An example of a template that was cut through by the reciprocating saw. The top half of the middle sleeve, as indicated by the dashed oval, has been torn down.


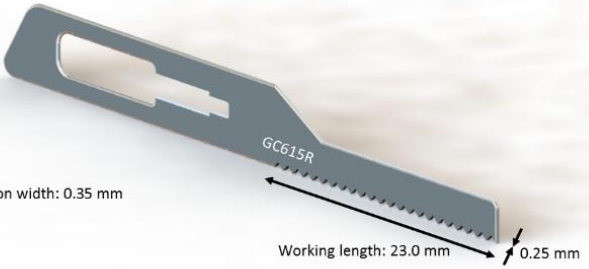
B.2 Current devices

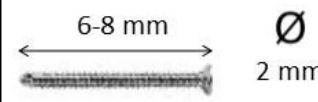
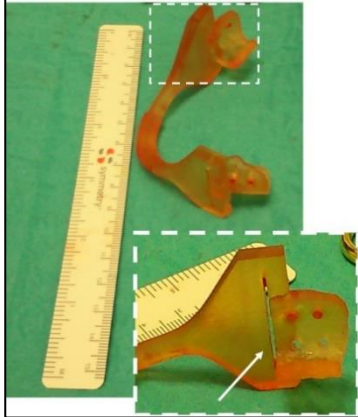
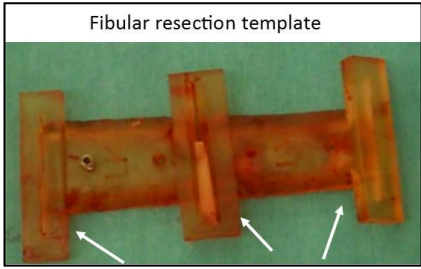
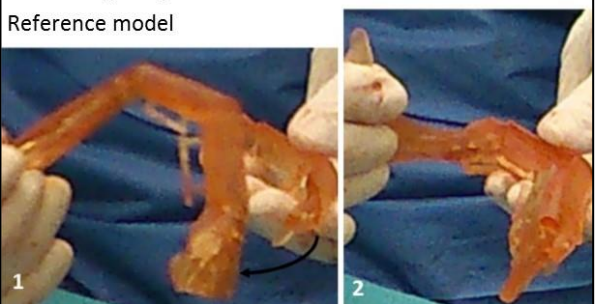
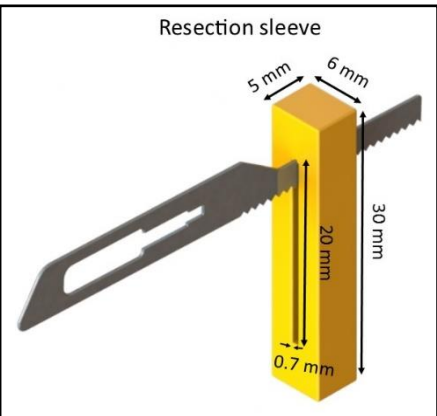
As mentioned before, the aim of this study is to reduce the difference between the planned and the obtained osteotomy trajectory by adjusting the interaction between the currently applied devices and the patient-specific designed and manufactured resection templates.

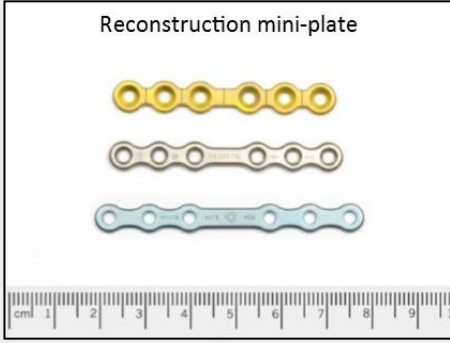
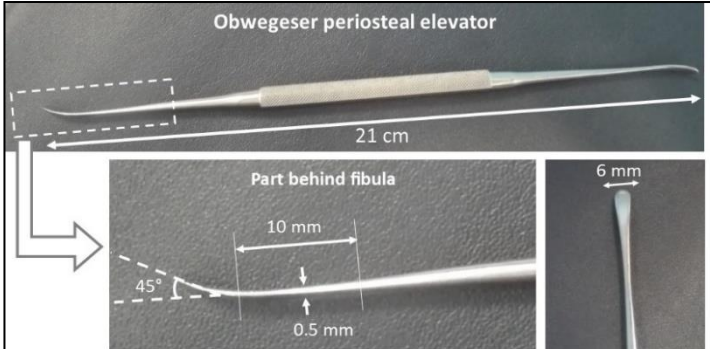
In order to adjust this interaction, the properties of interest with regard to the currently applied devices and templates will be described. According to the planned angles and lengths of the osteotomy and segmentation, patient-specific resection templates will be designed and manufactured. The cutting sleeves of the resection templates have dimensions as presented in table 1.

The surgical instruments that have interaction with the resection templates, and may be of interest, are a periosteal elevator, a reciprocating saw, drill and saw blade from Braunn Aesculap, reconstruction plates, and the connecting screws. (Table 1)

Table 1. Properties of the instruments of interest that are applied during fibula reconstruction.

Instrument	Material	Image (incl. dimensions)
Handpiece	Stainless steel	<p>Braunn Aesculap Microspeed uni handpiece</p>  <p>Speed: 18,000 rpm</p>
Reciprocating saw blade	Stainless steel	<p>Braunn Aesculap reciprocating saw blade</p>  <p>Incision width: 0.35 mm</p> <p>Working length: 23.0 mm</p> <p>0.25 mm</p>

Screw	Titanium	<p>Synthes self-tapping screw</p> 
Resection templates	<p>Nextdent SG: Composition of methacrylic oligomers, colorants, pigments and phosphine oxides ^{70,71}</p> <p>Polyamide: A composition of PA 2200 and PA 12⁴⁷</p>	<p>Mandibular resection template</p>  <p>Fibular resection template</p>  <p>Positioning template Reference model</p>  <p>Resection sleeve</p> 
Reconstruction plate	Titanium	

	 <p>Reconstruction mini-plate</p> <p>Three mini-plates are shown in yellow, silver, and blue. Below them is a ruler showing centimeters from 1 to 9.</p>
<p>Periosteal elevator (modified freer)</p>	<p>Stainless steel ⁷²</p>  <p>Obwegeser periosteal elevator</p> <p>21 cm</p> <p>Part behind fibula</p> <p>10 mm</p> <p>0.5 mm</p> <p>45°</p> <p>6 mm</p>

The currently applied cutting sleeve of the resection template has a width 0.7 mm. The thickness of the currently applied saw blade is 0.25 mm. Therefore, during insertion of the saw blade through the cutting sleeve, angulations up to 5.13° are allowed, as visualized in figure 2. During osteotomy, an angulation of insertion of 5.13° may end up in a deviation from the intended cutting path, as visualized in figure 3. Therefore, it is suggested that the interaction between devices contributes highly to the cutting deviation of 5.43°±4.39° (mean±SD) that was found during the literature study.⁴¹

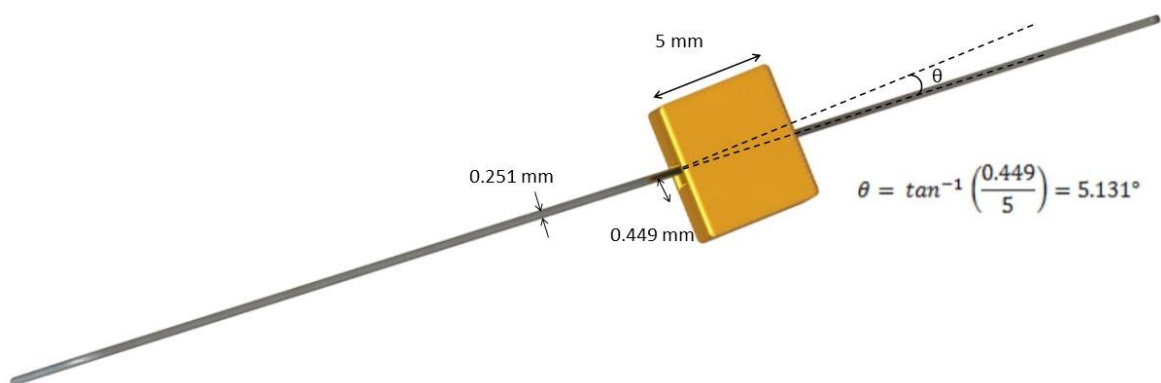


Figure 2. Topview of the maximal angulation of the saw blade into the cutting sleeve allowed by the currently applied dimensions of parts is about 5.13°.

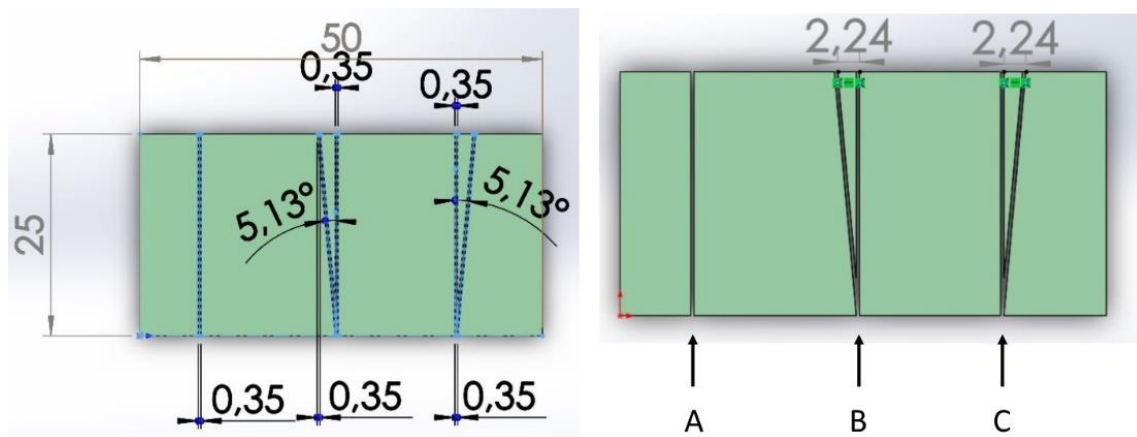


Figure 3. Three different cutting paths in a block with dimensions of 25x50 mm, cut through with a saw blade (cutting width of 0.35 mm, as the current blade)³⁸. Path A) the straight and intended path. Path B) The resulting cutting path after the saw blade perceives a counter-clockwise angulation of 5.13° results in a 2.24 mm distance at the left from the intended path. Path C) The resulting cutting path after the saw blade perceives a clockwise angulation of 5.13° results in a 2.24 mm distance at the right from the intended path.³⁸

B.3 Visualization of a deviated formation of the neomandible

As a result of deviations in the osteotomy trajectory or angulations of the fibula segments for mandible reconstruction, the morphology of the obtained neomandible can be different from the original and virtually planned neomandible. This will have consequences for the functioning of the temporomandibular joint (TMJ).⁴⁰ A clinical example of morphologic deviations between the native mandible and neomandible was found in literature. A difference in pre- and postoperative location and orientation of the mandibular angle due to a bad fit of the fibula segments, is visualized in figure 4. Other deformations of the mandible as a result of mandibular tumor resection and reconstruction with a fibula graft are visualized in figure 5.⁴⁰

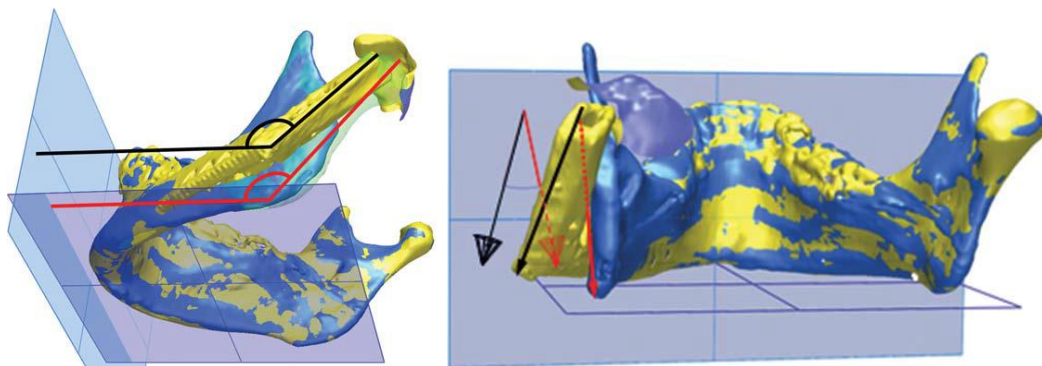


Figure 4. The difference between the native mandibular morphology (blue), and the postoperative reconstructed mandibular morphology (yellow). Left: the lateral view of the mandibular angle, right: the posterior view of the mandibular angle.⁴⁰

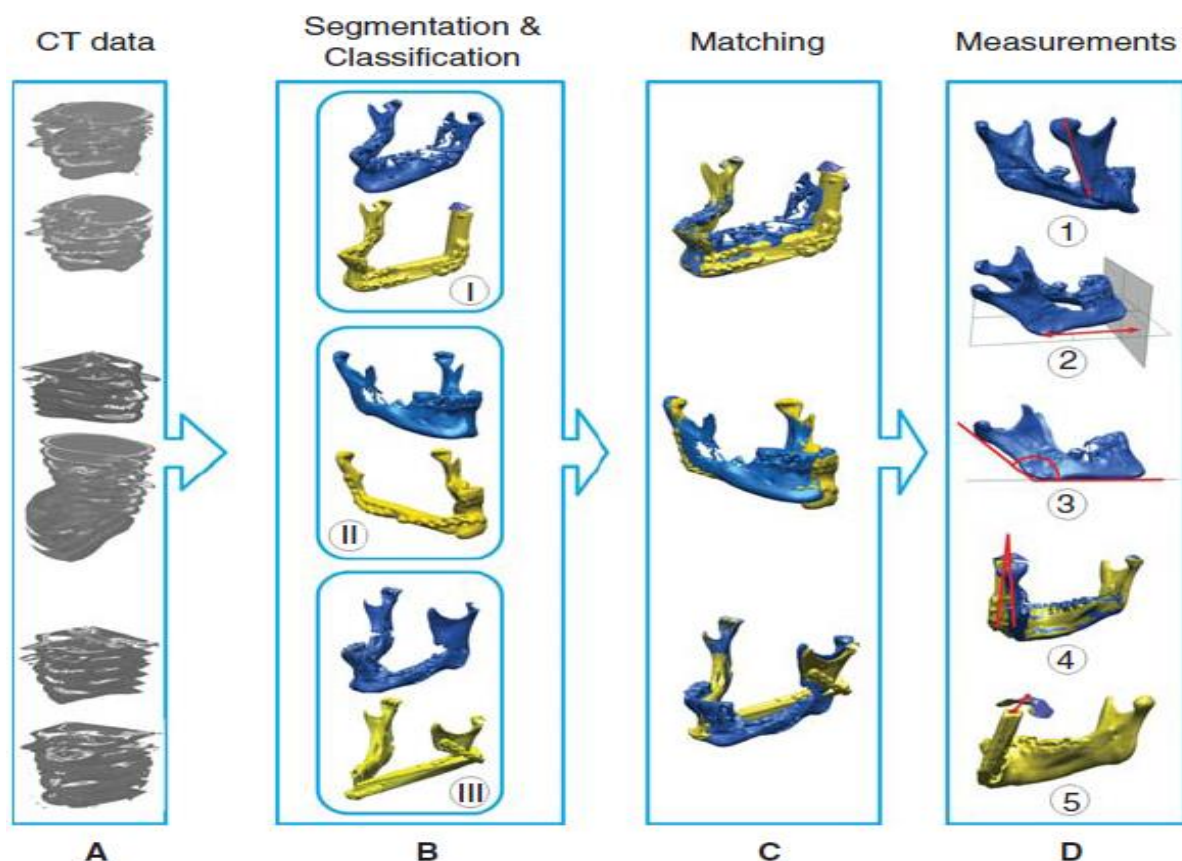


Figure 5. The method applied for the morphologic analysis between the pre-operative and postoperative mandibles that were reconstructed with fibula free flaps. A) The segmentation of CT data. B) The preoperative mandibles (blue) and reconstructed mandibles (yellow) after different types of resections. Type I: large segmental resection, type II: medium segmental resection, type III: small segmental resection. C) Matched preoperative mandibles and postoperative mandibles. D) The five measurements applied: 1. Ascending ramus 2. Horizontal ramus 3. Mandibular angle 4. Deviation of the pre- and postop ascending ramus 5. The shift of the condyle in relation to the fossa.⁴⁰

Table 2. Outcome of the measurements performed during a morphologic analysis of the preoperative and postoperative reconstructed mandibles of six patients that were treated with segmentation II and III (segmental resection).⁴⁰

Performed measurement	Mean \pm SD	Minimum (resection type)	Maximum (resection type)
Ascending ramus preoperative vs postoperative	4.7 mm \pm 4.9 mm	0.4 mm (type II)	14.3 mm (type III)
Horizontal ramus	6.5 mm \pm 4.5 mm	0.6 mm (type I)	14.3 mm (type I)
Lateral view mandibular angle (fig. 3)	5.0° \pm 5.5°	0° (type III)	17.1° (type II)
Posterior view mandibular angle (fig. 3)	9.1° \pm 9.9°	0.2° (type I)	27.3° (type I)
Condyles	10.0 mm \pm 6.0 mm	2.3 mm (type III)	23.4 mm (type I)
Ascending ramus simulated vs postoperative	4.8 mm \pm 6.3 mm	0.1 mm (type I)	21.0 mm (type III)

All mandibles included in this study have shown morphologic deviations. The largest dislocation (10 mm shift) occurred at the condyle when a large segmental resection was performed, where also the condyle was removed. After type II and III segmental resection, a type of resection in which the condyle is maintained, a mean condylar shift of 7.35 mm occurred. (Table 2)⁴⁰

This study is focused on the treatment that applies type II and III segmental resection. To define potential morphologic changes of the mandible as a result of the osteotomy deviations and angulations of the fibula segments, different situations are visualized. Therefore, different initial conditions for the angulation and cutting deviation, as retrieved from literature, are simulated using SolidWorks (SolidWorks Corp. 2015).

The mandibular residue is bound to the condyle, a part of the mandible of which is presumed that it is partially fixated in the TMJ (temporomandibular joint). Thus, when the condyles create the impression that no dislocation has occurred, it will be presumed by the surgeon that the positioning template is in the correct position and the fibula segments are connected to the mandibular residue. Therefore, the mandibular residue, including the condyle, is set as fixed in this simulation. The simulations that are sketched in figure 7 and figure 8 have a cutting deviation of 5.43° as initial condition for the mandible resection and fibular segmentation.^{41,48} Moreover, the fibula perceived two different angulations to the mandibular residue in both directions (clockwise and counterclockwise), as may result from manual placement. The first angulation is 5.3° , since this is found as mean angulation in literature. The second angulation applied in the simulation was chosen to be 9.82° , since this was the SD added to the mean, according to literature.¹⁷

An optimal neomandible was simulated as well to create a reference model that can be used to compare the resulting neomandibles. Distances, angles and thicknesses applied to create the simulated mandibular models are retrieved from literature.^{73,74} To verify that the optimal reconstruction is sufficient, three different views from the optimal model are superimposed on the native, unresected model. (Fig. 6) Simultaneously, the deviated neomandible models are superimposed on the optimal neomandible, to compare the different initial conditions. (Fig. 7, and fig. 8)

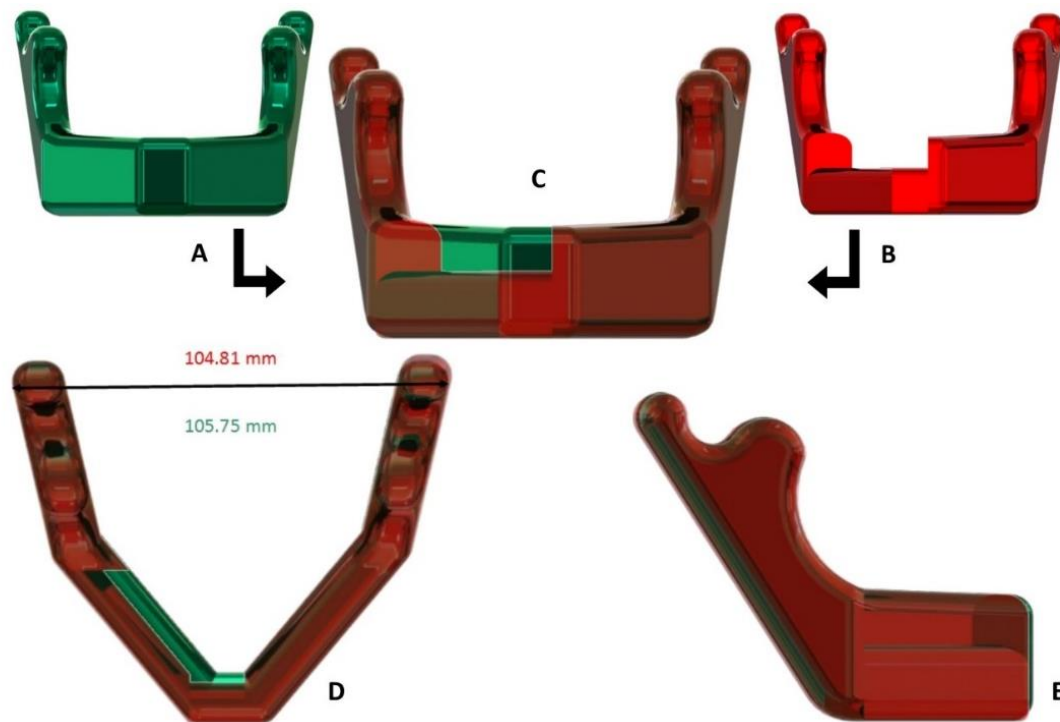


Figure 6. Three schematic views of the original mandible (green) and superimposed reconstructed mandible (red). A) Front view of the original mandible. B) Front view of the optimally reconstructed mandible. C) Front view of the superimposed mandibles. D) Top view of the superimposed mandibles, including the intercondylar distance of the original mandible (green) and the reconstructed mandible (red). E) Side view of the superimposed mandibles.

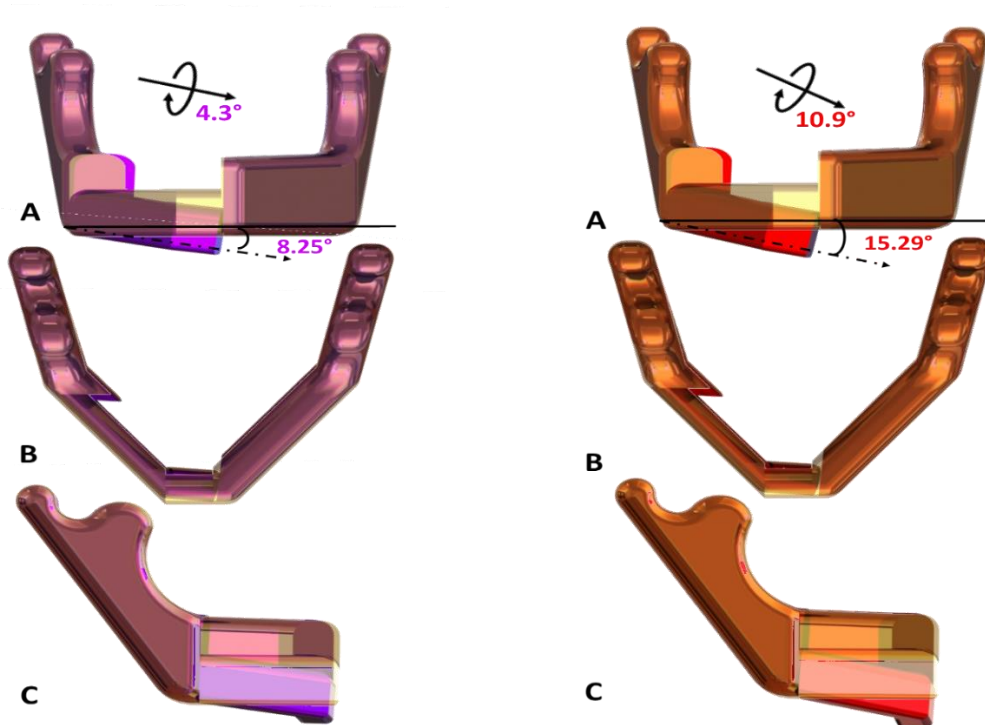


Figure 7. Three schematic views of the optimally reconstructed mandible (red) superimposed on the reconstructed mandible with an angular cutting deviations of 5.43° (purple and red). A) Front view of the superimposed mandibles, including clockwise fibula graft rotations of 5.3° (purple), and 9.82° (red), what will result in rotations of the reconstructed mandibular body of 9.36° and 14.17° respectively. The resulting rotation of the base B) Top view of the superimposed mandibles C) Side view of the superimposed mandibles.

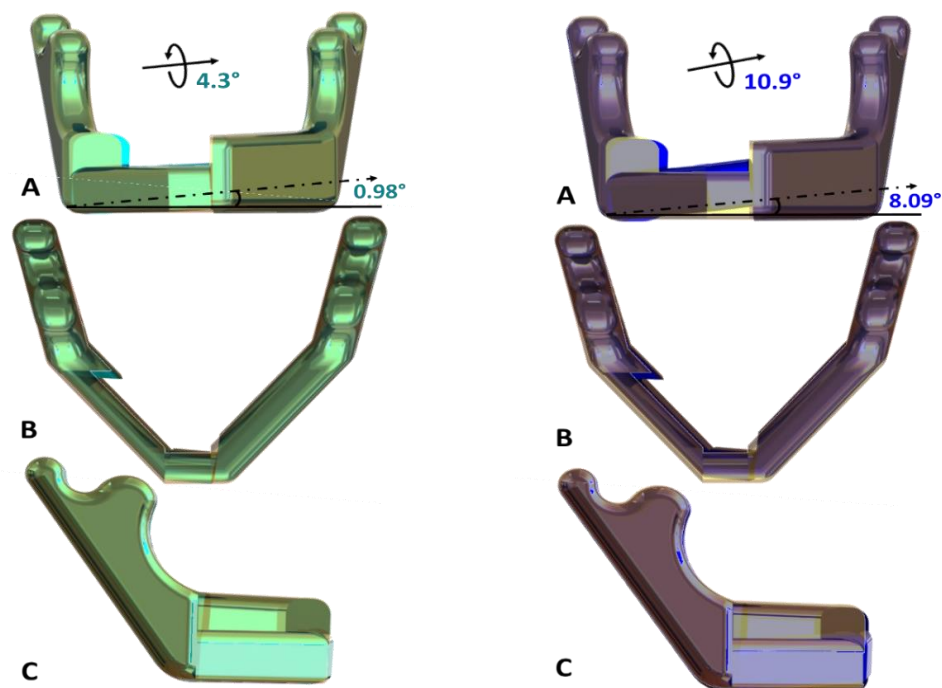


Figure 8. Three schematic views of the optimally reconstructed mandible (red) superimposed on the reconstructed mandible with an angular cutting deviations of 5.43° (green and blue). A) Front view of the superimposed mandibles, including the resulting counter-clockwise fibula graft rotations of 5.3° (green) and 9.82° (blue), what will result in rotations of the reconstructed mandibular body of 2.04° and 6.92° respectively. B) Top view of the superimposed mandibles C) Side view of the superimposed mandibles.

An altered contour shape was perceived for the resulting neomandible in all simulations. The mean angulations with respect to the optimal neomandible are 11.8° and 4.5° ($RMS_c=12.01^\circ$, $RMS_{cc}=5.10^\circ$) for the clockwise and counter-clockwise rotations, respectively. (Figure 7a and 8a) According to this simulation, the altered shape seems more prone to clockwise rotations (fig. 7), than counter-clockwise rotations. (Fig. 8)

Furthermore, the contact area between the fibula graft and mandibular residue can be altered or decreased, this is detectable in figure 7a and 8a. This affects the force transmission over the mandible, as will be discussed in appendix B.4.⁷⁵

B.4 Stress distributions on the (neo-) mandible

Besides direct morphologic changes due to a bad reconstruction, it is of interest what impact the extent of the resection and subsequent reconstruction has on the stress distribution over the mandible.

Ma et al. studied the difference in stress distribution at the condyles between the native mandible and the neomandible, during simulations of opening and closing of the mouth. During mouth closure, maximum Von Mises stress levels at the posterior condyles was 93.87 MPa in the native mandible and 51.91 MPa in the neomandible. Moreover, during mouth opening, Von Mises stress levels at the posterior condyles were 106.28 MPa on the native mandible and 54.30 MPa on the neomandible. Thus, more stress is generated at the condyles during mouth opening, and the amount of stress at the condyles reduced after reconstruction with a fibula graft.⁷⁶

This reduction of stress at the condyles after reconstruction is supported by a study of Ji et al, as presented in table 3. Additionally, they found that the level of resection has impact on both the location of the highest stresses as well as the value of the highest Von Mises stress level. (Fig. 9, table 3)⁷⁷

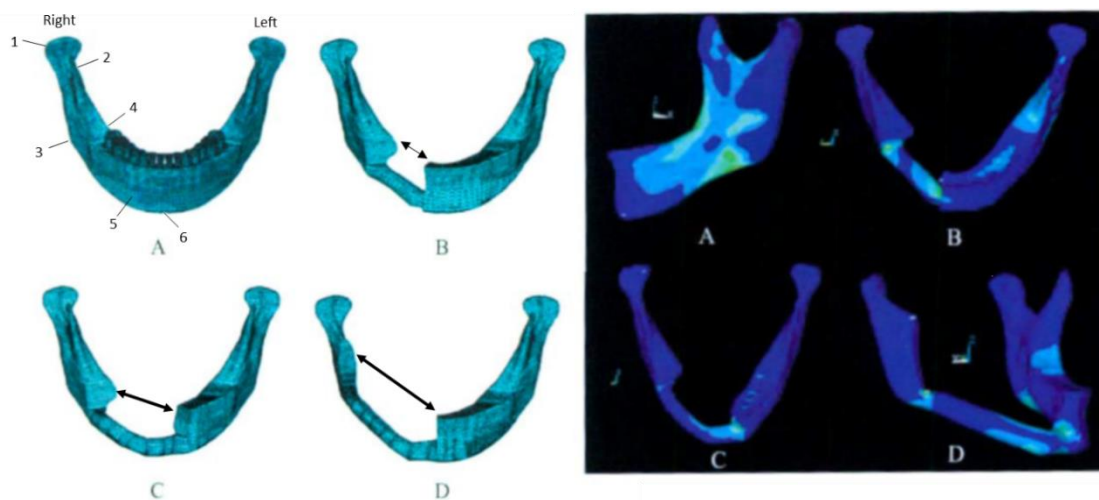


Figure 9. Von Mises stress distribution over the mandible after different extents of segmental resection and reconstruction using a fibula graft. A) A healthy mandible shows highest stresses at region 3. B) A small segmental resection, reconstructed with a fibula graft, shows highest stresses at regions 3 and 5. C) Medium segmental resection, reconstructed with a fibula graft, shows highest stresses at region 5. D) Large segmental resection, reconstructed with a fibula graft, shows highest stresses at regions 5 and 3.⁷⁷

Table 3. Von Mises Stress distributions over different regions of the mandible. The highest stress level for each side are bolt.⁷⁷

Location	Region	A Stress level (MPa)	B Stress level(MPa)	C Stress level (MPa)	D Stress level (MPa)
		Right / Left	Right / Left	Right / Left	Right / Left
1. Condyle		0.74 / 1.63	0.16 / 1.63	0.13 / 1.18	0.01 / 1.25
2. Condylar neck		0.94 / 2.00	0.41 / 3.55	0.25 / 2.78	0.04 / 4.02
3. Mandibular angle		2.15 / 4.23	1.16 / 6.99	0.97 / 5.73	5.29 / 7.14
4. Retromolar area		4.64 / 3.58	11.78 / 6.07	13.54 / 7.80	8.44 / 7.78
5. Mental foramen		1.76 / 1.97	3.20 / 2.20	4.30 / 9.02	3.81 / 2.68
6. Chin		1.73	2.47	5.81	5.38

* A = Unresected, B = Reconstructed small resection, C = Reconstructed medium resection, D = Reconstructed large resection

From figure 9 and the values highlighted in table 3, the amount of resection has impact on the stress distribution. In general, this study supports that highest stresses occur at the connection between the fibula graft and mandibular residue.⁷⁷ Deviations from the planned osteotomy trajectory or angulations during placement of the fibula segments could compromise this connection further by decreasing the contact area between both bony parts. Thereby, the stress distribution will be even more concentrated. This may affect bone healing and mandible functioning, since the stress distribution is an important factor for the biomechanical properties of the reconstructed mandible. A highly concentrated stress distribution will cause bone resorption instead of the desired bone regeneration.⁷⁵ The resorption of fibula segments in reconstructed mandibles was studied by Mertens et al. They observed fifteen patients over periods of six months, eleven months and seventeen months. After six months, 5.30% of the fibula was resorbed, after 11 months, 8.26% was resorbed, and 16.95% of the fibula was resorbed after 17 months. However, the amount of bone volume that remained in all patients was sufficient for implant placement.⁷⁸

These findings are supported by a study of Makiguchi et al., where fibula height resorption was observed in 19 patients during a follow-up period of 12 months. They found that bony union was present in all patients. Furthermore, the extent of fibula height resorption over time was on average 17.6%, and the extent of fibula height hypertrophy (growth) over time was on average 7.8%.⁷⁹

Appendix C: Design requirements

To make the design feasible, multiple aspects have to be taken into account during the design process. These aspects include the design requirements, the boundary conditions, and the requirements with regard to both human anatomy as well as the usability towards the surgeon. By fulfilling these requirements, it should be enabled that *any surgeon* can use the design on *any patient*, with *minimum operation time* and *costs*, while a *sufficient result* is obtained. In this section, the boundary conditions and a list of requirements for the newly designed or modified device will be presented. Since medical instruments have to deal with both clinical and technical requirements, these requirements will be discussed separately.

A summary of the design requirements is presented in table 1. The boundary conditions are discussed in appendix C.1. The clinical requirements will be explained in appendix C.2 and the technical requirements will be discussed in appendix C.3.

Table 1. The design requirements with corresponding values.

#	Clinical requirement	Value	Technical requirement	Value
1	Usability	Amount of the required training time	Accuracy osteotomy	$\leq 2^\circ$ or ≤ 5 mm
2	Adjustable to anatomy shapes	(x-,y-,z-plane)	Simple production method	≤ 500 euro's
3	Haptic feedback	Availability of the interacting forces to the surgeon	Angulation graft placement	$\leq 2^\circ$
4	Ischemia / disassembly time	≤ 100 min. ¹⁰	Bone thickness that should be bridged during osteotomy	3.02 mm - 51.50 mm
5	Clean ability	Shape, gap sizes	Resistant material / design to withstand forces during osteotomy	Young's modulus, tensile strength
6	Sterilization	121°C - 148°C	Simple construction	Amount of parts
7	Biocompatible	Risk of injury, toxicity or rejection by the immune system		
8	Safety	Amount of collateral damage		

C.1. Boundary conditions

To obtain a feasible design or modification of the current (surgical) devices, three boundary conditions have to be met: a) The deviation of the achieved osteotomy trajectory in comparison with the planned osteotomy trajectory should not exceed $\pm 2^\circ$, while b) the production costs of the patient-specific devices do not exceed 350 euro's and c) the ischemia time does not exceed 100 minutes.

To generate ideas for improvement, problems related to the current surgical device are divided into the following sub-problems for which solutions should be generated:

- How to create an optimal fit of the resection templates?
- How to make the osteotomy trajectory more reliable?
- How to prevent collateral damage?
- How to minimize ischemia time?
- How to minimize production costs?

As mentioned before, the newly designed device(s) should keep the deviation of the osteotomy trajectory within a range of 358° to 2° from the planned trajectory to improve the accuracy and the reliability of the current method. The production costs should not exceed 350 euro's, since the current costs are about 250 euro's and a far more expensive design will make the design less feasible and attractive. Additionally, the ischemia time should be kept within 100 minutes, considering that a higher time span is associated with an increased chance on skin island failure. Because the sub-problems act on different aspects, highest priority was assigned to the problems

with highest impact and feasibility. Therefore, the main issue that should be solved during the idea generation is “How to make the osteotomy trajectory more reliable, while keeping the ischemia time within boundaries”.

C.2. Clinical requirements

Clinical requirements are requirements that should be fulfilled to enable *any surgeon* to use the design on *any patient*. To achieve this, the design should be adjustable to the anatomies involved, such as the fibula and the mandible. Therefore, dimensions of the anatomies should be known. The rationale for the setting up the dimensions found for the anatomies will be provided in *subsection C.II.I and C.II.II*

C.2.I. Mandible

The height and thickness of the mandible should be taken into account for determine the dimensional design requirements. Patients suitable for mandibulectomy and reconstruction with the fibular free flap are usually edentulous (without teeth). Edentulous patients have a different morphology of the mandible, such as thickness and height, due to bone resorption. A good visualization of this process of morphologic change resulting from tooth loss is presented in figure 1. ⁴²

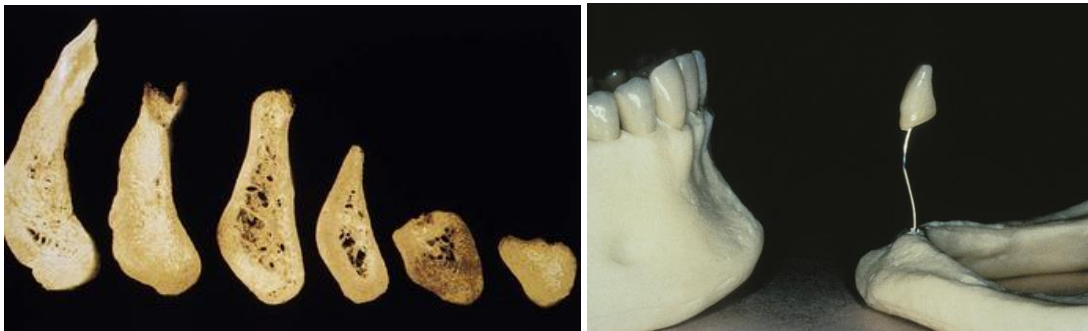
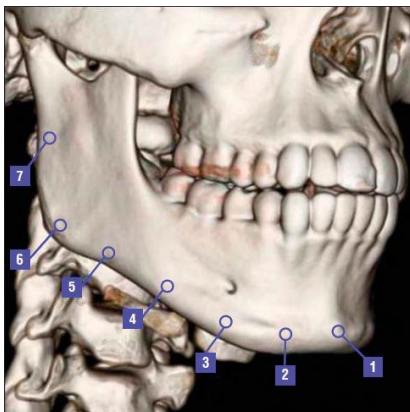


Figure 1. Bone resorption in edentulous patients (without teeth) over time, and a visualization of a decreased mandible height (right image).⁴²

Mandible thickness

According to a study in dentate young adults by Beaty et al., mandible thickness differs between mandibular regions. Regions that were included in this study are presented in figure 2.



Anatomical position	Gender	Men (n=150) Mean \pm SD (mm)	Woman (n=75) Mean \pm SD (mm)
1		14.03 \pm 1.53	13.21 \pm 1.46
2		11.17 \pm 1.37	10.00 \pm 1.08
3		9.48 \pm 1.28	8.72 \pm 1.00
4		10.33 \pm 1.24	9.45 \pm 0.92
5		7.27 \pm 0.82	7.10 \pm 0.88
6		5.42 \pm 0.90	5.39 \pm 0.66
7		5.90 \pm 0.86	5.85 \pm 0.71

Figure 2. Seven mandibular regions of young dentate adults with corresponding thicknesses as presented in the table at the right. The minimum and maximum thicknesses found are indicated in red. ⁴³

A minimal dentate mandible thickness of 5.39 mm, and a maximal dentate mandible thickness of 14.03 mm were found.⁴³ Since the mandible is shaped like an oval, it is relatively easy to define its thickness. Therefore, the thicknesses found according to the cross section of the mandible in this study are sufficient to use as base for determining the dimensional design requirements. (Fig. 3)

The maximum thickness found in this study for dentate patients is applicable for our design, assuming that the thickness of edentulous mandibles will not exceed the thickness of healthy dentate mandibles due to the occurrence of bone resorption. On the contrary, the minimum thickness of dentate mandibles is not a sufficient dimensional boundary, as a result from bone resorption in edentulous mandibles should be taken into account. It is assumed that mandible thickness is decreased in edentulous mandibles.

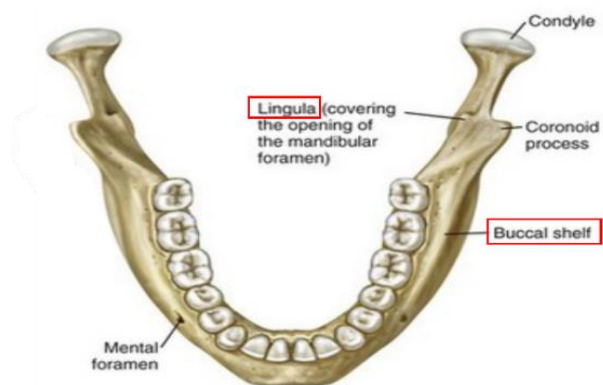


Figure 3. Illustration of a few regions of the mandible. The buccal side of the mandible is the outer surface area, in this illustration pinpointed by the buccal shelf. The lingual side of the mandible, the inner surface area, is pinpointed by the lingual in this illustration.⁸⁰

This assumption is confirmed by a study of Flanagan et al. They studied 17 edentulous mandibles, in which 704 sites over the mandible were analyzed. These sites included the buccal area and the lingual area of the mandible, as presented in figure 3. They found a minimum buccal cortical thickness of 1.36 mm and a minimum lingual cortical thickness of 1.66 mm. By merging these thicknesses, a minimum mandible thickness of 3.02 mm is found. In comparison with the dentate mandible thickness of 5.39 mm that was found by Beaty et al, the mandible thickness in edentulous patients is considerably less with a minimum thickness of 3.02 mm.⁴⁴

Mandible height

In a study of Sağlam et al., 192 radiographs of 96 dentate mandibles and 96 edentulous mandibles were compared to measure differences in mandible body heights as a result of tooth loss and the resulting bone resorption. According to table 2, they found a minimum mandible height of 8.00 mm in female edentulous mandibles at the vertical distance Y3 of figure 3.⁴⁵ This region is known as the mandibular body.⁸¹ Furthermore, a maximal mandibular body height of 51.50 mm was found at the symphysis in male dentate mandibles. (Y1, fig. 3)

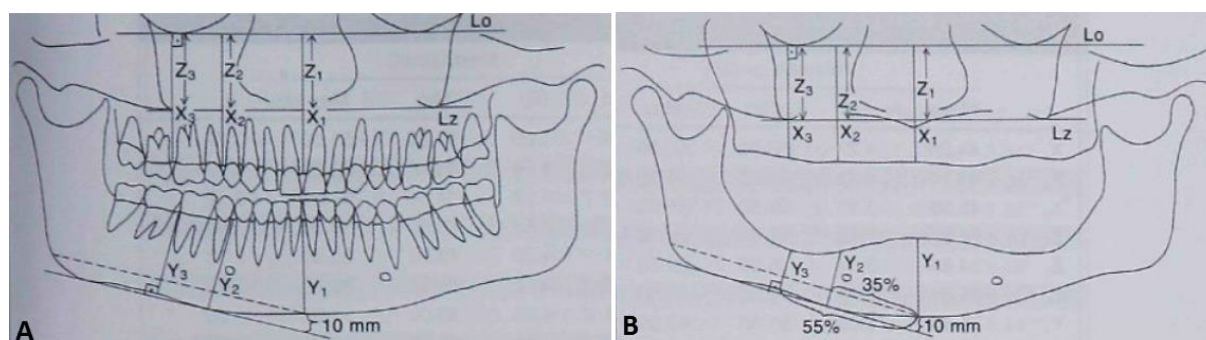


Figure 4. An illustration of measuring mandible heights at different locations of both dentate (A) and edentulous (B) mandibles, according to the study of Sağlam et al. They found a maximal mandible height (51.50 mm) for dentate men at vertical distance Y1, and a minimum mandible height (8.00 mm) for edentulous woman at vertical distance Y3.⁴⁵

Table 2. Vertical heights of mandibular bones found over 96 dentate and 96 edentulous mandibles, according to the study of Sağlam et al. The maximum and minimum mandible heights are indicated in bold.⁴⁵

	Section	Women		Men	
		Mean (\pm SD)	Min. – Max. (mm)	Mean (\pm SD)	Min. – Max. (mm)
Dentate n=96	Y1	35.85 (\pm 3.06)	31.00 – 43.00	39.54 (\pm 4.08)	33.00 – 51.50
	Y2	35.76 (\pm 3.95)	27.50 – 42.00	38.65 (\pm 4.05)	32.00 – 49.50
	Y3	30.91 (\pm 4.37)	19.50 – 38.00	32.83 (\pm 4.63)	26.00 – 46.00
Edentulous n=96	Y1	22.13 (\pm 6.67)	10.50 – 36.50	28.37 (\pm 6.68)	19.50 – 40.00
	Y2	21.43 (\pm 7.18)	10.00 – 33.50	27.35 (\pm 7.99)	13.50 – 40.00
	Y3	18.19 (\pm 6.46)	8.00 – 29.00	22.00 (\pm 6.58)	11.00 – 34.00

Conclusion

In conclusion, to make the device applicable to *any* patient, dimensional requirements can be set according to the mandible thicknesses and heights found for both dentate and edentulous patients. The design should allow mandibular thicknesses ranging from 3.02 mm to 14.03 mm, and mandibular heights ranging from 8.00 mm to 51.50 mm. These dimensions will be applied within the design requirements concerning the area of bone that should be bridged by the (surgical) devices during surgery.

C.2.II. Fibula

The minimum and maximum height of the fibula will also be applied to create a design that is feasible to *any* patient. Ide et al. studied CT scans of 20 different fibula bones to determine mean fibula heights and widths. They applied a method as presented in figure 4.1.⁴⁶

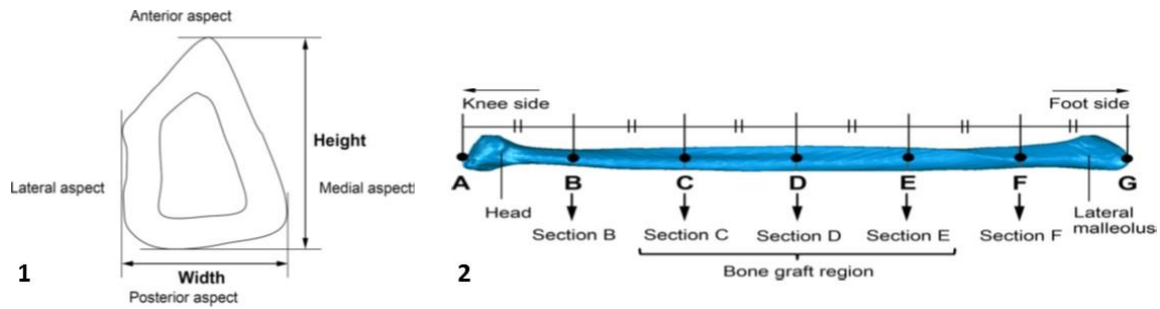


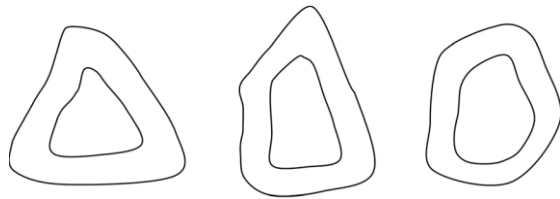
Figure 5. 1) The method applied to measure mean height and width of the fibular cross-section. 2) The fibula bone divided into different sections, of which sections “c”, “d”, and “e” are used for bone grafting.⁴⁶

Since section “C”, “D” and “E” (fig. 19.2) are used for bone grafting, the dimensional design requirements based on the fibula is based on dimensions found over these regions. The mean height and width of the fibula in these regions are presented in table 3.⁴⁶

Table 3. The mean heights and widths of the sections included in the bone graft region for both male and female subjects.
⁴⁶The minimum and maximum of both height and width are highlighted in bold.

Section	C		D		E	
	Mean \pm SD (mm)		Mean \pm SD (mm)		Mean \pm SD (mm)	
Gender	Height	Width	Height	Width	Height	Width
Male	16.8 \pm 1.8	12.8 \pm 1.2	17.0 \pm 1.6	14.2 \pm 1.9	16.4 \pm 2.0	12.0 \pm 1.4
Female	15.8 \pm 1.4	10.4 \pm 1.2	15.6 \pm 1.3	12.0 \pm 1.4	14.4 \pm 1.4	10.8 \pm 1.0

Because the patients that are included in the treatment are both males and females, the design should allow a minimum fibula height of 14.4 mm, and a maximum fibula height of 17.0 mm, according to highlighted values in table 3. Subsequently, the design should allow a minimum fibula width of 10.4 mm, and a maximum fibula width of 14.2 mm (table 3). However, different cross-sectional fibula shapes are found in literature, as presented in figure 5. Because the cross-sectional shape has impact on the resulting design requirements according to the minimum and maximum fibula height and width, a simulation was performed to retrieve dimensional design requirements, as indicated in figure 6.



Triangular type Quadrilateral type Irregular type

Figure 6. Different types of cross-sections of the fibula bone. ⁴⁶

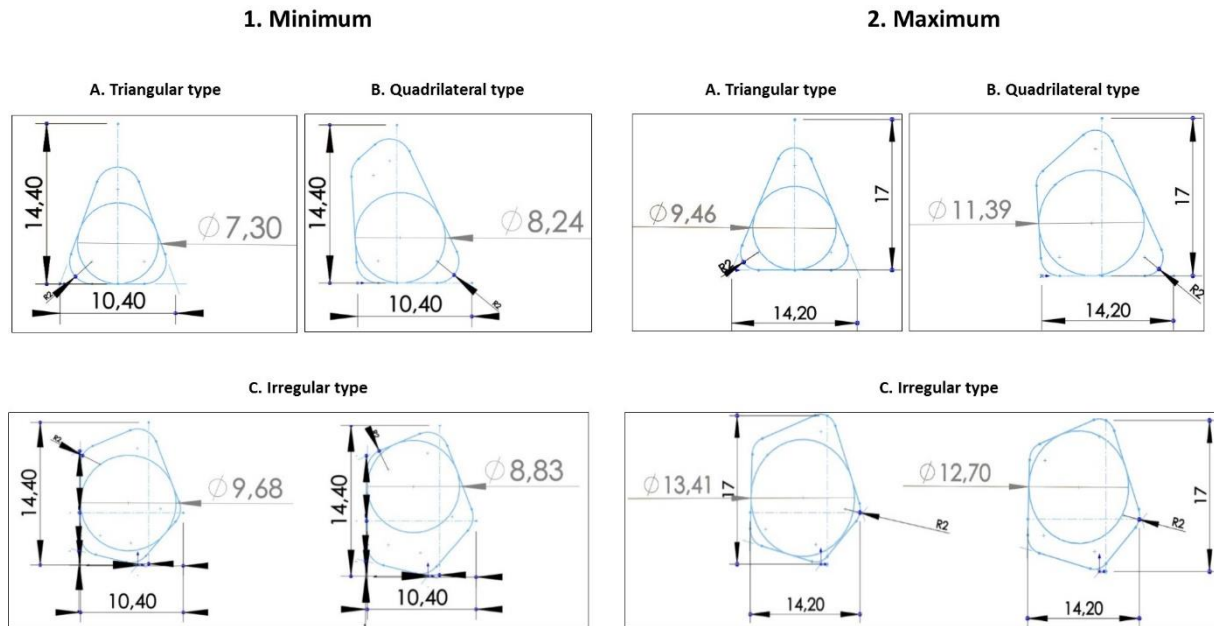


Figure 7. The different types of fibula shapes illustrated in figure 18 are simulated in SolidWorks, showing the impact of different fibula shapes on the mean cross-sections when 1) minimum width and height from table 6 are applied. 2) The maximum width and height from table 6 are applied.

Conclusion

Using the minimum and maximum fibula height and width for the shapes that are presented in figure 20, different cross sectional areas are found. Therefore, the boundaries of the dimensional design requirement according to the fibula will be based on the minimum and maximum cross sections according this method. A minimum cross section of 7.30 mm was found for the triangular type and a maximum cross section of 13.41 mm was found for the irregular type.

C.2.III. Conclusion

To make the design applicable to the anatomies involved, the dimensional design requirements should be based on the minimum and maximum dimensions that were found according to both the mandible and the fibula. Therefore, the design should be suitable for thicknesses of 3.02 mm to 14.03 mm and heights of 8.00 mm to 51.50 mm. In conclusion, the lower boundary is set at 3.02 mm and the upper boundary is set at 51.50 mm.

C.2.IV. Haptic feedback

Haptics is referred to as the interaction between cutaneous sensors of the skin and the kinesthetic sensors of muscles, tendons, and joints. Appliance of lateral motions or vibrations provides information about object's texture, and by the execution of pressure, object's hardness can be detected. Additionally, static contact can be applied for thermal sensing, and object's weight can be determined using unsupported holding. Finally, volume and contour shape of the object are retrieved through enclosure, and contour following can be applied for the global shape and precise contour information.⁸² The obtained interacting forces, torques and movements are known as *haptic feedback*. Haptic feedback enables surgeons to explore, detect and distinguish between

structures in absence of visual feedback. Using this information, the surgeon can apply appropriate pressure and tension to facilitate tissue exposure, and perform dissections without inducing collateral damage.⁸³ Collateral damage is referred to as causing damage to surrounding tissues.

For example, bone provides higher haptic forces than soft tissues, thus if the haptic force alters during the osteotomy, the surgeons will realize not only bone is involved. Haptic feedback can be attenuated or distorted through the intervention of (metal) instruments, which may lead to surgical errors, such as damage of critical structures.⁸⁴

To increase the chance of skin island survival, it is of major importance that critical structures are left undamaged during mandibulectomy or osteotomy of the fibula. Examples of these critical structures are the peroneal vessel at the back of the fibula, and the jugular vein and other facial arteries close to the mandible. The new design can improve to the amount of haptic feedback that is provided to the surgeon during osteotomy in comparison with the current design. The amount of feedback during osteotomy can be enhanced by improved enclosure and contour following, or by increasing the amount of visual feedback.

C.2.V. Sterilization

For application of the device in the operating room, each device should be able to withstand cleaning and sterilization methods that are currently available (table 4). The sterilization requirements for the design are embedded in possible problematic parameters and the compatibility of the design to the sterilization methods, such as exposure to high temperatures and chemicals. The design should be conform these sterilization requirements, according to the shape and the materials that are applied. The dimensions of the lumens and cavities of the medical instruments applied in this study are small, <3 mm. According to the FDA, an increased lumen length or a decreased lumen diameter impairs penetration of sterilant, and forced flow will be required to achieve sterilization. This impact increases for low-temperature sterilization. Therefore, it is encouraged to prevent both small gaps and lumens, and use autoclave steam as sterilization technique for the instruments involved in this study. Autoclave steam applies high temperatures for an adequate sterilization and has limited requirements with regard to compatibility.³⁷

Table 4. Existing methods and forthcoming problematic parameters and required compatibility of the device that will be sterilized.^{85, 86}

Method	(Problematic) parameters	Compatibility
Autoclave steam	- 15-60 min. - 121°C – 148°C	- Humidity - May affect embedded batteries
Ethylene oxide	- 480-720 min - 30°C-60°C	- Vacuum may affect embedded batteries - Highly flammable - Carcinogenic
Chlorine dioxide	- 150 min. - 15°C-40°C	- No moisture - Non-flammable - Non-carcinogenic
Vaporized hydrogen peroxide	- 690 min. - 25°C-50°C	- Oxidative stress by H ₂ O ₂ radicals - No moisture - Lower penetration capabilities
Hydrogen peroxide plasma	- 60-180 min. - 40°C-65°C	- Affects electronics
Gamma rays	- ≤15 min - 20°C	- Affects electronics - Produces nuclear waste
Electron beams	- Faster than gamma - 20°C	- Lower penetration depth than gamma - No nuclear waste

C.3 Technical requirements

Additional to the clinical requirements from the surgeon, the patient and the sterilization department, there will be technical requirements to the design. Technical requirements are introduced to minimize production time and costs. Furthermore, technical requirements are important for providing a sufficient result of the design. The currently applied combination of instruments allow osteotomy deviations up to 5.13° . This may lead to deviations of 2.24 mm of the planned osteotomy trajectory, as discussed in section B.2, figure 3. However, the cross section that should be bridged during osteotomy is composed by the bone and the cutting sleeve of the template. When the mandible height is maximum, this combination may reach to a cross section of 51.5 mm instead of the 50 mm that was applied in section B.2. Thereby, a deviation of 4.62 mm at the end of the osteotomy trajectory may be obtained, as visualized in figure 8.1.

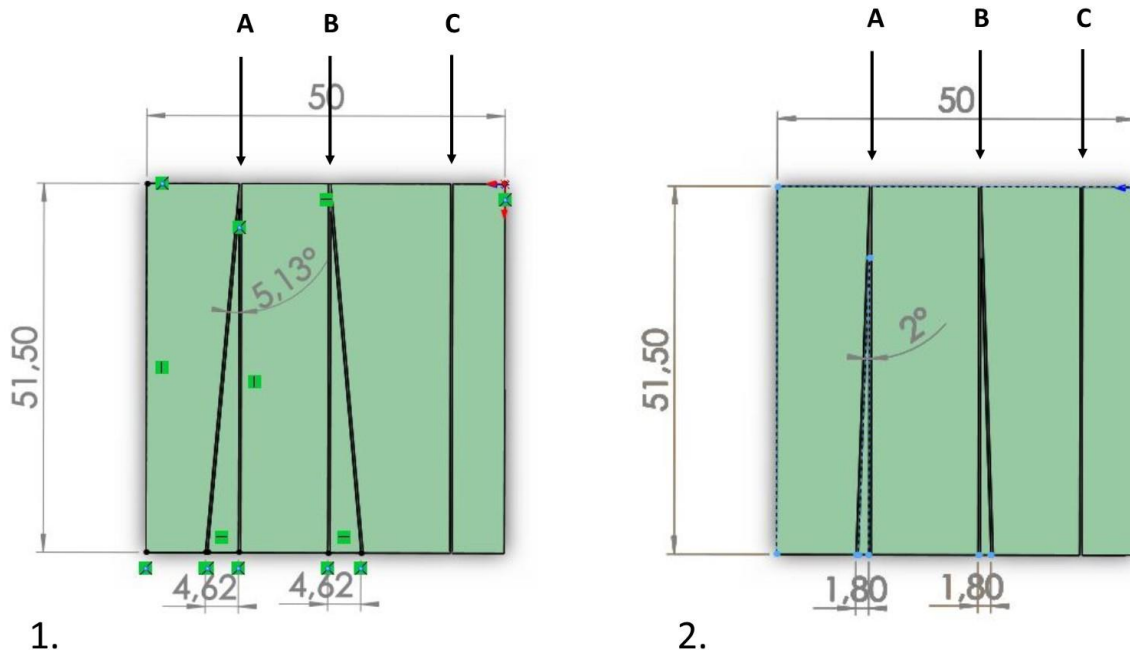


Figure 8. 1. The resulting osteotomy trajectory of an osteotomy with a deviation of 5.13° , which results in a distance of 4.62mm to the intended path (A,B). 2. The resulting osteotomy trajectory of an osteotomy with a deviation of 2.0° , which results in a distance of 1.80 mm to the intended path (A, B). C) A straight osteotomy trajectory that behaves as intended.

A maximum angulation of 2.0° was set as design requirement regarding to the angulation of the osteotomy trajectory. To motivate this choice, a simulation was preformed to determine the distance to the planned trajectory. The simulation showed that this angulation will contribute to a maximum of 1.8 mm to the planned osteotomy trajectory, as presented in figure 9.2. To detect further consequences, the impact of this amount of deviation was simulated in SolidWorks simultaneously to the method applied in appendix B.2. Both clockwise and counterclockwise simulations were performed. With this simulation, it was found again that the quality reconstructed mandible is more prone to clockwise rotations of the fibula. With these initial conditions, a maximal rotation of 2.9° of the neomandibular body occurs when the fibular graft receives a clockwise angulation of 2.0° . (Fig. 9.3A) This is considerable less than a rotation of 8.25° of the reconstructed mandibular body, as was found in appendix B.3 for a clockwise rotation of 4.3° .

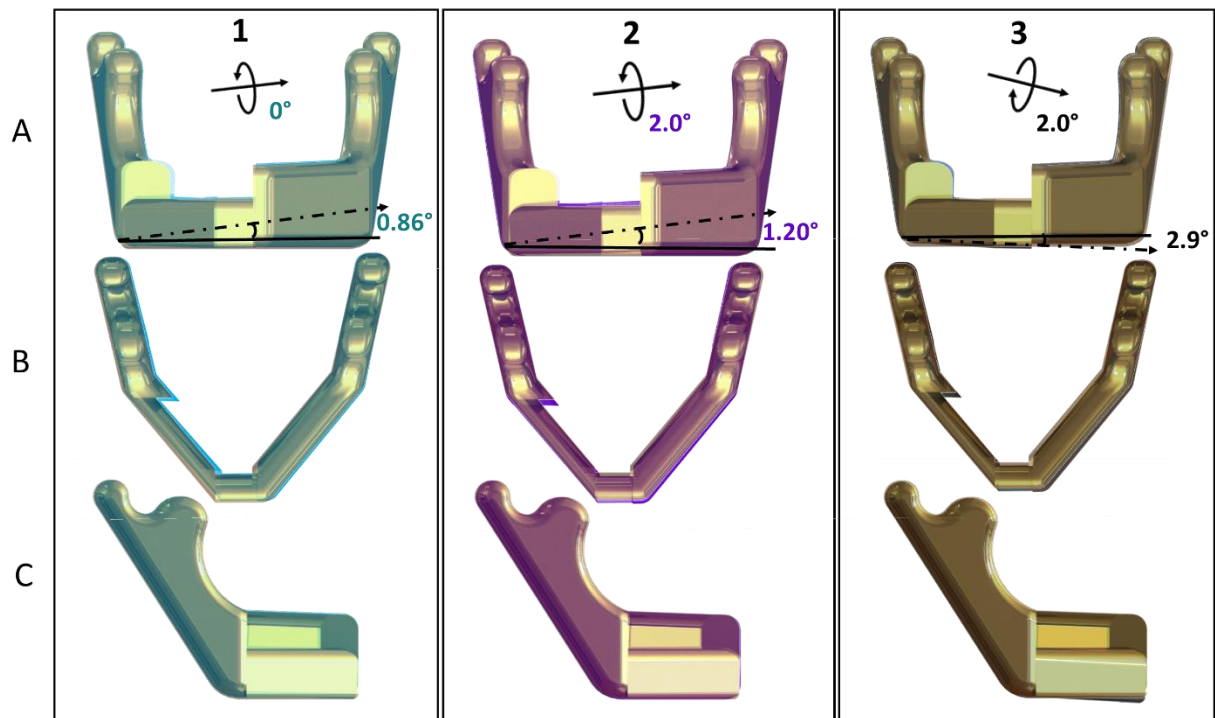


Figure 9. Simulations of a reconstructed mandible where an osteotomy deviation of 2° is present, in front view (A), top view (B) and lateral view (C). 1. The left frame represents a situation where no segmental angulations occurred, as a result, the base of the fibula graft rotated 0.86° from the original mandibular base. 2. The middle frame represents a situation where the fibula graft is placed with a counter-clockwise angulation of 2.0° , this results in a rotation the reconstructed mandibular body of 1.20° . 3. The right frame represents a situation in which the fibular graft angulated 2.0° clockwise during the placement, and as a result the reconstructed mandibular body is rotated 2.9° .

Appendix D. Concept generation

This section will provide ideas to improve the current interaction of devices and their feasibility towards the design requirements described in appendix C. In appendix D.1, an overview of the solutions will be given by a morphologic analysis. Additionally to this analysis, a scoring system is generated to eliminate non-suitable options and select most suitable ideas. The residual design solutions are established into concepts in appendix D.2. Additionally, a motivation for these concepts and their design models is presented. Finally, several concepts are selected that will be produced using 3D-printing for further evaluation.

D.1 Ideas and idea selection

One suitable methodology to change the interaction between the currently applied devices and the resection templates is by adjusting the resection templates. Another suitable approach is by changing or adjusting the applied osteotomy device. A morphologic analysis was performed to provide an overview of the created options that fulfill one of the requirements mentioned in appendix C. (Fig. 1) Within the morphologic analysis, four major functions of the design are discussed:

- A) Connection between bone and template
- B) Fit of the template
- C) Strength of the template
- D) Guiding perspective

For these functions, multiple options were generated. By selection of an option for each function, a pathway is created. This pathway can be compiled into a concept. The options that were selected and combined into concepts are presented and discussed in appendix D.2.V to D.2.VI. Since it is suspected that remarkable progress can be made by adjusting the current design of the template, the concept choices that will be created will be based on adjustments to the current design of the resection templates. Additionally, because the surgeon is experienced with using the reciprocating saw, it was chosen to make no adjustments to the device applied for osteotomies. However, when no progress is registered by the approach of adjusting the resection template, a transfer can be made to changing or adjusting the cutting device.

Option Function	1	2	3	4	5	6	7
A. Connection bone-template	Current: screw 	Vacuum-fitted 	Shape-memory 	Contact fit 			
B. Fit template - orientation - location	Current: shape-forced 	Coating: Gel-supported fit 	Material 	Shape: increase contact area 	Bone contouring click-connection 	Bone contouring bend-connection 	Navigation 
C. Strength tem-plate	Current: biocompatible material 	Coating: Enforcing 	Composite material: anisotropic structure 	Material: insertion of metal 	Alter material: introduce outline 		
D. Cutting devia- tion	Current: 0.25 mm thick saw blade 0.70 mm cutting sleeve width 	Strengthen saw blade: material or thickness 	Additional guidance 	Alter width of cutting sleeve 	Fixation of anatomies 	Alternative device: Laser 	Alternative device: piezoelectric osteotome 

Figure 1. The morphologic analysis that provides the generated solutions to the sub-problems that were encountered with the current design or major requirements the design should fulfill.

D.2. Concepts

In this section, different choices of the morphologic analysis were combined to generate five concepts. A short description and the implementation of the four major functions in each design is given in the following subsections.

D.2.I. Concept B – Reduced sleeve width

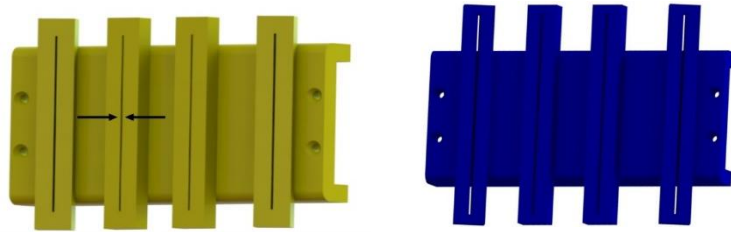


Figure 1. Left: A CAD model of concept B, a resection template with a reduced resection sleeve width to reduce the chance of angulations of the saw blade into the cutting sleeve. Right: The current template, with a larger resection sleeve width.

- A) The connection between the bone and the template will be obtained using screws. The template will be screwed onto the bone, which is equal to the currently applied principle.
- B) For the fit of the template to the bone, a shape-forced surface was selected, as applied currently. The shape of the bone should force the template onto the planned location.
- C) The strength of the template depends, amongst other things, on the material applied. PA 2200 was selected as template material, since this material is labeled as biocompatible and it is applicable for medical applications according to ISO 13485. Furthermore, PA 2200 can be processed to relatively low costs into a model using selective laser sintering (SLS).⁴⁷
- D) The cutting deviation is attempted to be tackled by adjusting the width of the cutting sleeve. (Fig. 1) The current cutting sleeve width is 0.70 mm, while the saw blade thickness is 0.25 mm. It is suspected that due to this difference, angulations of the saw blade may occur as explained in figure 2 of appendix B.2. Two approaches that are possible to adjust this difference are 1) reducing the width of the cutting sleeve or 2) increasing the width of the saw blade. For this concept, the first option was selected and executed by reducing the width of the cutting sleeve of 0.7 mm to a width of 0.4 mm.

D.2.II. Concept C – Contact-fitted

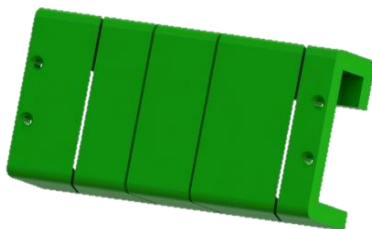


Figure 2. A CAD model of concept C, a resection template that is contact-fitted and has a reduced cutting sleeve depth to increase visual feedback during surgery.

- A) The connection between the bone and the template will be obtained using screws. The template will be screwed onto the bone, which is equal to the currently applied principle. Additionally, the contact area between the bone and template is increased to allow a contact-fit between the bone and template. (Fig. 2)
- B) For the fit of the template to the bone, a shape-forced surface was selected, which is equal to the method that is currently applied. The shape of the bone should force the template onto the planned location. Additionally, the contact area between the template and the bone was increased by a contact area at the top, and partially at the back bottom to provide a better fit.
- C) The strength of the template depends, amongst other things, on the material applied. PA 2200 was selected as template material, since this material is labeled as biocompatible and it is applicable for medical applications according to ISO 13485. Furthermore, PA 2200 can be processed to relatively low costs into a model using selective laser sintering (SLS).⁴⁷

D) The cutting deviation is attempted to be tackled by the introduction of additional guidance at the top of the resection template. Additionally, the depth of the cutting sleeves was reduced from 10 mm to 5 mm to improve the sight on the saw path.

D.2.III. Concept D – Top guidance

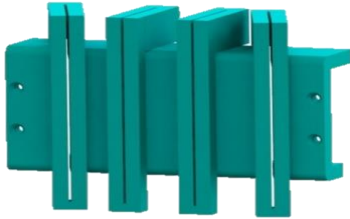


Figure 3. A CAD model of concept D, a resection template that introduces guidance from the top to increase the control of the angle of insertion of the saw blade.

A) The connection between the bone and the template will be obtained using screws. The template will be screwed onto the bone, which is equal to the currently applied principle. Additionally, the contact area between the bone and template is increased to allow a contact-fit between the bone and template. (Fig. 3)

B) For the fit of the template to the bone, a shape-forced surface was selected, which is equal to the method that is currently applied. The shape of the bone should force the template onto the planned location. Additionally, the contact area between the template and the bone was increased by an increased amount of contact area at the top, to provide a better fit.

C) The strength of the template depends, amongst other things, on the material applied. PA 2200 was selected as template material, since this material is labeled as biocompatible and it is applicable for medical applications according to ISO 13485. Furthermore, PA 2200 can be processed to relatively low costs into a model using selective laser sintering (SLS).⁴⁷

D) The cutting deviation is attempted to be tackled by the introduction of a guiding sleeve at the top. This should improve the guidance of the saw blade into the correct orientation onto the bone prior to initiating a bone cut.

D.2.IV. Concept E – Metal insert

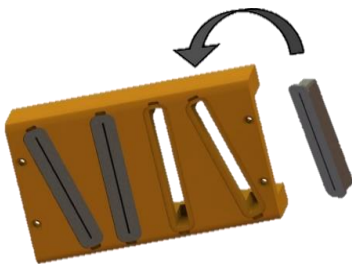


Figure 4. A CAD model of concept E, a titanium insert is introduced to enforce the template locally around the cutting sleeves to prevent the saw from cutting into the template.

A) The connection between the bone and the template will be obtained using screws. The template will be screwed onto the bone, which is equal to the currently applied principle.

B) For the fit of the template to the bone, a shape-forced surface was selected, which is equal to the method that is currently applied. The shape of the bone should force the template onto the planned location.

C) The strength of the template depends, amongst other things, on the material applied. PA 2200 was selected as template material, since this material is labeled as biocompatible and it is applicable for medical applications according to ISO 13485. Furthermore, PA 2200 can be processed to relatively low costs into a model using selective laser sintering (SLS).⁴⁷ Additionally, a metal insert with resection sleeve was designed. (Fig. 4) The reciprocating saw is guided through this sleeve while resecting the bone, thus the insert strengthens the template locally. This should prevent the saw from cutting into the template. The metal applied for this insert is titanium, since this is biocompatible and wear resistant.⁸⁷ The titanium insert can be generated using milling or laser-cutting of titanium, or by using Direct Metal Laser Sintering (DMLS).

D) The cutting deviation is attempted to be tackled by additional guidance through this titanium insert. The rationale is similar the principle of the concept of a reduced sleeve width, since the sleeve width was reduced from 0.7 mm to 0.35 mm in this concept.

D.2.V. Concept F – Bone-contouring guidance

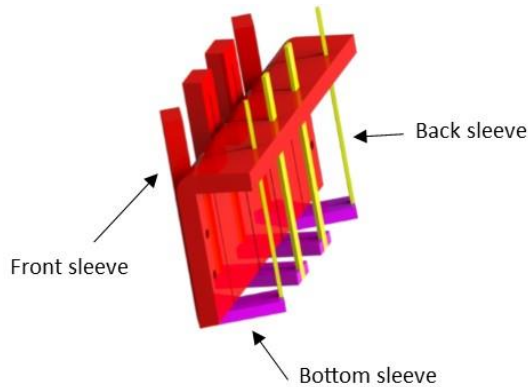


Figure 5. A CAD model of concept F, guiding cutting sleeves are introduced at the back and the bottom of the template, to guide the saw in all directions.

A) The connection between the bone and the template will be obtained using screws. The template will be screwed onto the bone, which is equal to the currently applied principle. Additionally, the contact area between the bone and template is increased to allow a contact-fit between the bone and template. (Fig. 5)

B) For the fit of the template to the bone, a shape-forced surface was selected, which is equal to the method that is currently applied. The shape of the bone should force the template onto the planned location. Furthermore, there will be sleeves inserted at the back of the fibula, between the bone and the peroneal artery, and at the bottom of the fibula. Therefore, there will be a connection and contact-fit obtained by introducing contact area's at the top, back, and bottom of the template.

C) The strength of the template depends, amongst other things, on the material applied. PA 2200 was selected as template material, since this material is labeled as biocompatible and it is applicable for medical applications according to ISO 13485. Furthermore, PA 2200 can be processed to relatively low costs into a model using selective laser sintering (SLS).⁴⁷

D) The cutting deviation is attempted to be tackled by an increased guidance at the back of the fibula. This design is based on a miter box, a woodworking tool that is applied to guide a hand saw performing a wood cut with angles of 45° or 90°, by the presence of guiding slots at the front, the bottom, and the back of the box. This design consists of three parts; a front template that contains cutting sleeves (red), a guiding part at the bottom (purple) and a guiding part at the back (yellow). The parts are connected through a male-female pin-connection.

Appendix E. Concept evaluation: Exploring test

To create feasible design solutions, the major functions that should be fulfilled by the design were summarized in a scoring (Table 1). A weighing factor was added to the requirements to select the best options. The weighing factor represents the degree of importance of the requirement for receiving a successful design. According to this outcome, feasible design solutions can be created.

Table 1. Scoring guidelines for the design requirements described in section 3.

Requirement	Score 1 when	Score 10 when	Weighing factor
<i>Usability</i>	Device is custom made or physician needs intensive training	Device is feasible to all patients and physicians	8
<i>Adjustable to anatomy shapes</i>	Device is only applicable to one shape type of one anatomy	Device applicable to all anatomies and their shape types	7
<i>Haptic feedback</i>	No haptic feedback is given	Same or improved feedback is present	6
<i>Ischemia time / disassembly time</i>	> 100 minutes / slow fixation or removal during surgery	≤ 100 minutes / quick fixation or removal during surgery	8
<i>Sterilization</i>	Device cannot withstand sterilization methods	Device can withstand sterilization methods	6
<i>Biocompatible</i>	No	Yes	8
<i>Reusable</i>	No	Yes	4
<i>Safety</i>	The device causes collateral damage, (e.g. fixation method is invasive)	The device does not cause collateral damage (e.g. noninvasive fixation)	8
<i>Accuracy</i>	> 2° / > 5 mm	≤ 2° / ≤ 5 mm	10
<i>Simple production method</i>	No CAD/CAM is feasible or different methods are required	The design is fully produced using CAD/CAM	8
<i>Simple construction</i>	Device consists of many (small) parts, difficult to disassemble	Device consists of a few parts and is a solid construction, easy to disassemble	6
<i>Clean ability</i>	Device contains tiny gaps and/or device cannot be disassembled	Device contains no gaps or gaps are rounded-off and device can be disassembled	8
<i>Hardness and strength of material / design</i>	Elastic or/and brittle, easy to cut into, high amount of debris	Stiff material that can withstand cutting forces, or design increases the resistibility towards forces of the saw blade	9

It is difficult to score the concepts purely based on CAD models and theoretical assumptions. Therefore, the production of the concepts and by executing an exploring test to gain practical experience on their performance, information will be retrieved that aids in scoring them with regard to the design requirements. The design requirements of interest during the exploring test include the accuracy, safety, disassembly time, usability, simplicity of manufacturing, hardness and strength of the design and the amount of feedback. Each concept, including the current design, is evaluated during as well as after executing four bone cuts. This will give an impression of the performance and ease in use of each concept. As a result, the scoring table can be completed and concept(s) can be selected by means of their total scores.

E.1. Materials

During the exploring test, the manufactured concepts will be evaluated according to their simplicity, ease in use, safety during use, the amount of feedback they provide and the accuracy of their performance. Therefore, each concept was printed using Selective Laser Sintering. Subsequently, the performance of each concept was studied using a synthesized bone block as test medium (Saw bones, Pacific Research Laboratories)⁸⁸ and a reciprocating bone saw to perform the bone cut.

E.1.I. 3D-printed concepts

The material applied for the realization of the three dimensional models is a white polyamide (PA 2200 with PA 12, Océan). PA 2200 has high strength and stiffness with a Young's modulus (E) of 1650 MPa and a tensile strength (σ) of 48 MPa. It is resistant to chemicals, has a melting temperature of 176 °C and other properties that make the material promising towards withstanding sterilization methods as described in appendix C.2. Additionally, according to ISO 10993-1, the material is biocompatible through which it is suitable for use in is according to EN ISO 10993-1. Moreover, by the application of 3D-printing as manufacturing method, the production costs are relatively low, while the resolution that can be achieved using 3D-printing is relatively high. Therefore, PA 2200 is applicable and suitable for the 3D-printing of the templates used in this study.

E.1.II. Bone block

A synthesized bone block (Sawbone, Pacific Research Laboratories Inc.) was applied for the exploring test. (Fig. 1) The largest amount of the synthesized bone block represents human cancellous bone. This is made of solid and rigid polyurethane foam, since this mimics the relevant mechanical properties of cancellous bone. Additionally, the block was laminated with an epoxy sheet on one side. This is a short fiber filled epoxy sheet which is a mixture of short glass fibers and epoxy resin, with mechanical properties similar to cortical bone.⁸⁹

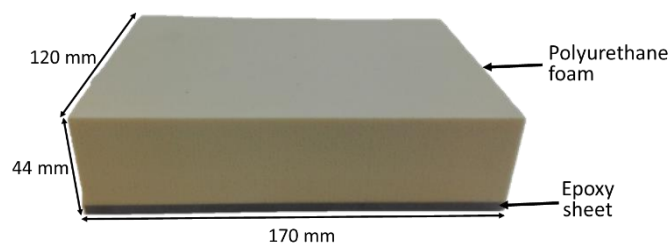


Figure 1 A synthesized bone block (Sawbone, Pacific Research Laboratories Inc.).⁸⁹

E.1.III. Reciprocating saw

During the exploring test, a reciprocating saw with a saw blade (microspeed uni, Braunn Aesculap) as applied during current surgery was used during this test. (Fig. 3) The dimensions and properties of this instrument was already discussed in Appendix B.2.



Figure 2. The reciprocating saw with a saw blade (microspeed uni, Braunn Aesculap) as applied during the exploring test.³⁸

E.2. Methods

E.2.I. Dimensions bone blocks

A synthesized bone block with dimensions of 190x120x44 mm was processed by a computer numerical controlled milling machine (CNC milling machine) into nine slices of 12x90x35 mm. (Fig. 1) The thickness of the slices (12 mm) corresponds to possible thicknesses of both the fibula and the mandible, as discussed in section C.1., On

the contrary, the height of the slices (35 mm) is doubled in comparison with the anatomies involved. An increased height of the bone block surface will provide more information, since a larger surface can be analyzed. An increased amount of information is suspected to aid in distinguishing between the bone block surfaces obtained with the different designs. The width of the small bone blocks corresponds to a reasonable width of a harvested fibula graft and allows multiple osteotomies without interference of the trajectory of two bone osteotomies. The obtained osteotomy trajectories and surfaces will be analyzed in terms of smoothness and deviation from the planned trajectories.

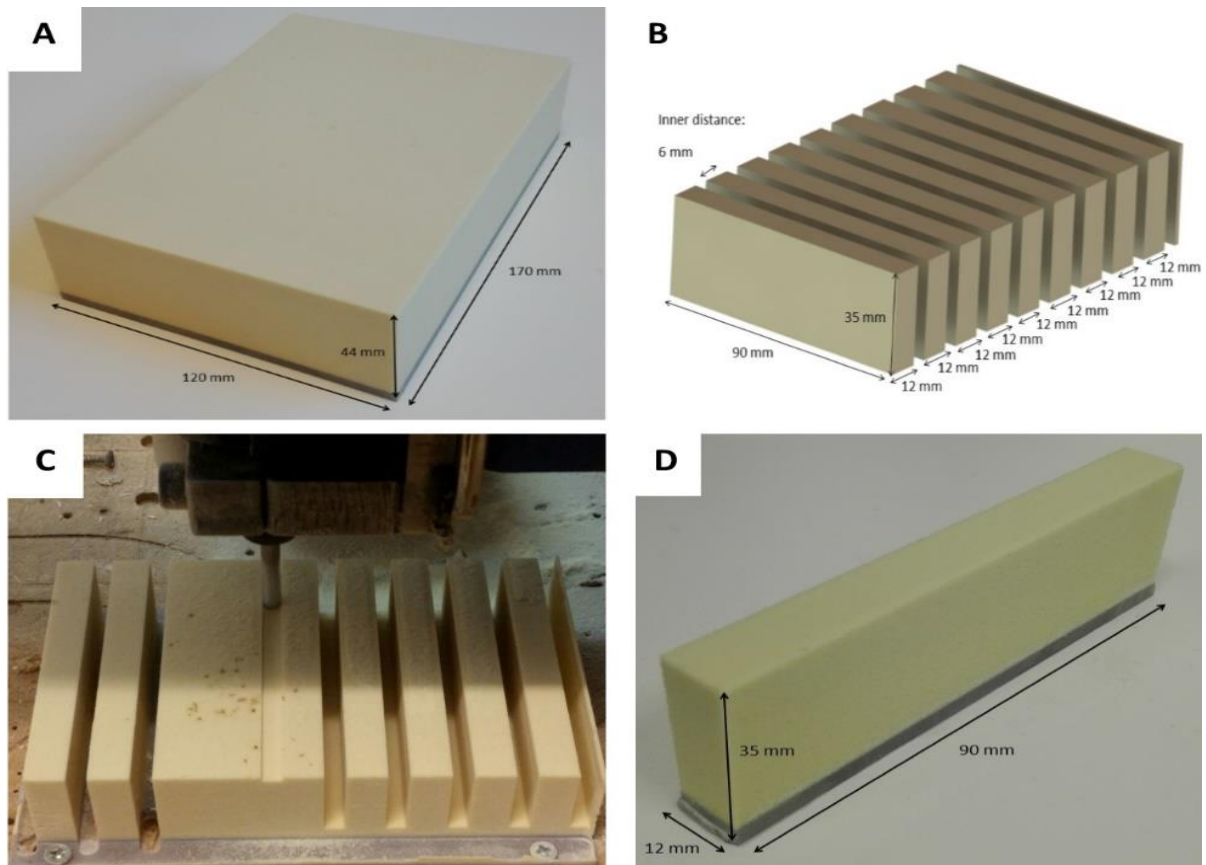


Figure 1. A) An unprocessed synthesized bone block with dimensions as indicated. B) Planned segmentation of the bone block into slices with dimensions as presented. C) The bone block being processed into 9 slices by a milling machine. D) The obtained bone block slices with dimensions as indicated.

The dimensions of nine sliced bone blocks were measured three times by a digital caliper, as presented in figure 2. (Powerfix Profi+). The mean dimensions that were measured are presented in table 1. These dimensions could be used to create simulated bone blocks that represent the planned osteotomy trajectories and thereby act as reference blocks. Within this study, the simulated bone blocks were created using SolidWorks since this program was also applied for creating the models, thus the locations of the resection sleeves are known. The expected osteotomy trajectory can be based on these locations, when an incision width of the saw blade of 0.35 mm is applied. (Fig. 3) The distance between two sleeves are combined with the measured bone block thicknesses and heights to generate dimensions that represent the planned osteotomy trajectories and surfaces.

Table 1. Dimensions found for nine sliced blocks (A to I).

Block	Mean width (mm)	Mean height (mm)
A	11,97667	34,99
B	11,97	34,94
C	11,99333	34,76167
D	11,64167	34,54833
E	11,9	34,67833
F	11,79167	34,935
G	11,89167	34,935
H	11,73667	34,88833
I	11,83	34,86667

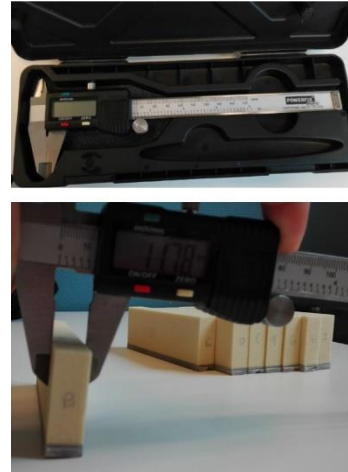


Figure 2. The measuring method for measuring the dimensions of the sliced bone block.

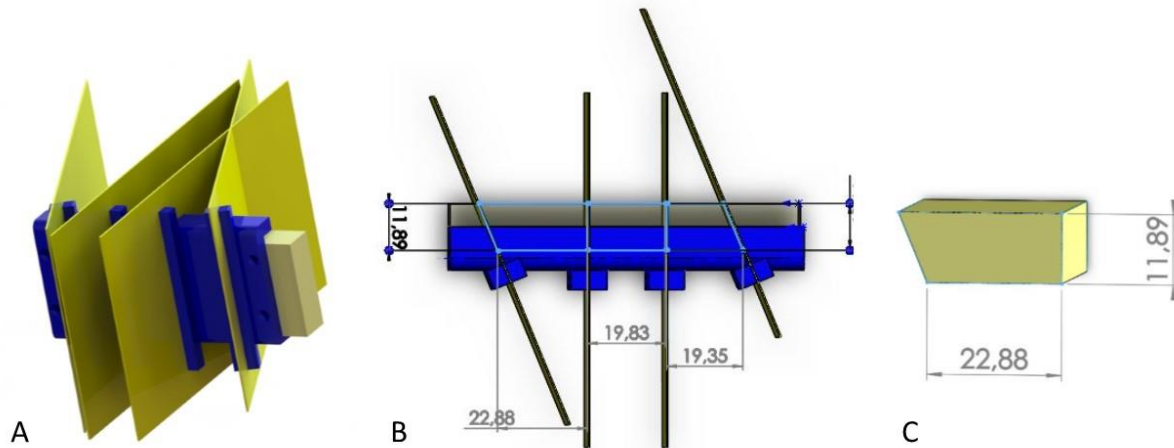


Figure 3. The process of creating simulated bone blocks that represent the planned osteotomies. A) The model situated on a bone block with dimensions that correspond to the values presented in table 9, additionally, simulated osteotomy planes with a thickness of 0.35 mm are sketched. B) The resulting width of the simulated bone blocks, in this case for concept 1, normal guidance. C) The resulting simulated bone block with dimensions corresponding to the width found in B, and the thickness and height of the involved bone block as measured in table 9.

E.2.II. Laser surface scanner

It is hypothesized that a sufficient performance of a concept can be detected as a straight, smooth, and plain surface that corresponds to the planned osteotomy trajectory. The osteotomy surface can be scanned and converted into a virtual 3D model by a laser surface scanner (D500 3D scanner, 3Shape, Copenhagen, Denmark).⁹⁰ The laser surface scanner applies two 1.3 MP cameras and a red laser to obtain a high resolution 3D virtual model. Accuracies of 10 μ m are claimed by the company.³⁹ With this scanner, the synthesized bone block can be scanned and the surface can be retrieved that is obtained after performing an osteotomy. The scanned blocks including the resected surfaces can be exported in a stereolithographic format (STL-file) to allow calculations and manipulations using computational software.

E.2.III. Performing the test

The templates were fixated on the bone blocks according to the method applied during real surgery. (Fig. 4)

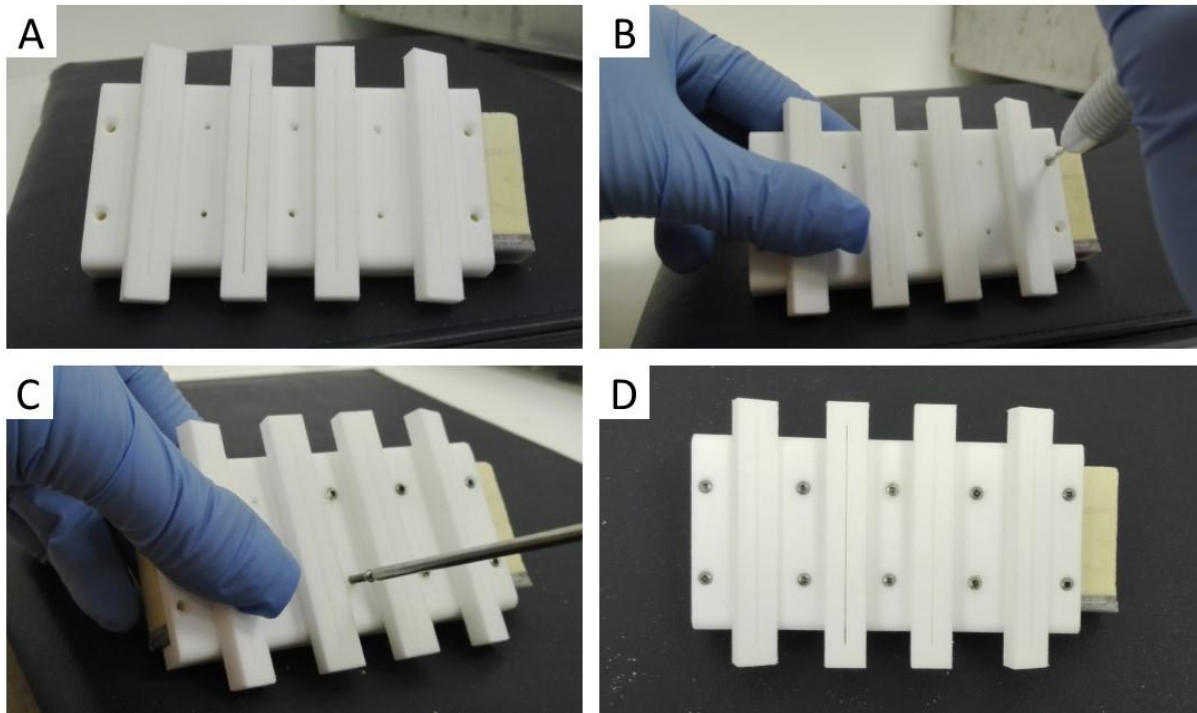


Figure 4. Fixation of the resection templates on the bone blocks. A) The initial placement of the template on the bone block. B) Pre-drilling the holes. C) Screwing the template on the bone block. D) Fixated template on the bone block.

Then, osteotomy was performed using the middle two guiding sleeves using a reciprocating saw and saw blade. (Fig. 5) The experimental set-up is presented in figure 28. The bone blocks with models are temporarily fixated into a vise, to reduce chance of variance due to different angles of insertion.

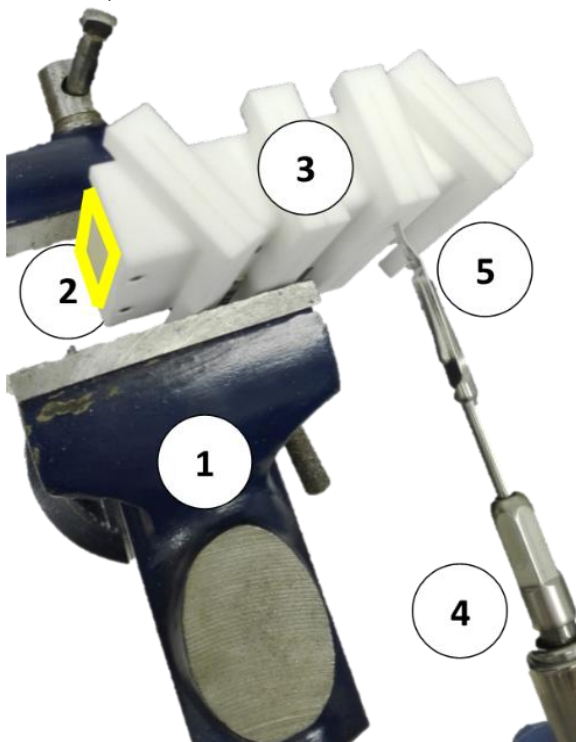


Figure 5. The experimental set-up as applied during the exploring test. The set-up includes a vise (1), in which a piece of Sawbone (2) with a fixated template is fixated (3), and a reciprocating saw (4) with a type of sawblade that is applied during surgery (5).

E.2.IV. Evaluation of the concepts

Distance mapping

After performing osteotomies by the reciprocating saw, the bone block was segmented into five segments. Each segment was scanned by the laser scanner and converted into a STL format. These STL-files can be imported into software (Maxilim V2.3.0.3, Medicim NV, Mechelen, Belgium) to apply a surface-based registration algorithm between two STL files. The other STL file used for this registration is a planned bone block that was simulated in SolidWorks, as described in appendix E.2.III. After surface-based registration, the surfaces of two models are aligned and a distance map between the surfaces can be obtained. This distance map shows the correspondence between the two inserted 3D models, by creating a point cloud of the models, and measure the distances between the points of both clouds. In this study, the surface of the bone block that was obtained after osteotomy was registered on the planned osteotomy surface of the simulated bone block. (Fig. 6, 7) Therefore, the distance map retrieved in this study is a measure of the performance of a template in successively guiding the reciprocating saw during osteotomy.

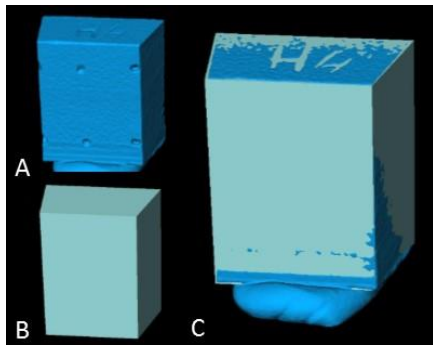


Figure 6. The registration of surfaces according to the surface-based registration algorithm of Maxilim. A) The real resected bone block. B) The simulated resected bone block that defines the planned resection surfaces. C) Resulting registration of the simulated bone block on the real bone block.

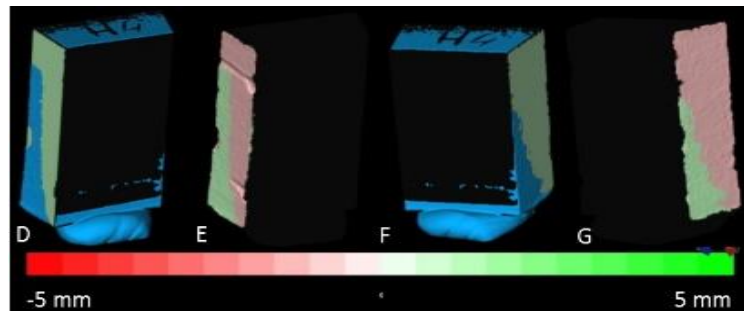


Figure 7. Distance maps of the registered surfaces in a range from -5 mm to 5 mm, using a point-cloud. D) The registration of the left resected surface. E) The resulting distance map of the left resected surface to the planned osteotomy surface. F) The registration of the right resected surface. G) The resulting distance map of the right resected surface to the planned osteotomy surface.

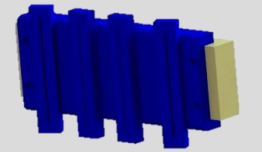
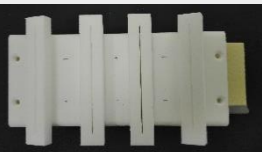
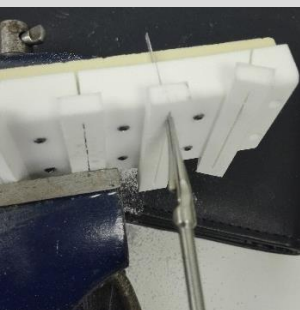



E.3. Results

During the exploring test, several design requirements could be scored according to the use and performance of each design. Remarks about the ease in use or performance of the concepts and some examples of the things that were noticed during the test are presented in table 3. The performance of a concept was mainly assessed by the accuracy of the osteotomy using the distance map values. The distances were put in a distance kit. The distance kits contain the distances between all points of the surfaces and represent the amount of correspondence between the planned and the obtained osteotomy surfaces. The accuracy was scored on the resulting ranking of concepts with regard to their mean value, standard deviation and 95 percentile of the calculated distances of the distance kit. Lower distances represent a better match between the planned and the obtained surface, and vice versa. (Table 2)

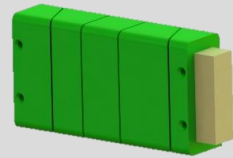
Concept	Mean (absolute)	SD	Mean+SD	95th percentile	Resulting ranking
A	0,5840	0,6103	1,1943	1,4269	5
B	0,3357	0,9428	1,2785	0,4995	4
C	0,4229	1,0037	1,4266	1,1869	6
D	0,3009	0,6968	0,9977	0,7068	2
E	0,3054	0,6030	0,9084	0,5601	1
F	0,3279	0,6983	1,0263	0,5545	3

Table 2. Results of the exploring test with regard to the absolute mean, standard deviation and 95th percentile, as retrieved from the distance kits. The resulting ranking represents the accuracy of the design, with the highest rank for the design that performs most accurate according to the match between the planned and obtained osteotomy surface.

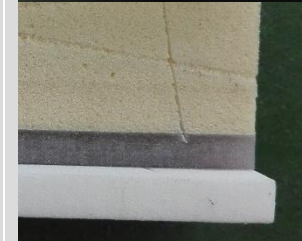
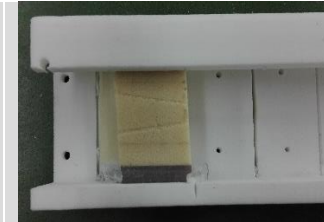
Table 3. The experimental set-up of the exploring test, the, results, remarks and photographic evidence of the remarks.

Concept choice	CAD and CAM model	Experimental set-up	STL	Remarks	Examples
A. Current design	 			Deviations occurred during the osteotomy, the osteotomy trajectory is not straight, as can be noticed by the naked eye.	
B. Reduced sleeve width	 			The design was easy in use, the bone saw did not get stuck in the reduced sleeve width	

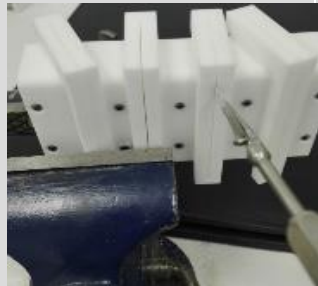
C. Increased contact area



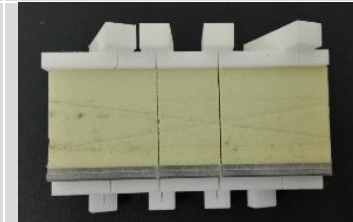
1. Bad sight during cutting
2. Vise got loose during cutting
3. One segment got stuck after cutting
4. One osteotomy could not be performed fully, the osteotomy to create segment 1 and 2 could only be fulfilled after the template was removed.



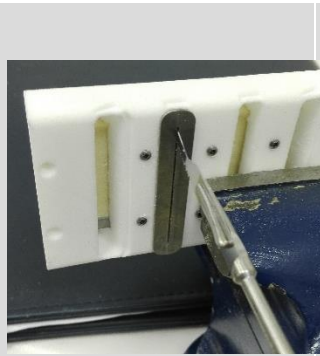
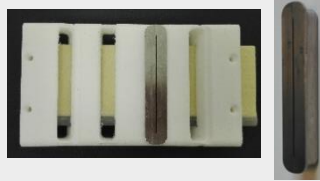
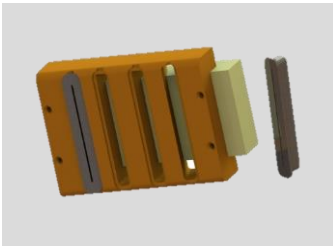
D. Additional top guidance



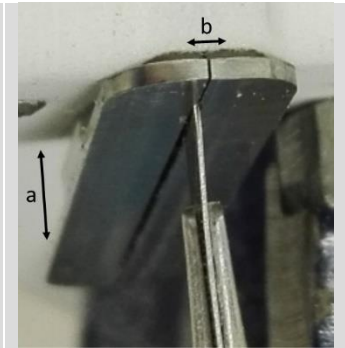
The outer cutting sleeves had a bad fit in the vise. This may have impact on the fixation and the performance of the design, since the design may move in the vise during a bone cut.



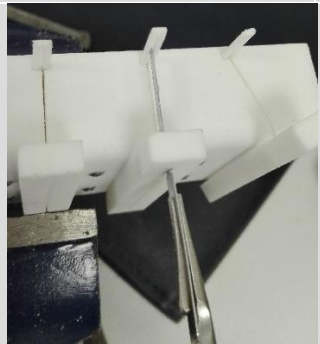
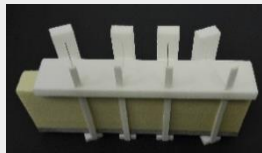
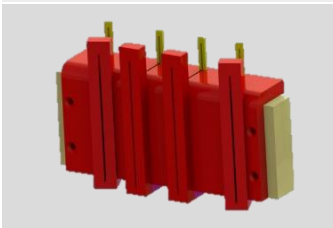
E. Enforcing titanium insert



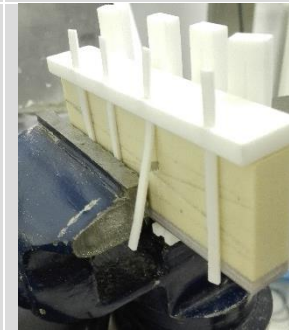
Due to a loose fit of the titanium insert into the template, two situations occurred:
 a) The titanium insert vibrated out of the template and the insert required manual pressure to keep it at the intended location. b) The connection of the two parts that create the cutting sleeve became loose. Therefore, it is encouraged to reduce the width of the template to 6.50 mm



F. Bone-contouring guidance



The 3D-printed model requires lots of adjustments to create a fit between parts. Additionally, the back sleeve is flexible, and the designed connection between back sleeve and under sleeve was not sufficient.



The resulting osteotomy trajectories of the six different concepts that were included in the exploring test were photographed to retrieve a global impression about their performance to guide the reciprocating saw. (Fig. 8) Furthermore, complications such as template material failure were registered.

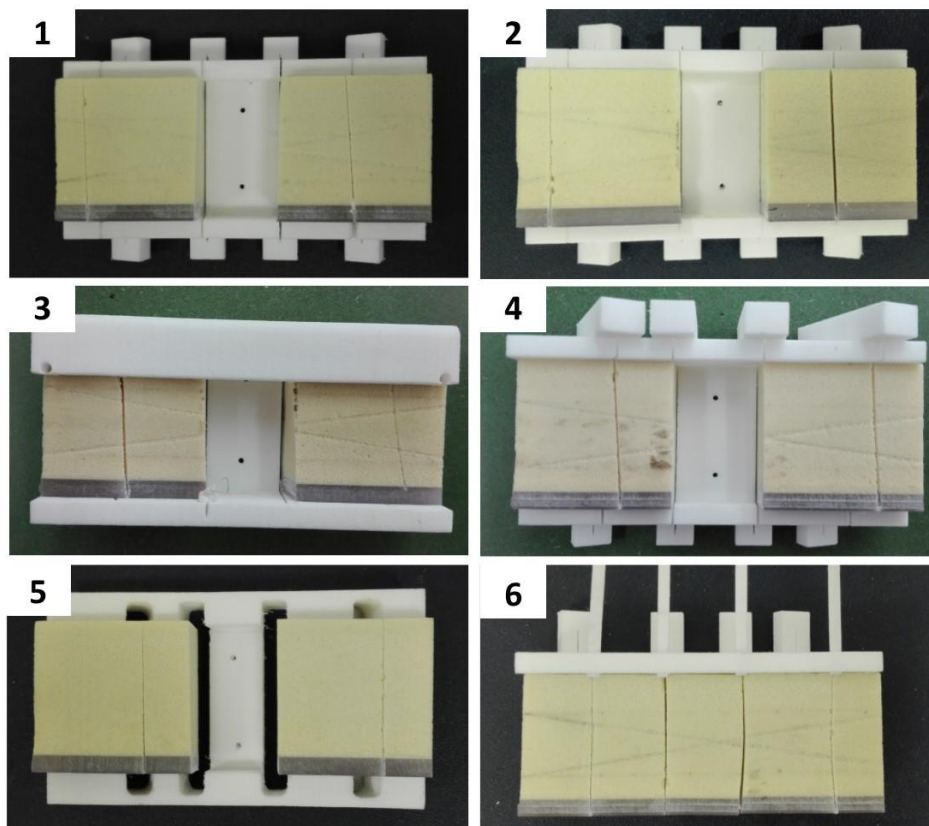


Figure 8. The visualization of the resulting osteotomy trajectories of the six different concepts that were included in the exploring test. 1) Concept A, the current template, 2) Concept B, reduced sleeve width, 3) Concept C, increased contact area, 4) Concept D, top guidance, 5) Concept E, titanium insert, 6) Concept F, bone contouring guidance

E.4. Discussion

According to the ease in use, the obtained remarks and the performances of each design resulting from the exploring test, the scoring table was completed. (Table 4)

The exploring test provided insight in (dis)assembly time, time required for correct placement, the amount of feedback provided to the surgeon, the strength of the design according to withstanding the forces of the saw blade, the usability of the design and the simplicity of the construction. As described in table 3, concept B did not introduce major user changes in comparison with the current concept. However, it did improve the current concept, what should not be surprisingly since the design tackles the gap between the saw width and sleeve width, thereby reducing the amount of possible angulations of the saw blade.

The increased contact area of concept C eliminated the sight on the bone block. There was less visual or haptic feedback provided by concept C in comparison with the current design, while it was basically expected that this concept would increase feedback. Additionally, it was easy to cut into the template of concept C, and the resulting debris led to a stuck bone block inside the template. This all may contribute to the resulting lowest rank in accuracy as presented in table 2. Therefore, concept C was scored lowest in strength of the design, and scored lowest in safety and accuracy.

On the contrary, the top guidance from concept D was easy in use and allowed more visual and haptic feedback as a result of the additional and elongated guidance towards the saw at the top. The model achieved a high accuracy even though the model did not achieve a good fit in the vise. Therefore, it will be a little safer in use than concept C.

Concept E scored best in accuracy, however, the titanium insert did become loose during use because of a loose fit of the insert into the design. Therefore, it was suspected that even an improved accuracy will be achieved when a better fit is obtained.

The construction of concept F, the bone contouring guidance, for which the guidance from the back is the major change and most important working part, did not work properly. The man-female pin connection acts in the same direction as the lateral vibrations of the reciprocating saw, which leads to a loose connection. Additionally, the back sleeve was flexible and the depth was not sufficient to restrict the saw blade in horizontal movements. However, this concept achieved rank 3 in accuracy and is most inventive regarding to safety. Therefore, it is still a promising alternative to the current concept.

Table 4. The completed scoring table with the design requirements from chapter 3, and the scores given in compliance with the scoring guidelines described in table 8, at the beginning of this chapter. The best scoring concept are highlighted in bold.

<i>Requirement</i>	<i>Weighing factor</i>	<i>Score Concept A: Current</i>	<i>Score Concept B: Smaller</i>	<i>Score Concept C: Contact</i>	<i>Score Concept D: Top guidance</i>	<i>Score Concept E: Titanium</i>	<i>Score Concept F: Contouring</i>
<i>Usability</i>	8	8	8	7	8	7	5
<i>Adjustable to anatomy shapes</i>	6	5	5	5	5	5	5
<i>Haptic feedback</i>	8	4	5	3	5	5	9
<i>Ischemia time / disassembly time</i>	8	8	8	8	8	7	5
<i>Sterilization</i>	6	8	8	8	8	7	8
<i>Biocompatible</i>	8	9	9	9	9	9	9
<i>Safety</i>	9	5	5	3	5	5	9
<i>Accuracy</i>	10	5	7	6	9	9	8
<i>Simple production method</i>	7	9	9	9	9	6	7
<i>Simple construction</i>	6	10	10	7	9	8	5
<i>Resistant material</i>	9	6	6	6	6	9	6
<i>Total score (%)</i>	850	582	610	540	624	602	596

E.5. Conclusion: Concept selection

From table 5, concept B, “smaller guidance” and concept D, “top guidance” scored considerably higher in comparison with the current concept (concept A). However, since the requirements of accuracy and safety are of major importance to improve the surgery and surgical outcome, it was chosen to select, adjust, and test concepts E, “titanium insert, and concept F, “bone contouring guidance”, as well in the next phase.

Appendix F. Design choices

As described in *Appendix E*, multiple concepts were promising in improving the current design. Therefore, this section discusses the design choices that were made. All sharp edges at the inner surfaces of the concepts were altered into a notch, to smoothen the connection between the bone block and the template. (Fig. 1) Concept F, “bone contouring guidance” that was assessed during the exploring test did not work properly. The man-female pin connection between the back and bottom was not sufficient, and the back sleeve was too shallow and flexible. To solve these problems, two different principles were created for this concept, as will be described in section F.1 and F.2. Because concept B, “reduced sleeve width”, and concept D, “additional top guidance” both achieved a high score with regard to the requirements of major importance and the total score according to the scoring table, these were combined into a new design, as discussed in F.3.

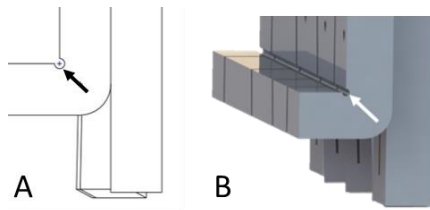


Figure 1. A: Schematic drawing of the notch that was created at the inner surfaces of the templates, to smoothen the connection between the template and the synthesized bone block. B: The CAD model of the notch.

F.1. Design 1 – Backguidance 1

The working principle of the design as presented in figure 2 is based on the concept of bone contouring guidance, except the bottom guidance was eliminated. The back sleeve was preserved, since this can replace the periosteal elevator that is currently applied as a non-controlled safety measure to protect the periosteal artery at the back of the fibula during segmentation of the bone, as described in appendix C.2.IV. Within this design, the shape of the gap and the design of back sleeve are adjusted. The sharp edge of the gap was altered into a notch for a smoother insertion of the back sleeve. Furthermore, the thickness of the sleeve was increased to achieve both a deeper sleeve to restrict the lateral movements of the saw blade as well as to increase the stiffness of the back sleeve. Additionally, the connection of the back sleeve to the front sleeve was altered. Within this design, a conical connection was introduced. By pushing the back sleeve from the top to the bottom, the sleeve will eventually get stuck and is connected to the rest of the model. The back sleeves are identical, and the amount of back sleeves required corresponds to the amount of resection sleeves at the front. Additionally, to suppress the manufacturing costs of this design, reuse of a back sleeve may be possible.

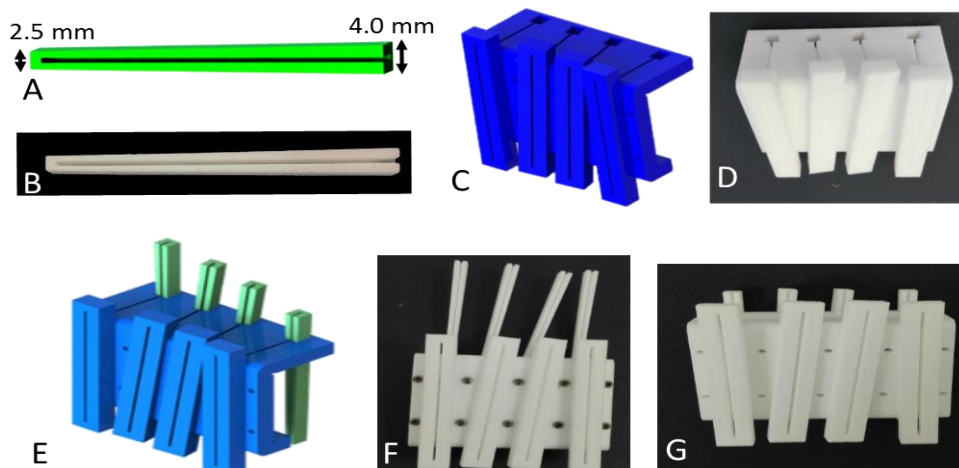


Figure 1. A) CAD model the back sleeve of design “backguidance 1”. B) 3D printed model of back sleeve of design “backguidance 1”. C) CAD model of the major part of the template. D) 3D printed model of the major part of the template. E) The assembled CAD model. F) G) The assembled 3D model.

F.2. Design 2 – Backguidance 2

The working principle of this design as presented in figure 3 is similar to design 1. However, another connection was introduced. Within this design, the man-female pin connection was introduced once again. On the contrary of the original bone contouring guidance, this connection is located at the top of the model, instead of at the back as applied within the concept this design is based on. Therefore, it should not interfere with the lateral movements during vibrations of the saw blade during osteotomy. Thereby, the connection will be maintained during osteotomy. Additionally, the back guidance sleeves are a unity. This provides inter distance control between the back sleeves and should improve the correspondence between the front and the back sleeves.

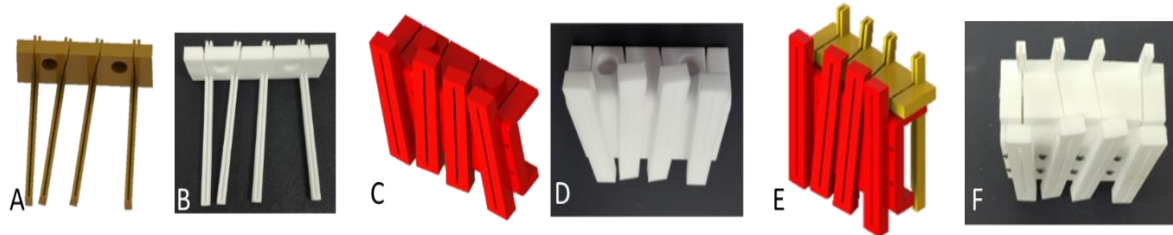


Figure 2. A) CAD model the back part of design “backguidance 2”. B) 3D printed model of back part of design “backguidance 2”. C) CAD model of the major part of the template. D) 3D printed model of the major part of the template. E) The assembled CAD model. F) The assembled 3D model.

F.3. Design 3 – Smaller top guidance

This design as presented in figure 3 implies both best assessed conceptual ideas during the exploring test, concept B, “reduced sleeve width” and concept D, “Top guidance”. The design provides guidance from the top, while the sleeve width is reduced. Thereby, mainly the angulations of the saw blade will be tackled. By these measures, the saw blade will be restricted to angulate within the guiding sleeves. Moreover, the design has no major differences in shape or ease in use from the current design, thus it is suspected to this design is easily adapted by the surgeon.

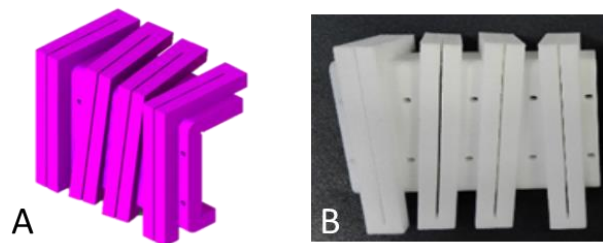


Figure 3. A) CAD model of design “smaller combined with topguidance”. B) 3D printed model of design “smaller combined with topguidance”.

F.4. Design 4 – Current model

The current design as presented in figure 4 is also included within this test phase, to create a reference framework. The newly designed models can be compared with this model and their performances can be assessed.

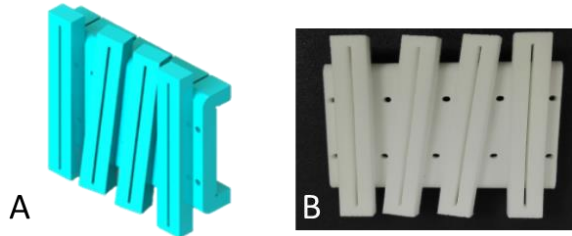


Figure 4. A) CAD model of design “current model”. B) 3D printed model of design “current model”.

F.5 Design 5 – Titanium insert

The dimensions of this design were adjusted to provide a more tight fit of the titanium insert into the model. Thereby, the titanium insert should not get loose during osteotomy, as occurred during the exploring test. Therefore, it is suspected that an even more accurate osteotomy will be obtained. The CAD/CAM models are presented in figure 5.

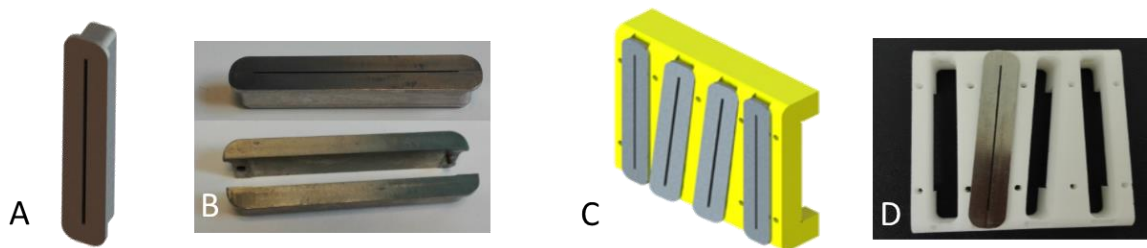


Figure 5. A) CAD model of design “titanium insert”. B) 3D printed model of design “titanium insert”.

Appendix G. Evaluation of the design choices

The proof of principle of all design choices that were made in appendix F, are assessed simultaneously to the method that was applied during the exploring test. However, a larger sample size of osteotomies is required to provide sufficient power and create a statistical significant outcome of the test.

G.1. Materials

The same materials are applied during the exploring test were applied for both the models as well as the synthesized bone blocks. Thus, the synthesized bone block consists mainly of solid and rigid polyurethane foam with a thin fiber filled epoxy sheet, which is a mixture of short glass fibers and epoxy resin (Sawbone, Pacific Research Laboratories Inc.) The models are printed using a white polyamide (a mixture of PA 2200 with PA 12, Oceanz).⁴⁷

G.2. Methods

G.2.I. Dimensions bone blocks

A similar synthesized bone block as applied for the exploring test, with equal dimensions of 190x120x44 mm, was simultaneously processed by a milling machine. However, to provide a larger sample size, the block was divided into 20 slices with dimensions of 11.5x54x30 mm. (Fig. 1) The thickness of the slices (11.5 mm), the width (54 mm) and the height (30 mm) were required to create space for a sufficient fixation of the block to allow good performance of the milling machine. These dimensions still correspond to realistic dimensions of both the mandible and the fibula, while the height is set maximal to create a larger surface for the analysis of the osteotomy trajectory.

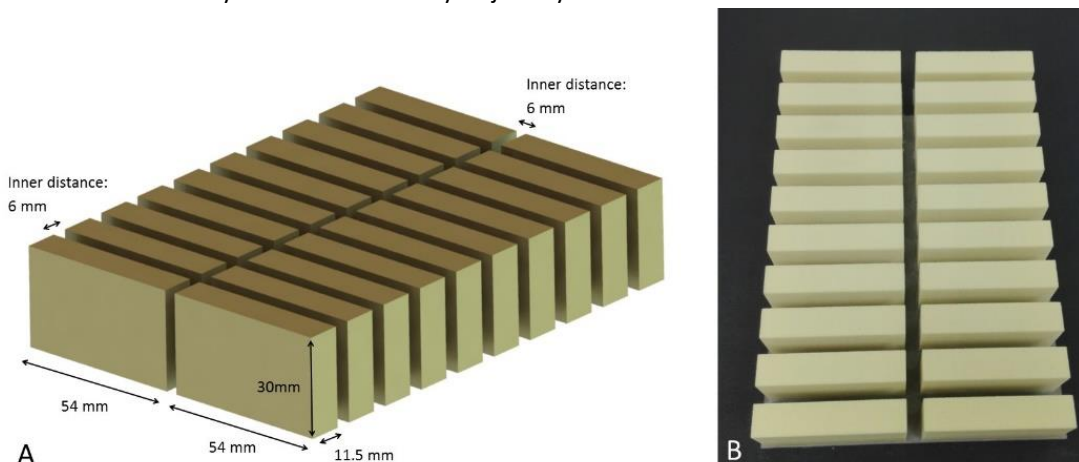


Figure 1. A) The planned segmentation of the bone block, with dimensions as sketched. B) The obtained segmented bone block, as processed by the milling machine.

Simultaneously, the dimensions of the bone blocks were measured by a digital caliper. (Table 1) These dimensions were once more required to create the simulated bone blocks, on which the real bone blocks could be matched to determine the accuracy of the osteotomy trajectory.

Table 1. The dimensions found for the twenty sliced bone blocks.

block	Mean (mm)	thickness (mm)	Mean (mm)	height (mm)	block	Mean (mm)	thickness (mm)	Mean height (mm)
a1	11,55		30,215		c1	11,49		30,235
a2	11,45		30,25		c2	11,435		30,205
a3	11,41		30,245		c3	11,44		30,15
a4	11,45		30,235		c4	11,44		30,195
a5	11,46		30,22		c5	11,455		30,21
b1	11,45		30,19		d1	11,55		30,2
b2	11,45		30,2		d2	11,455		30,21
b3	11,47		30,24		d3	11,44		30,235
b4	11,52		30,21		d4	11,45		30,23
b5	11,57		30,255		d5	11,71		29,225

Additionally, the resection sleeves of the model were manipulated in such a way that an angulation of insertion is introduced, in both the XY-direction as the YZ-direction. During the exploring test, only an angulation in the YZ-direction was introduced. Therefore, the method for creating the simulated bone blocks needed to be adjusted as well. This method is described and visualized in figure 2.

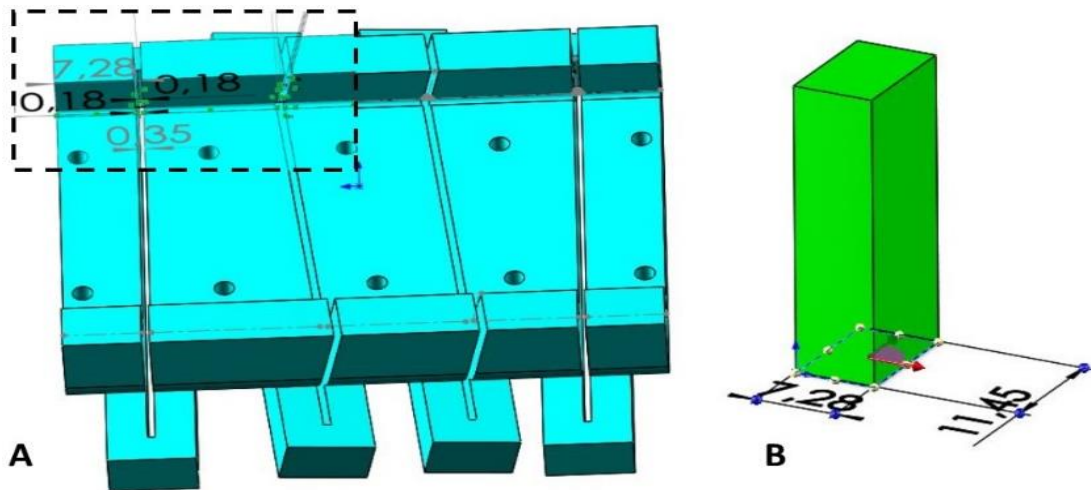


Figure 2. An example of the methodology applied to generate simulated bone blocks that will act as reference blocks. A) The designed model in SolidWorks can be used to determine the width of the bone block that will be applied for matching in Maxilim. According to this method, the simulated bone block a4 should have a width of 7.28 mm. B) The resulting simulated bone block with a width of 7.28 as determined in the designed model, and a thickness of 11.45 as retrieved from table 13, block a4.

G.2.II. Performing the test

Simultaneous methodologies as performed during the exploring test were applied for fixation of the templates on the bone blocks, osteotomy of the bone blocks, and the processing of the obtained resected smaller bone blocks, as described in Appendix E.2. (Fig. 3) Five designs were tested and every design contained four resection sleeves, of which two were angulated and two were straight. Because 20 sliced bone blocks were created for this test, each design could be tested four times. Thereby, eight equally angulated and eight straight cuts were performed.

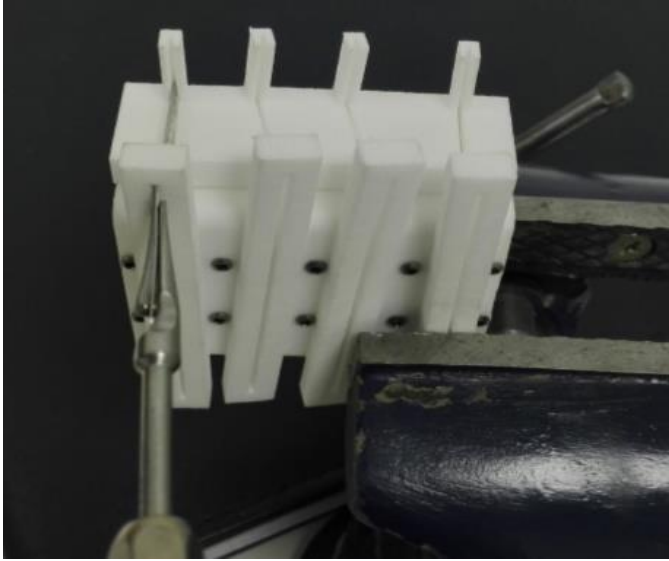


Figure 3. Design 1, "backguidance 1" during the test. It can be noticed that the backsleeve keeps the saw blade in the correct direction, even though the handpiece is a little angulated.

G.2.III Design evaluation

Two different methods were applied to analyze the performance of each design according to their accuracy with regard to the osteotomy trajectory. Once again, distances were calculated between the obtained and the planned trajectories. Furthermore, since literature search showed that during osteotomy, the osteotomy trajectory may angulate up to 5.43° , the angulation of the trajectories was assessed as well.⁴¹

Therefore, besides evaluating the distance between the planned osteotomy surface and the obtained osteotomy surface, a region of interest is the angulation of the osteotomy surface with regard to the obtained surface. This can be evaluated using the yaw, pitch and roll of the obtained trajectory and their deviations from the planned trajectory. (Fig. 4) The roll deviation represents the extent to which the osteotomy trajectory is followed from the front to the back of the bone block. The pitch deviation describes the performance of following the trajectory regarding to deviations to left and right. From the yaw deviation, the trajectory from the top to the bottom can be analyzed.

To retrieve those angulations, normal vectors of the surface of both the planned as well as the obtained surfaces were created. The normal vectors were averaged into one normal vector and a plane was drawn perpendicular to this normal vector. The plane of the obtained surface was compared to the plane of the planned surface, and differences in the yaw, pitch and roll were calculated. (Fig. 5)

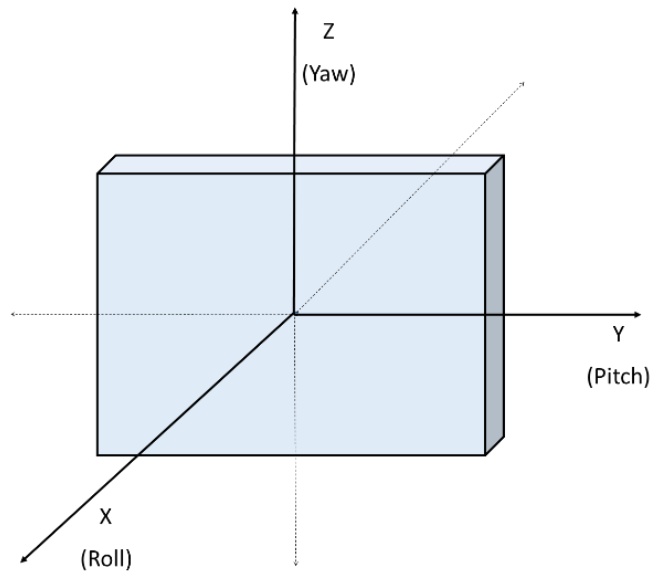


Figure 4. The yaw, pitch and roll of the planes used to determine the angulations of the obtained osteotomy trajectory in comparison with the planned trajectory.

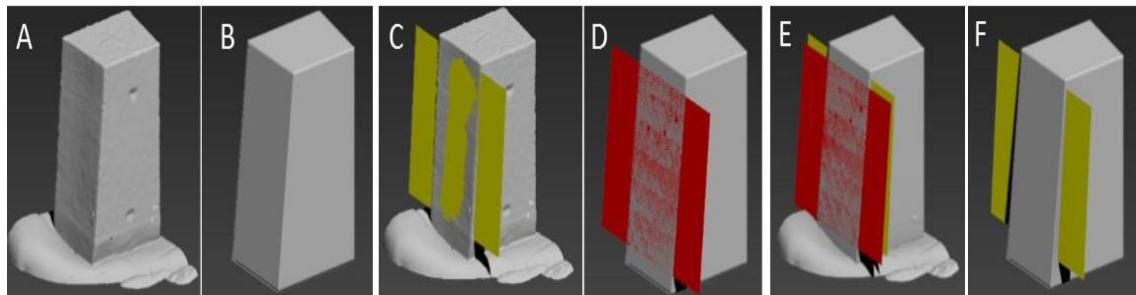


Figure 5. The method of calculating the angulation of the osteotomy trajectory. A) The obtained bone block as scanned by the laser surface scanner. B) The planned bone block. C) The obtained osteotomy plane perpendicular to the calculated averaged normal vector of the resected surface. D) The planned osteotomy plane perpendicular to the calculated averaged normal vector of the planned surface. E) The difference in angulation of both planes that can be calculated. F) The obtained osteotomy plane compared to the planned bone block that contains the planned osteotomy trajectory.

G.3. Results

After performing the four osteotomies using each of the five designs, the osteotomy trajectories were photographed to generate a global impression of their ability of guiding the reciprocating saw and obtain the planned osteotomy trajectory. (Fig. 1) Furthermore, the behavior of the designs were studied and filmed during the osteotomy, of which remarks were noted.

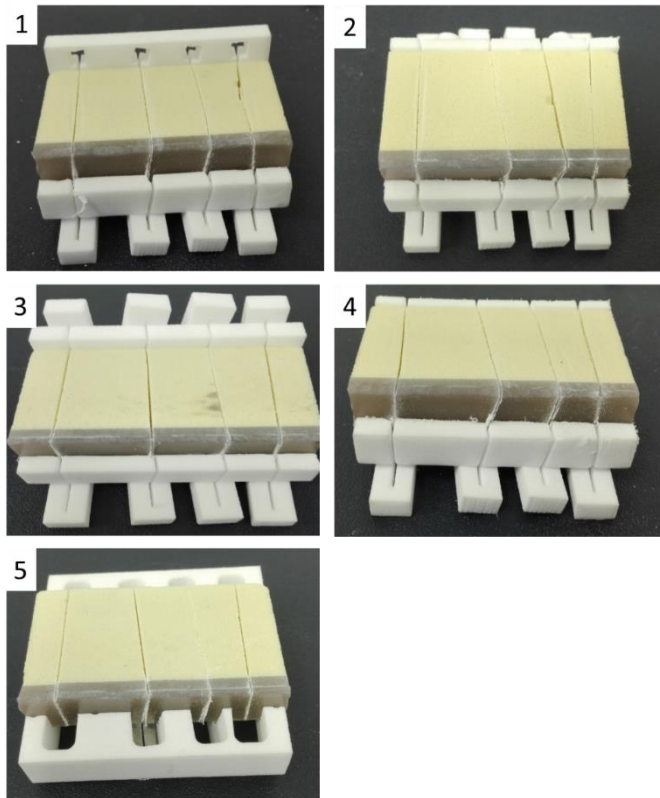


Figure 1. The visualization of the resulting osteotomy trajectories of the five different design that were included in this experiment. 1) Back guidance 1, 2) Back guidance 2, 3) Smaller combined with top, 4) Normal guidance, 5) Titanium insert.

G.3.I. Usability and adaptability

Because all designs are based on the current design and no major changes are introduced with regard to their use, the amount of training time to apply each design is assumed be equal. Furthermore, each template is adjusted and shape-fitted to the scans retrieved from the patient, thus each template is adaptable to the anatomies involved.

G.3.II. Biocompatibility, clean ability and sterilization

All designs are made of PA 2200, a material that fulfills the requirement according to biocompatibility. Additionally, PA 2200 is a material that melts at 176°. Therefore, all designs are suitable for sterilization by means of autoclave steam. Furthermore, the lumens, gap sizes relative to their depth, are similar and sufficient to allow appropriate cleaning and sterilization.³⁷

Solely design 5, “titanium insert”, which is intended to be reusable to may compromise these requirements. However, it is designed in such a way, that the titanium insert can be disassembled in two parts to allow sufficient cleaning and sterilization. (Fig. 2)



Figure 2. A disassembled titanium insert, to allow appropriate cleaning and sterilization.

G.3.III. Simplicity, production method and costs

Because design 1 to 4 and the base of design 5 are manufactured using PA 2200, their production method and costs will be similar. Designs “backguidance 1” and “backguidance 2” both consist of multiple parts, and it is suspected that a multi-part design may compromise the simplicity and production costs. However, it is presumed that these design fulfill the design requirement to keep the production costs under 500 euros, since both material and production method are at relatively low cost. Furthermore, because design 5, “titanium insert” introduces a titanium part that needs to be manufactured as well. Therefore, both the production and the costs will increase for design 5, “titanium insert”. However, because the part made of titanium is presumed to be reusable, also this design will keep production costs within boundaries.

G.3.IV. Ischemia time

The ischemia time, the duration that the blood supply of the fibula graft is disrupted should not exceed 100 min to ensure survival of the bone and skin flap.¹⁰ Design “backguidance 1” and “backguidance 2” may compromise this duration, because they require additional placement of backguidance sleeves between the fibula graft and the peroneal artery. However, this principle is based on the placement of a periosteal elevator that is already performed during surgery as safety measure to protect the peroneal artery. Using these designs, the surgeon has to create space for a backsleeve instead of a periosteal elevator. Therefore, it is suspected that these designs does not compromise ischemia by exceeding the duration of 100 min.

G.3.V. Safety and strength

According to the requirements related to safety, each design is able to provide visual feedback during the osteotomy. Because all designs were manufactured of PA 2200, the safety features that are provided by the material is assumed to be similar. The shape is the only factor that could alter template strength with regard to withstanding vibrational forces of the saw blade. Two designs that are promising in increasing the safety during osteotomy are Design 1, “backguidance 1” and design 2, “backguidance 2”. Both designs aim at protecting the peroneal artery at the back of the fibula by the presence of back sleeves. However, design 2, “backguidance 2” did not perform sufficiently during the experiment, since a part of a backsleeve broke off. As a result, backguidance 1 is suspected to provide the best additional safety measure. (Fig. 3)

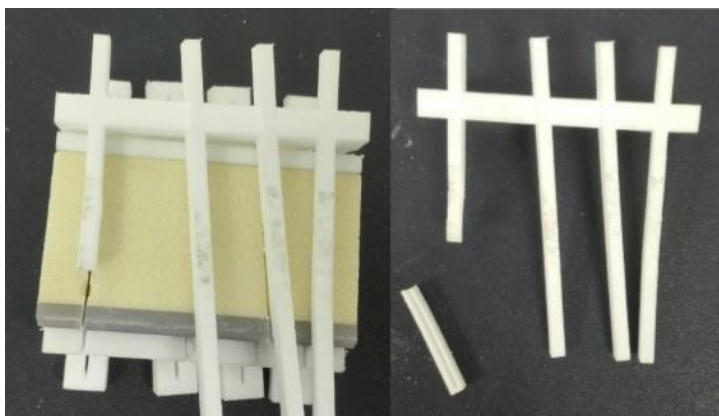


Figure 3. During the fourth and final use of the template to resect a synthesized bone block, a part of one of the sleeves at the back of design “backguidance 2”, broke off.

G.3.VI. Accuracy trajectory (statistics)

The experiment consisted of two parts, since there was a straight and an angulated osteotomy performed. Thereby, two type of datasets were created. Additionally, two methods were applied to assess the accuracy of the osteotomy.

These datasets are suitable for the ANOVA test, because over two models are compared, the acquired data is independent and distributed normally, and the model data has equal sample sizes with equally ranged standard deviations.⁹¹ To reduce the chance on a type 1 error (the error of rejecting a true null hypothesis) while comparing five models using the t-test, it was chosen to use the post hoc Tukey test to determine significant differences between the designs. The Post hoc Tukey test takes the number of means that are being compared into account.

For the distance kits of the straight osteotomies, no significant differences were found between the five designs. However, for the distance kits of the angulated osteotomies, a significant difference was found within the dataset ($p=0.023$). Therefore, a post hoc Tukey was added to localize if there are significant differences between one or multiple designs. From this test, design 3, “smaller topguidance” showed a significantly lower distance towards the planned osteotomy trajectory ($p=0.042$). The distance between the obtained trajectories with respect to the planned trajectories over four angulated cuts was 0.18 ± 0.11 mm (mean \pm SD). For the current design, a deviated trajectory of 0.30 ± 0.09 mm (mean \pm SD) was obtained. Therefore, it was assumed that design 3 achieves a higher accuracy during an angulated cut than the current design, according to the distance kit.

According to evaluation method 2, the deviation of the yaw, pitch and roll of the obtained trajectory in comparison with the planned trajectory were calculated. A significant difference was found within the dataset of the straight trajectories according to the roll ($p=0.001$). (Table 6) Therefore, a post hoc Tukey test was performed to localize if there are significant differences between one or multiple designs. From this test, it occurred the roll was better controlled by design 5, “titanium insert” ($p=0.001$). The current design caused an angulation of $1.24 \pm 0.19^\circ$ (mean \pm SD), while design 5 kept the roll within $0.32 \pm 0.07^\circ$.

Additionally, a significant difference was found within the dataset of the angulated trajectories according to the yaw ($p=0.014$) and pitch ($p=0.039$). The current design caused a yaw deviation of $0.25 \pm 0.32^\circ$ (mean \pm SD). Design 1, “backguidance 1” reduced this deviation to $0.07 \pm 0.16^\circ$ (mean \pm SD), ($p=0.05$). Design 3, “smaller topguidance” reduced this to $0.05 \pm 0.06^\circ$ (mean \pm SD), ($p=0.016$) and design 5, “titanium insert” reduced this to a deviation of $0.07 \pm 0.08^\circ$ (mean \pm SD), ($p=0.045$). Furthermore, the pitch was controlled better by design 1, “backguidance 1”, because the pitch was reduced from $2.14 \pm 1.81^\circ$ (mean \pm SD) of the current design to $0.85 \pm 0.84^\circ$ (mean \pm SD), ($p=0.017$) for design “backguidance 1”.

It can be concluded that all designs were able to bridge the intended bone thickness during the osteotomy. Furthermore, from the statistical analysis, all designs fulfill the requirement of keeping deviation of the osteotomy trajectory under $\leq 2^\circ$ or ≤ 5 mm from the planned trajectory. All generated designs seem to improve the current design, but not all findings were significant. Furthermore, different designs were suggested to perform best, according to the two types of osteotomy and the two evaluation methods. According to the angulated osteotomies, design 3, “smaller topguidance” was able to perform significantly better with regard to both the distance kit and the analysis of angulation. Also design 1, “backguidance 1” and design 5, “titanium insert” kept better control over the angulations of the angulated osteotomies. For the straight osteotomies, solely design 5, “titanium insert” had positive impact on controlling the angulation of the osteotomy trajectory.

G.3.VII. Discussion

Besides improving the reliability and accuracy of the trajectory, other advances can be made to improve this treatment. This study mainly focused on the interaction between the resection templates and the instruments.

Multiple designs of the resection template were generated to improve the reliability and accuracy of the osteotomy trajectory during mandibulectomy and mandible reconstruction with fibula graft segments. It can be concluded that all designs were able to bridge the bone thicknesses as were set in the design requirements, while deviations over the osteotomy trajectory were kept between boundaries. However, adjusting the design of the resection template is just one way, there are other ways to achieve a more reliable use of the resection template. Literature search has shown that other osteotomy devices are available with a higher accuracy, such as the Er:YAG laser and the piezoelectric device. However, it was argued that these osteotomy devices have difficulties in bridging the bone thicknesses that are involved within this treatment or require further development before they are suitable for clinical applications. Therefore, operating time may increase, which subsequently increases the chance on complications and graft failure.^{92,93,49} Furthermore the time required to perform an osteotomy was suspected to increase with these devices, this may compromise ischemia time. Therefore, it was chosen to use the reciprocating saw during this study. But when these devices are developed further, it may be of interest to get into this and test these devices as well.

From the experiment and evaluation, several designs within this study showed improvements towards the current design, even though the differences are small. The main aim of this study was a proof of principle, which is achieved and therefore the results may be interpreted as a promising area of improving the current treatment. Multiple designs are suggested as alternative to the current resection template according to improving the accuracy and reliability of the trajectory. However, besides improving the accuracy of the trajectory, it is important that the treatment is safe. It is important that the peroneal artery remains undamaged to increase the chance on survival of the donor bone and skin flap. Currently, a periosteal elevator is put between the fibula bone and the vessel to act as safety measure in protecting the vessel. The location of the elevator is solely determined by the surgeon, there is no base or reference point available to check if the location is correct. The saw blade slides easily next to this elevator, while no visual or haptic feedback of this occasion is provided towards the surgeon. The surgeon believes the vessel is protected and starts with the osteotomy.

Within design “backguidance 1”, the location of the back sleeves is controlled, thanks to a connection at the top of the template. Therefore, it is assumed that design 1 and 2 improve the safety in two ways in comparison with the current device. Design “backguidance 1” was not prone to the vibrations of the saw blade, and performed better according to the accuracy of the angulated osteotomy trajectory. Therefore, design “backguidance 1” is recommended for further development and clinical applications in future surgeries as alternative to the currently applied resection template. (Fig. 4)

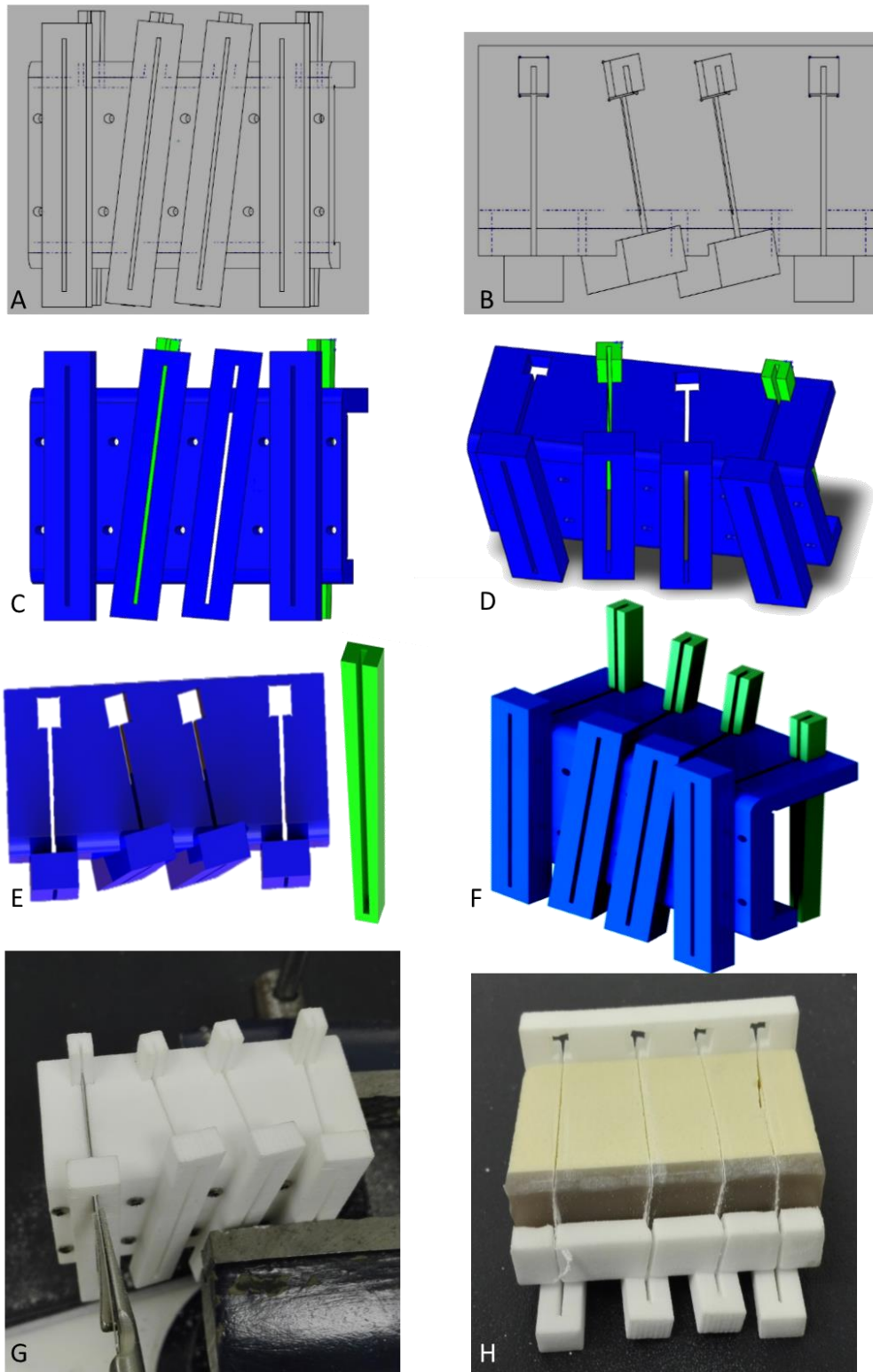


Figure 4. An overview of the recommended resection template as result from this study, design “backguidance 1”. A) Front view of schematic drawing. B) Top view of schematic drawing. C) Front view of partly assembled design in SolidWorks. D) Top view of partly assembled design in SolidWorks, the resection sleeve in the middle shows the planned trajectory and the correspondence between the front, top and the back sleeve. E) The rendered CAD design of both the template (left) as well as the back sleeve that should be put into the hole at the back (right). F) The assembled CAD design. G) The resection template in use during the experiment, it shows that the saw blade follows the trajectory, despite of an angulated insertion of the saw blade through the front sleeve. H) The resulting four osteotomy trajectories, resulting in five small synthesized bone blocks.

G.3.VIII. Recommendations

Most commonly, a sufficient reconstruction is obtained by angulated trajectories to create inter-angles between the fibula segments that can be formed into the shape of a mandible. Design “backguidance 1” performs best in controlling both the yaw and pitch of an angulated trajectory. Moreover, this design is most innovative by introducing a controllable protective measure towards the peroneal artery of the fibula. The back sleeves replace the periosteal elevator that is usually applied as protection. Since difficulties were detected by insertion of the straight elevator, it is recommended that design “backguidance 1” is adjusted to the shape of the fibula. A way of achieving this, is by introducing an angle of about 45° within the straight back sleeve. This is conform the surgeons that were involved during this study, they already adjusted the periosteal elevators manually to facilitate placement of the elevator behind the triangular-shaped fibula, without damaging the underlying peroneal artery. (Fig. 5)

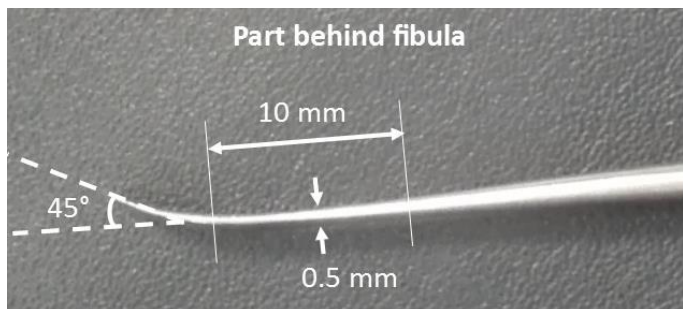


Figure 5. The currently applied periosteal elevator with an angle of 45°, on which the back sleeve is based on, to facilitate placement of the back sleeve behind the triangular-shaped fibula in front of the peroneal artery.

Furthermore, to control the location of the resection template on the mandible and fibula, it is proposed to use intraoperative navigation techniques and perform the osteotomy by a robotically controlled laser.⁴⁹ Using intraoperative navigation techniques, feedback towards the surgeon during placement of the resection templates can be provided. Additionally, the osteotomy trajectory can be loaded into software of the navigation system. This will improve the transfer between the virtually planned surgery and the operation theatre. However, because the space of making advances to improve this treatment lies in a range of 0 to 5 mm, these techniques should be further developed to make them sufficient for improving this treatment. During navigation guided osteotomy in the pelvis, still a difference of 2.52 ± 2.32 mm (mean \pm SD) between the planned osteotomy surface and the performed osteotomy surface was found.¹⁹ Additionally, according to a study of Baek et al. it was concluded that real-time interaction in terms of real-time monitoring and depth control of the navigation system and robot has to be improved before it is a reliable and safe method to assist during osteotomy.^{49,51}

Because resection template “backguidance 1” that was designed amongst others during this study can easily be adapted in the current treatment, it is recommended to develop this design further and test this template during a cadaver study.

Abbreviations

3D	– Three-dimensional
CT	– Computed Tomography
CBCT	– Cone Beam Computed Tomography, high resolution
CAD	– Computer-Aided Design
CAM	– Computer-Aided Manufacturing
CAS	– Computer-Aided Simulation
CNC	– Computer Numerical Control
CTA	– Cone Beam Angiography
DMLS	– Direct Metal Laser Sintering
DSMH	– Dutch Association for Experts Sterile Medical Devices
Er:YAG	– Erbium-doped Yttrium Aluminum Garnet
MRI	– Magnetic Resonance Imaging
ORN	– Osteoradionecrosis
PA 2200	– Polyamide 2200
SCC	– Squamous Cell Carcinoma
SLS	– Selective laser sintering, a production method to print a three-dimensional model
STL	– Stereolithography
TMJ	– Temporomandibular Joint

Glossary of terms

Term	Definition
Anastomosis	Connection of vessels
Autogenous	Originating from the patient
Bone regeneration	Regrowth of bone
Biocompatible	The property of being coexistent with living tissues without producing a toxic, injurious or immunologic response in living tissues
Collateral damage	Causing damage to surrounding tissues
Dentate	With teeth
Edentulous	Without teeth
Fibula	the outer and narrower of two bones of the human lower leg, extending from the knee to the ankle
Follow-up period	Period of observation and data acquisition of the patients included in a study
Graft	A piece of tissue created for transplantation
Harvesting	Extraction of tissue from a living body for transplantation, in this case the fibula
Image fusion	Registration of MR images on CT images
Ischemia	A decreased or disrupted blood supply to an organ or tissue by constriction or obstruction of the blood vessels
Mandible	Lower jaw
Mandibulectomy	Resection of the mandible
Mandibular residue	bony part left after mandible resection, the gap that exists after resection of the defect
Maxilla	Upper jaw
Maxillofacial region	A region consisting of the face, neck, mouth, tongue, upper jaw and lower jaw
Metastasis	Progression of cancer from the original location to another location
Native mandible	The original mandible
Neomandible	The newly constructed mandible
Osteotomy	Bone cutting
Pathology	The anatomic or functional manifestations of a disease
Pedicle	Part of a tissue graft that is left temporarily attached to the original site
Piezostome	Piezoelectric device applied for bone cutting
Pitch deviation	The osteotomy trajectory regarding to deviations to left and right

<i>Positioning template</i>	Designed template to guide the surgeon to obtain the correct orientation and positioning of the fibula segments
<i>Recipient</i>	Receiving site, opposite to the donor site
<i>Registration</i>	Matching of different types of images
<i>Resection</i>	Surgical removal of a part of a structure
<i>Resection template</i>	Designed template with cutting sleeves to guide osteotomy
<i>Roll deviation</i>	The osteotomy trajectory regarding to deviations from the front to the back
<i>Safety margin</i>	The surgical margin required to insure safety
<i>Segment</i>	Part of a structure after it was cut into pieces
<i>Segmentation</i>	Dividing the structure into several segments
<i>Vascularized</i>	Tissue supplied with blood vessels
<i>Vise</i>	Clamping tool, applied in this study to fixate a synthesized bone block
<i>Yaw deviation</i>	The osteotomy trajectory regarding to deviations from the top to the bottom

Bibliography

1. Antoni van Leeuwenhoek. Mondkanker en tongkanker. Antoni van Leeuwenhoek - Nederlands Kanker Instituut. <http://www.avl.nl/kankersoorten/mondkanker/>.
2. Chim H, Salgado C, Mardini S, Chen H-C. Reconstruction of Mandibular Defects. *Semin Plast Surg.* 2010;24(2):188-197. doi:10.1055/s-0030-1255336.
3. Guven Y, Zorlu S, Cankaya AB, Aktoren O, Gencay K. A Complex Facial Trauma Case with Multiple Mandibular Fractures and Dentoalveolar Injuries. *Case Rep Dent.* 2015;2015:1-6. doi:10.1155/2015/301013.
4. Lonie S, Herle P, Paddle A, Pradhan N, Birch T, Shayan R. Mandibular reconstruction: meta-analysis of iliac- versus fibula-free flaps. *ANZ J Surg.* 2015:n/a-n/a. doi:10.1111/ans.13274.
5. Rana M, Warraich R, Kokemüller H, et al. Reconstruction of mandibular defects - Clinical retrospective research over a 10-year period - Clinical r. *Head Neck Oncol.* 2011;3(1):23. doi:10.1186/1758-3284-3-23.
6. Zavattero E, Fasolis M, Garzino-Demo P, Berrone S, Ramieri G a. Evaluation of plate-related complications and efficacy in fibula free flap mandibular reconstruction. *J Craniofac Surg.* 2014;25(2):397-399. doi:10.1097/SCS.0000000000000656.
7. Kalra GS, Goel P, Singh PK. Reconstruction of post-traumatic long bone defect with vascularised free fibula: A series of 28 cases. *Indian J Plast Surg.* 2013;46(3):543. doi:10.4103/0970-0358.122013.
8. Minami A, Kasashima T, Iwasaki N, Kato H, Kaneda K. Vascularised fibular grafts. *J Bone Jt Surg - Ser B.* 2000;82(7):1022-1025. <http://ovidsp.ovid.com/ovidweb.cgi?T=JS&PAGE=reference&D=emed5&NEWS=N&AN=2000335393>.
9. Cordeiro PG, Disa JJ, Hidalgo D a, Hu QY. Reconstruction of the mandible with osseous free flaps: a 10-year experience with 150 consecutive patients. *Plast Reconstr Surg.* 1999;104(5):1314-1320. <http://www.ncbi.nlm.nih.gov/pubmed/10513911>.
10. Kääriäinen M, Kuuskeri M, Gremoutis G. Utilization of Three-Dimensional Computer- Aided Preoperative Virtual Planning and Manufacturing in Maxillary and Mandibular Reconstruction with a Microvascular Fibula Flap. 2015.
11. Hidalgo D a. Fibula free flap: a new method of mandible reconstruction. *Plast Reconstr Surg.* 1989;84(1):71-79. doi:10.1016/S0901-5027(05)80583-1.
12. Antony AK, Chen WF, Kolokythas A, Weimer K a., Cohen MN. Use of Virtual Surgery and Stereolithography-Guided Osteotomy for Mandibular Reconstruction with the Free Fibula. *Plast Reconstr Surg.* 2011;128(5):1080-1084. doi:10.1097/PRS.0b013e31822b6723.
13. Leong J-L, Batra PS, Citardi MJ. CT-MR image fusion for the management of skull base lesions. *Otolaryngol Head Neck Surg.* 2006;134(5):868-876. doi:10.1016/j.otohns.2005.11.015.
14. Wong KC, Kumta SM, Antonio GE, Tse LF. Image fusion for computer-assisted bone tumor surgery. *Clin Orthop Relat Res.* 2008;466(10):2533-2541. doi:10.1007/s11999-008-0374-5.
15. Zhang WB, Wang Y, Liu XJ, et al. Reconstruction of maxillary defects with free fibula flap assisted by computer techniques. *J Cranio-Maxillofacial Surg.* 2015;43(5):630-636. doi:10.1016/j.jcms.2015.03.007.
16. Tsai MJ, Wu CT. Study of mandible reconstruction using a fibula flap with application of additive manufacturing technology. *Biomed Eng Online.* 2014;13(1):57. doi:10.1186/1475-925x-13-57.

17. Schepers RH, Raghoobar GM, Vissink A, et al. Accuracy of fibula reconstruction using patient-specific CAD/CAM reconstruction plates and dental implants: A new modality for functional reconstruction of mandibular defects. *J Craniomaxillofac Surg.* 2015;43(5):649-657. doi:10.1016/j.jcms.2015.03.015.
18. Shu D, Liu X, Guo B, Ran W, Liao X, Zhang Y. Accuracy of using computer-aided rapid prototyping templates for mandible reconstruction with an iliac crest graft. *World J Surg Oncol.* 2014;12(1):190. doi:10.1186/1477-7819-12-190.
19. Ritacco LE, Milano FE, Farfalli GL, Ayerza M a., Muscolo DL, Aponte-Tinao L a. Accuracy of 3-D Planning and Navigation in Bone Tumor Resection. *Orthopedics.* 2013;36(7):e942-e950. doi:10.3928/01477447-20130624-27.
20. Soule WC, Fisher LH. Mandibular Fracture Imaging. Medscape. <http://emedicine.medscape.com/article/391549-overview>. Published 2015.
21. Kim MG, Lee ST, Park JY, Choi SW. Reconstruction with fibular osteocutaneous free flap in patients with mandibular osteoradionecrosis. 2015. doi:10.1186/s40902-015-0007-3.
22. Chronopoulos A, Zarra T, Tröltzsch M, Mahaini S, Ehrenfeld M, Otto S. Osteoradionecrosis of the mandible: A ten year single-center retrospective study. *J Cranio-Maxillofacial Surg.* 2015;43(6):837-846. doi:10.1016/j.jcms.2015.03.024.
23. Lin C-H, Kang C-J, Tsao C-K, et al. Priority of Fibular Reconstruction in Patients with Oral Cavity Cancer Undergoing Segmental Mandibulectomy. *PLoS One.* 2014;9(4):e94315. doi:10.1371/journal.pone.0094315.
24. Gardner DG, Pecak a M. The treatment of ameloblastoma based on pathologic and anatomic principles. *Cancer.* 1980;46(11):2514-2519. doi:10.1002/1097-0142(19801201)46:11<2514::AID-CNCR2820461133>3.0.CO;2-9.
25. Matsushita Y, Yanamoto S, Yamada S, et al. Correlation between degree of bone invasion and prognosis in carcinoma of the mandibular gingiva: Soft tissue classification based on UICC classification. *J Oral Maxillofac Surgery, Med Pathol.* 2015;27(5):631-636. doi:10.1016/j.ajoms.2014.12.002.
26. Lam KH, Lam LK, Ho CM, Wei WI. Mandibular invasion in carcinoma of the lower alveolus. *Am J Otolaryngol - Head Neck Med Surg.* 1999;20(5):267-272. doi:10.1016/S0196-0709(99)90026-1.
27. Shan X-F, Li R-H, Lu X-G, Cai Z-G, Zhang J, Zhang J-G. Fibular Free Flap Reconstruction for the Management of Advanced Bilateral Mandibular Osteoradionecrosis. *J Craniofac Surg.* 2015;26(2):1. doi:10.1097/SCS.0000000000001391.
28. Lee M, Chin RY, Eslick GD, Sritharan N, Paramaesvaran S. Outcomes of microvascular free flap reconstruction for mandibular osteoradionecrosis: A systematic review. *J Cranio-Maxillofacial Surg.* 2015. doi:10.1016/j.jcms.2015.03.006.
29. Metzler P, Geiger EJ, Alcon A, Ma X, Steinbacher DM. Three-Dimensional Virtual Surgery Accuracy for Free Fibula Mandibular Reconstruction: Planned Versus Actual Results. *J Oral Maxillofac Surg.* 2014;72(12):2601-2612. doi:10.1016/j.joms.2014.07.024.
30. Cornelius C-P, Smolka W, Giessler G a., Wilde F, Probst F a. Patient-specific reconstruction plates are the missing link in computer-assisted mandibular reconstruction: a showcase for technical description. *J Cranio-Maxillofacial Surg.* 2015;43(5):624-629. doi:10.1016/j.jcms.2015.02.016.
31. So TYC, Lam Y-L, Mak K-L. Computer-assisted Navigation in Bone Tumor Surgery: Seamless Workflow Model and Evolution of Technique. *Clin Orthop Relat Res.* 2010;468(11):2985-2991. doi:10.1007/s11999-010-1465-7.
32. Chan HHL, Siewerdsen JH, Vescan A, Daly MJ, Prisman E, Irish JC. 3D Rapid Prototyping for

33. Coppen C, Weijs W, Bergé SJ, Maal TJJ. Oromandibular reconstruction using 3D planned triple template method. *J Oral Maxillofac Surg.* 2013;71(8):243-247. doi:10.1016/j.joms.2013.03.004.
34. Hanasono MM, Skoracki RJ. Computer-assisted design and rapid prototype modeling in microvascular mandible reconstruction. *Laryngoscope.* 2013;123(3):597-604. doi:10.1002/lary.23717.
35. Huang J-W, Shan X-F, Lu X-G, Cai Z-G. Preliminary clinic study on computer assisted mandibular reconstruction: the positive role of surgical navigation technique. *Maxillofac Plast Reconstr Surg.* 2015;37(1):20. doi:10.1186/s40902-015-0017-1.
36. Yu H, Wang X, Zhang S, Zhang L, Xin P, Shen SG. Navigation-guided en bloc resection and defect reconstruction of craniomaxillary bony tumours. *Int J Oral Maxillofac Surg.* 2013;42(11):1409-1413. doi:10.1016/j.ijom.2013.05.011.
37. Rutala WA, Ph D, Weber DJ. Guideline for Disinfection and Sterilization in Healthcare Facilities , 2008. *Centers Dis Control Prev.* 2008:1-158. doi:10.1086/423182.
38. Braunn. *Aesculap Power Systems Burrs & Blades Katalog.*; 2009. [http://webcache.googleusercontent.com/search?q=cache:43hpXzLDJSwJ:www.veterinary-instrumentation.co.uk/skin1/admin/UserFiles/File/JS PDF/BRAESBUR.pdf+&cd=1&hl=nl&ct=clnk&gl=nl](http://webcache.googleusercontent.com/search?q=cache:43hpXzLDJSwJ:www.veterinary-instrumentation.co.uk/skin1/admin/UserFiles/File/JS%20PDF/BRAESBUR.pdf+&cd=1&hl=nl&ct=clnk&gl=nl).
39. Hollenbeck K, Allin T, Poel M Van Der. Dental Lab 3D Scanners – How they work and what works best. 2012;(January):1-5.
40. Leiggener CS, Krol Z, Gawelin P, Buitrago-Téllez CH, Zeilhofer H-F, Hirsch J-M. A computer-based comparative quantitative analysis of surgical outcome of mandibular reconstructions with free fibula microvascular flaps. *J Plast Surg Hand Surg.* 2014;6764(April):1-7. doi:10.3109/2000656X.2014.920711.
41. Cartiaux O. Computer-Assisted and Robot-Assisted Technologies to Improve Bone-Cutting Accuracy When Integrated with a Freehand Process Using an Oscillating Saw. *J Bone Jt Surg.* 2010;92(11):2076. doi:10.2106/JBJS.I.00457.
42. Misch CE. *Rationale for Dental Implants.* Second Edi. Elsevier Inc.; 2014. doi:10.1016/B978-0-323-07845-0.00001-4.
43. Beaty NB, Le TT. Mandibular thickness measurements in young dentate adults. *Arch Otolaryngol Head Neck Surg.* 2009;135(9):920-923. doi:10.1001/archoto.2009.109.
44. Flanagan D. A Comparison of Facial and Lingual Cortical Thicknesses in Edentulous Maxillary and Mandibular Sites Measured on Computerized Tomograms. *J Oral Implantol.* 2008;34(5):256-258. doi:10.1563/0.915.1.
45. Sağlam AA. The vertical heights of maxillary and mandibular bones in panoramic radiographs of dentate and edentulous subjects. *Quintessence Int.* 2002;33(6):433-438. <http://www.ncbi.nlm.nih.gov/pubmed/12073723>.
46. Ide Y, Matsunaga S, Harris J, O 'connell D, Seikaly H, Wolfaardt J. Anatomical examination of the fibula: digital imaging study for osseointegrated implant installation. *J Otolaryngol - Head Neck Surg.* 2015:1-8. doi:10.1186/s40463-015-0055-9.
47. Oceanz your 3D printing professional. Medisch 3D printen. <http://www.oceanz.eu/branches/medisch>. Published 2016.
48. Cartiaux O, Paul L, Docquier PL, et al. Accuracy in planar cutting of bones: an ISO-based evaluation.

- Int J Med Robot.* 2009;5(1):77-84. doi:10.1002/rcs.237.
49. Baek K-W, Deibel W, Marinov D, et al. Clinical applicability of robot-guided contact-free laser osteotomy in cranio-maxillo-facial surgery: in-vitro simulation and in-vivo surgery in minipig mandibles. *Br J Oral Maxillofac Surg.* 2015;1-6. doi:10.1016/j.bjoms.2015.07.019.
 50. Stopp S, Deppe H, Lueth T. A new concept for navigated laser surgery. *Lasers Med Sci.* 2008;23(3):261-266. doi:10.1007/s10103-007-0476-4.
 51. Stübinger S, Kober C, Zeilhofer H-F, Sader R. Er:YAG laser osteotomy based on refined computer-assisted presurgical planning: first clinical experience in oral surgery. *Photomed Laser Surg.* 2007;25(1):3-7. doi:10.1089/pho.2006.2005.
 52. Horta R, Costa J, Valenc R, Amarante JM. ALT chimeric flap associated to a dura mater biomatrix substitute for severe desfigurative mandible osteoradionecrosis and deficient bone consolidation after a free fibula flap. 2014;52:3-5. doi:10.1016/j.bjoms.2014.01.024.
 53. Mehra M, Somohano T, Choi M. Mandibular fibular graft reconstruction with CAD/CAM technology: A clinical report and literature review. *J Prosthet Dent.* 2015;1-6. doi:10.1016/j.prosdent.2015.05.012.
 54. Lyons A, Ghazali N. Osteoradionecrosis of the jaws: current understanding of its pathophysiology and treatment. *Br J Oral Maxillofac Surg.* 2008;46(8):653-660. doi:10.1016/j.bjoms.2008.04.006.
 55. Kildal M, Wei F-C, Chang Y-M, Huang W-C, Chang K-J. Reconstruction of bilateral extensive composite mandibular defects after osteoradionecrosis with two fibular osteoseptocutaneous free flaps. *Plast Reconstr Surg.* 2001;108(4):963-967. doi:10.1097/00006534-200109150-00022.
 56. Weitz J, Kreutzer K, Bauer FJM, Wolff K-D, Nobis C-P, Kesting MR. Sandwich flaps as a feasible solution for the management of huge mandibular composite tissue defects. *J Cranio-Maxillofacial Surg.* 2015;43(9):1769-1775. doi:10.1016/j.jcms.2015.07.038.
 57. Babu N. Unicystic Ameloblastoma of Mandible Treated with an Innovative Approach: A Clinical Case Report. *J Clin Diagnostic Res.* 2015;9(7):11-13. doi:10.7860/JCDR/2015/13908.6177.
 58. Knoll W-D, Gaida A, Maurer P. Analysis of mechanical stress in reconstruction plates for bridging mandibular angle defects. *J Cranio-Maxillofacial Surg.* 2006;34(4):201-209. doi:10.1016/j.jcms.2006.01.004.
 59. Yamaguchi S, Nagasawa H, Suzuki T, et al. Sarcomas of the oral and maxillofacial region: a review of 32 cases in 25 years. *Clin Oral Investig.* 2004;8(2):52-55. doi:10.1007/s00784-003-0233-4.
 60. Hawrot A, Alam M, Ratner D. Squamous cell carcinoma. *Curr Probl Dermatol.* 2003;15(3):91-133. doi:10.1016/S1040-0486(03)00039-5.
 61. Wong KC, Kumta SM, Sze KY, Wong CM. Use of a patient-specific CAD/CAM surgical jig in extremity bone tumor resection and custom prosthetic reconstruction. *Comput Aided Surg.* 2012;17(6):284-293. doi:10.3109/10929088.2012.725771.
 62. Markiewicz MR, Bell RB, Bui TG, et al. Survival of microvascular free flaps in mandibular reconstruction: A systematic review and meta-analysis. *Microsurgery.* 2015;30(3):242-248. doi:10.1002/micr.
 63. Mazzoni S, Bianchi A, Schiariti G, Badiali G, Marchetti C. Computer-Aided Design and Computer-Aided Manufacturing Cutting Guides and Customized Titanium Plates Are Useful in Upper Maxilla Waferless Repositioning. *J Oral Maxillofac Surg.* 2015;73(4):701-707. doi:10.1016/j.joms.2014.10.028.
 64. Tarsitano A, Ciocca L, Ciprani R, Scotti R MC. Mandibular reconstruction using fibula free flap harvested using a customised cutting guide : how we do it. *Clin Tech Technol.* 2015;35:198-201.

65. Liu Y, Xu L, Zhu H, Liu SS-Y. Technical procedures for template-guided surgery for mandibular reconstruction based on digital design and manufacturing. *Biomed Eng Online*. 2014;13(1):63. doi:10.1186/1475-925X-13-63.
66. Zheng G Sen, Su YX, Liao GQ, Liu HC, Zhang SE, Liang LZ. Mandibular reconstruction assisted by preoperative simulation and accurate transferring templates: Preliminary report of clinical application. *J Oral Maxillofac Surg*. 2013;71(9):1613-1618. doi:10.1016/j.joms.2013.02.018.
67. Sternheim A, Daly M, Qiu J, et al. Navigated Pelvic Osteotomy and Tumor Resection. *J Bone Jt Surg*. 2015;97:40-46.
68. Gouin F, Paul L, Odri GA, Cartiaux O. Computer-Assisted Planning and Patient-Specific Instruments for Bone Tumor Resection within the Pelvis: A Series of 11 Patients. *Sarcoma*. 2014;2014:842709. doi:10.1155/2014/842709.
69. Weijs W, Coppens C. Research subject. 2016.
70. NextDent B.V. NextDent SG (Surgical Guide). <http://nextdent.com/products/sg-surgical-guide/>. Published 2016.
71. Vertex Dental. NextDent 3D printing materials. 2014;23:1-6. <http://nextdent.com/wp-content/uploads/2014/10/Safety-Data-Sheet-NextDent-Materials.pdf>.
72. Martin GmbH & Co. KG. Septum elevator Roger. <http://www.klsmartin.com/catalog/de/article/37/Periostelevatorien/>. Published 2015.
73. Matros E, Santamaria E, Cordeiro PG, Cam CAD. Standardized Templates for Shaping the Fibula Free Flap in Mandible Reconstruction. 2013.
74. Olayemi AB. Assessment and determination of human mandibular and dental arch profiles in subjects with lower third molar impaction in Port Harcourt, Nigeria. *Ann Maxillofac Surg*. 2011;1(2):126-130. doi:10.4103/2231-0746.92775.
75. Tie Y, Wang DM, Ji T, Wang CT, Zhang CP. Three-dimensional finite-element analysis investigating the biomechanical effects of human mandibular reconstruction with autogenous bone grafts. *J Cranio-Maxillofacial Surg*. 2006;34(5):290-298. doi:10.1016/j.jcms.2006.03.004.
76. Ma L, Zhou Y, Zhang Y, et al. Biomechanical Effects of Masticatory Muscles on Human Mandible After Reconstructed Mandibulectomy Tumor. *J Craniofac Surg*. 2015:1563-3732. doi:10.1097/SCS.0000000000000840.
77. Ji T, Tie Y, Wang D, Zhang C. Three-dimensional finite element analysis of the mandible reconstruction with fibula. *West China J Stomatol*. 2009;27(2):7-10.
78. Mertens C, Decker C, Engel M, Sander A, Hoffmann J, Freier K. Early bone resorption of free microvascular reanastomized bone grafts for mandibular reconstruction - A comparison of iliac crest and fibula grafts. *J Cranio-Maxillofacial Surg*. 2014;42(5):217-223. doi:10.1016/j.jcms.2013.08.010.
79. Makiguchi T, Yokoo S, Hashikawa K, Miyazaki H, Terashi H. Evaluation of bone height of the free fibula flap in mandible reconstruction. *J Craniofac Surg*. 2015;26(3):673-676. doi:10.1097/SCS.0000000000001509.
80. Elsevier, Netter FH. Teeth: Surfaces of a Tooth. Elsevier. <https://www.netterimages.com/teeth-surfaces-of-a-tooth-labeled-norton-1e-dentistry-dental-hygiene-frank-kip-11813.html>. Published 2016.
81. Ural Ç, Bereket C, Şener I, Aktan AM, Akpınar YZ. Bone height measurement of maxillary and mandibular bones in panoramic radiographs of edentulous patients. *J Clin Exp Dent*. 2011;3(1):5-9. doi:10.4317/jced.3.e5.

82. Klatzky RL, Lederman S, Reed C. Haptic Integration of Object Properties : Texture , Hardness , and Planar Contour. 1989;15:45-57.
 83. Bholat OS, Haluck RS, Murray WB, Gorman PJ, Krummel TM. Tactile feedback is present during minimally invasive surgery. *J Am Coll Surg*. 1999;189(4):349-355. doi:10.1016/S1072-7515(99)00184-2.
 84. Pinzon D, Byrns S, Zheng B. Prevailing Trends in Haptic Feedback Simulation for Minimally Invasive Surgery. *Surg Innov*. 2016. doi:10.1177/1553350616628680.
 85. Maxim integrated products inc. Sterilization Methods and Their Impact on Medical Devices Containing Electronics. <https://www.maximintegrated.com/en/app-notes/index.mvp/id/5068>. Published 2011.
 86. Patel M. *MEDICAL STERILIZATION METHODS*.; 2003. <https://www.digikey.com/WebExport/SupplierContent/lemo-1124/pdf/lemo-rf-medical-steril.pdf?redirected=1>.
 87. Wang K. The use of titanium for medical applications in the USA. *Mater Sci Eng A*. 1996;213(1-2):134-137. doi:10.1016/0921-5093(96)10243-4.
 88. Pacific Research Laboratories. Sawbones. <http://www.sawbones.com/Catalog/Biomechanical/Biomechanical Test Materials>. Published 2013.
 89. Sawbones. Catalogue biomechanical testmaterials. In: Pacific Research Laboratories, Inc; 2014. http://www.sawbones.com/UserFiles/Docs/biomechanical_catalog.pdf.
 90. De Waard O, Baan F, Verhamme L, Breuning H, Kuijpers-Jagtman AM, Maal T. A novel method for fusion of intra-oral scans and cone-beam computed tomography scans for orthognathic surgery planning. *J Cranio-Maxillofacial Surg*. 2016;44(2):160-166. doi:10.1016/j.jcms.2015.11.017.
 91. Field A, Hole G. *How to Design and Report Experiments*. London: SAGE Publications; 2003.
 92. Spinelli G, Lazzeri D, Conti M, Agostini T, Mannelli G. Comparison of piezosurgery and traditional saw in bimaxillary orthognathic surgery. *J Cranio-Maxillofacial Surg*. 2014;42(7):1211-1220. doi:10.1016/j.jcms.2014.02.011.
 93. Baek K, Deibel W, Marinov D, et al. A comparative investigation of bone surface after cutting with mechanical tools and Er:YAG laser. *Lasers Surg Med*. 2015;432(February):n/a-n/a. doi:10.1002/lsm.22352.
-
1. Antoni van Leeuwenhoek. Mondkanker en tongkanker. Antoni van Leeuwenhoek - Nederlands Kanker Instituut. <http://www.avl.nl/kankersoorten/mondkanker/>.
 2. Chim H, Salgado C, Mardini S, Chen H-C. Reconstruction of Mandibular Defects. *Semin Plast Surg*. 2010;24(2):188-197. doi:10.1055/s-0030-1255336.
 3. Guven Y, Zorlu S, Cankaya AB, Aktoren O, Gencay K. A Complex Facial Trauma Case with Multiple Mandibular Fractures and Dentoalveolar Injuries. *Case Rep Dent*. 2015;2015:1-6. doi:10.1155/2015/301013.
 4. Lonie S, Herle P, Paddle A, Pradhan N, Birch T, Shayan R. Mandibular reconstruction: meta-analysis of iliac- versus fibula-free flaps. *ANZ J Surg*. 2015:n/a-n/a. doi:10.1111/ans.13274.
 5. Rana M, Warraich R, Kokemüller H, et al. Reconstruction of mandibular defects - Clinical retrospective research over a 10-year period - Clinical r. *Head Neck Oncol*. 2011;3(1):23. doi:10.1186/1758-3284-3-23.

6. Zavattero E, Fasolis M, Garzino-Demo P, Berrone S, Ramieri G a. Evaluation of plate-related complications and efficacy in fibula free flap mandibular reconstruction. *J Craniofac Surg*. 2014;25(2):397-399. doi:10.1097/SCS.0000000000000656.
7. Kalra GS, Goel P, Singh PK. Reconstruction of post-traumatic long bone defect with vascularised free fibula: A series of 28 cases. *Indian J Plast Surg*. 2013;46(3):543. doi:10.4103/0970-0358.122013.
8. Minami A, Kasashima T, Iwasaki N, Kato H, Kaneda K. Vascularised fibular grafts. *J Bone Jt Surg - Ser B*. 2000;82(7):1022-1025. <http://ovidsp.ovid.com/ovidweb.cgi?T=JS&PAGE=reference&D=emed5&NEWS=N&AN=2000335393>.
9. Cordeiro PG, Disa JJ, Hidalgo D a, Hu QY. Reconstruction of the mandible with osseous free flaps: a 10-year experience with 150 consecutive patients. *Plast Reconstr Surg*. 1999;104(5):1314-1320. <http://www.ncbi.nlm.nih.gov/pubmed/10513911>.
10. Kääriäinen M, Kuuskeri M, Gremoutis G. Utilization of Three-Dimensional Computer- Aided Preoperative Virtual Planning and Manufacturing in Maxillary and Mandibular Reconstruction with a Microvascular Fibula Flap. 2015.
11. Hidalgo D a. Fibula free flap: a new method of mandible reconstruction. *Plast Reconstr Surg*. 1989;84(1):71-79. doi:10.1016/S0901-5027(05)80583-1.
12. Antony AK, Chen WF, Kolokythas A, Weimer K a., Cohen MN. Use of Virtual Surgery and Stereolithography-Guided Osteotomy for Mandibular Reconstruction with the Free Fibula. *Plast Reconstr Surg*. 2011;128(5):1080-1084. doi:10.1097/PRS.0b013e31822b6723.
13. Leong J-L, Batra PS, Citardi MJ. CT-MR image fusion for the management of skull base lesions. *Otolaryngol Head Neck Surg*. 2006;134(5):868-876. doi:10.1016/j.otohns.2005.11.015.
14. Wong KC, Kumta SM, Antonio GE, Tse LF. Image fusion for computer-assisted bone tumor surgery. *Clin Orthop Relat Res*. 2008;466(10):2533-2541. doi:10.1007/s11999-008-0374-5.
15. Zhang WB, Wang Y, Liu XJ, et al. Reconstruction of maxillary defects with free fibula flap assisted by computer techniques. *J Cranio-Maxillofacial Surg*. 2015;43(5):630-636. doi:10.1016/j.jcms.2015.03.007.
16. Tsai MJ, Wu CT. Study of mandible reconstruction using a fibula flap with application of additive manufacturing technology. *Biomed Eng Online*. 2014;13(1):57. doi:10.1186/1475-925x-13-57.
17. Schepers RH, Raghoobar GM, Vissink A, et al. Accuracy of fibula reconstruction using patient-specific CAD/CAM reconstruction plates and dental implants: A new modality for functional reconstruction of mandibular defects. *J Craniomaxillofac Surg*. 2015;43(5):649-657. doi:10.1016/j.jcms.2015.03.015.
18. Shu D, Liu X, Guo B, Ran W, Liao X, Zhang Y. Accuracy of using computer-aided rapid prototyping templates for mandible reconstruction with an iliac crest graft. *World J Surg Oncol*. 2014;12(1):190. doi:10.1186/1477-7819-12-190.
19. Ritacco LE, Milano FE, Farfalli GL, Ayerza M a., Muscolo DL, Aponte-Tinao L a. Accuracy of 3-D Planning and Navigation in Bone Tumor Resection. *Orthopedics*. 2013;36(7):e942-e950. doi:10.3928/01477447-20130624-27.
20. Soule WC, Fisher LH. Mandibular Fracture Imaging. Medscape. <http://emedicine.medscape.com/article/391549-overview>. Published 2015.
21. Kim MG, Lee ST, Park JY, Choi SW. Reconstruction with fibular osteocutaneous free flap in patients with mandibular osteoradionecrosis. 2015. doi:10.1186/s40902-015-0007-3.

22. Chronopoulos A, Zarra T, Tröltzsch M, Mahaini S, Ehrenfeld M, Otto S. Osteoradionecrosis of the mandible: A ten year single-center retrospective study. *J Cranio-Maxillofacial Surg.* 2015;43(6):837-846. doi:10.1016/j.jcms.2015.03.024.
23. Lin C-H, Kang C-J, Tsao C-K, et al. Priority of Fibular Reconstruction in Patients with Oral Cavity Cancer Undergoing Segmental Mandibulectomy. *PLoS One.* 2014;9(4):e94315. doi:10.1371/journal.pone.0094315.
24. Gardner DG, Pecak a M. The treatment of ameloblastoma based on pathologic and anatomic principles. *Cancer.* 1980;46(11):2514-2519. doi:10.1002/1097-0142(19801201)46:11<2514::AID-CNCR2820461133>3.0.CO;2-9.
25. Matsushita Y, Yanamoto S, Yamada S, et al. Correlation between degree of bone invasion and prognosis in carcinoma of the mandibular gingiva: Soft tissue classification based on UICC classification. *J Oral Maxillofac Surgery, Med Pathol.* 2015;27(5):631-636. doi:10.1016/j.ajoms.2014.12.002.
26. Lam KH, Lam LK, Ho CM, Wei WI. Mandibular invasion in carcinoma of the lower alveolus. *Am J Otolaryngol - Head Neck Med Surg.* 1999;20(5):267-272. doi:10.1016/S0196-0709(99)90026-1.
27. Shan X-F, Li R-H, Lu X-G, Cai Z-G, Zhang J, Zhang J-G. Fibular Free Flap Reconstruction for the Management of Advanced Bilateral Mandibular Osteoradionecrosis. *J Craniofac Surg.* 2015;26(2):1. doi:10.1097/SCS.0000000000001391.
28. Lee M, Chin RY, Eslick GD, Sritharan N, Paramaesvaran S. Outcomes of microvascular free flap reconstruction for mandibular osteoradionecrosis: A systematic review. *J Cranio-Maxillofacial Surg.* 2015. doi:10.1016/j.jcms.2015.03.006.
29. Metzler P, Geiger EJ, Alcon A, Ma X, Steinbacher DM. Three-Dimensional Virtual Surgery Accuracy for Free Fibula Mandibular Reconstruction: Planned Versus Actual Results. *J Oral Maxillofac Surg.* 2014;72(12):2601-2612. doi:10.1016/j.joms.2014.07.024.
30. Cornelius C-P, Smolka W, Giessler G a., Wilde F, Probst F a. Patient-specific reconstruction plates are the missing link in computer-assisted mandibular reconstruction: a showcase for technical description. *J Cranio-Maxillofacial Surg.* 2015;43(5):624-629. doi:10.1016/j.jcms.2015.02.016.
31. So TYC, Lam Y-L, Mak K-L. Computer-assisted Navigation in Bone Tumor Surgery: Seamless Workflow Model and Evolution of Technique. *Clin Orthop Relat Res.* 2010;468(11):2985-2991. doi:10.1007/s11999-010-1465-7.
32. Chan HHL, Siewerdsen JH, Vescan A, Daly MJ, Prisman E, Irish JC. 3D Rapid Prototyping for Otolaryngology — Head and Neck Surgery : Applications in Image-Guidance , Surgical Simulation and Patient-Specific Modeling. 2015:1-18. doi:10.1371/journal.pone.0136370.
33. Coppen C, Weijs W, Bergé SJ, Maal TJJ. Oromandibular reconstruction using 3D planned triple template method. *J Oral Maxillofac Surg.* 2013;71(8):243-247. doi:10.1016/j.joms.2013.03.004.
34. Hanasono MM, Skoracki RJ. Computer-assisted design and rapid prototype modeling in microvascular mandible reconstruction. *Laryngoscope.* 2013;123(3):597-604. doi:10.1002/lary.23717.
35. Huang J-W, Shan X-F, Lu X-G, Cai Z-G. Preliminary clinic study on computer assisted mandibular reconstruction: the positive role of surgical navigation technique. *Maxillofac Plast Reconstr Surg.* 2015;37(1):20. doi:10.1186/s40902-015-0017-1.
36. Yu H, Wang X, Zhang S, Zhang L, Xin P, Shen SG. Navigation-guided en bloc resection and defect reconstruction of craniomaxillary bony tumours. *Int J Oral Maxillofac Surg.* 2013;42(11):1409-1413. doi:10.1016/j.ijom.2013.05.011.
37. Rutala WA, Ph D, Weber DJ. Guideline for Disinfection and Sterilization in Healthcare Facilities ,

2008. *Centers Dis Control Prev.* 2008;1-158. doi:10.1086/423182.
38. Braunn. *Aesculap Power Systems Burrs & Blades Katalog*; 2009. [http://webcache.googleusercontent.com/search?q=cache:43hpXzLDJSwJ:www.veterinary-instrumentation.co.uk/skin1/admin/UserFiles/File/JS PDF/BRAESBUR.pdf+&cd=1&hl=nl&ct=clnk&gl=nl](http://webcache.googleusercontent.com/search?q=cache:43hpXzLDJSwJ:www.veterinary-instrumentation.co.uk/skin1/admin/UserFiles/File/JS%20PDF/BRAESBUR.pdf+&cd=1&hl=nl&ct=clnk&gl=nl).
 39. Hollenbeck K, Allin T, Poel M Van Der. Dental Lab 3D Scanners – How they work and what works best. 2012;(January):1-5.
 40. Leiggener CS, Krol Z, Gawelin P, Buitrago-Téllez CH, Zeilhofer H-F, Hirsch J-M. A computer-based comparative quantitative analysis of surgical outcome of mandibular reconstructions with free fibula microvascular flaps. *J Plast Surg Hand Surg.* 2014;6764(April):1-7. doi:10.3109/2000656X.2014.920711.
 41. Cartiaux O. Computer-Assisted and Robot-Assisted Technologies to Improve Bone-Cutting Accuracy When Integrated with a Freehand Process Using an Oscillating Saw. *J Bone Jt Surg.* 2010;92(11):2076. doi:10.2106/JBJS.I.00457.
 42. Misch CE. *Rationale for Dental Implants*. Second Edi. Elsevier Inc.; 2014. doi:10.1016/B978-0-323-07845-0.00001-4.
 43. Beaty NB, Le TT. Mandibular thickness measurements in young dentate adults. *Arch Otolaryngol Head Neck Surg.* 2009;135(9):920-923. doi:10.1001/archoto.2009.109.
 44. Flanagan D. A Comparison of Facial and Lingual Cortical Thicknesses in Edentulous Maxillary and Mandibular Sites Measured on Computerized Tomograms. *J Oral Implantol.* 2008;34(5):256-258. doi:10.1563/0.915.1.
 45. Sağlam AA. The vertical heights of maxillary and mandibular bones in panoramic radiographs of dentate and edentulous subjects. *Quintessence Int.* 2002;33(6):433-438. <http://www.ncbi.nlm.nih.gov/pubmed/12073723>.
 46. Ide Y, Matsunaga S, Harris J, O'Connell D, Seikaly H, Wolfaardt J. Anatomical examination of the fibula: digital imaging study for osseointegrated implant installation. *J Otolaryngol - Head Neck Surg.* 2015;1-8. doi:10.1186/s40463-015-0055-9.
 47. Oceanz your 3D printing professional. Medisch 3D printen. <http://www.oceanz.eu/branches/medisch>. Published 2016.
 48. Cartiaux O, Paul L, Docquier PL, et al. Accuracy in planar cutting of bones: an ISO-based evaluation. *Int J Med Robot.* 2009;5(1):77-84. doi:10.1002/rcs.237.
 49. Baek K-W, Deibel W, Marinov D, et al. Clinical applicability of robot-guided contact-free laser osteotomy in cranio-maxillo-facial surgery: in-vitro simulation and in-vivo surgery in minipig mandibles. *Br J Oral Maxillofac Surg.* 2015;1-6. doi:10.1016/j.bjoms.2015.07.019.
 50. Stopp S, Deppe H, Lueth T. A new concept for navigated laser surgery. *Lasers Med Sci.* 2008;23(3):261-266. doi:10.1007/s10103-007-0476-4.
 51. Stübinger S, Kober C, Zeilhofer H-F, Sader R. Er:YAG laser osteotomy based on refined computer-assisted presurgical planning: first clinical experience in oral surgery. *Photomed Laser Surg.* 2007;25(1):3-7. doi:10.1089/pho.2006.2005.
 52. Horta R, Costa J, Valenc R, Amarante JM. ALT chimeric flap associated to a dura mater biomatrix substitute for severe disfiguring mandible osteoradionecrosis and deficient bone consolidation after a free fibula flap. 2014;52:3-5. doi:10.1016/j.bjoms.2014.01.024.
 53. Mehra M, Somohano T, Choi M. Mandibular fibular graft reconstruction with CAD/CAM technology: A clinical report and literature review. *J Prosthet Dent.* 2015;1-6.

doi:10.1016/j.prosdent.2015.05.012.

54. Lyons A, Ghazali N. Osteoradionecrosis of the jaws: current understanding of its pathophysiology and treatment. *Br J Oral Maxillofac Surg*. 2008;46(8):653-660. doi:10.1016/j.bjoms.2008.04.006.
55. Kildal M, Wei F-C, Chang Y-M, Huang W-C, Chang K-J. Reconstruction of bilateral extensive composite mandibular defects after osteoradionecrosis with two fibular osteoseptocutaneous free flaps. *Plast Reconstr Surg*. 2001;108(4):963-967. doi:10.1097/00006534-200109150-00022.
56. Weitz J, Kreutzer K, Bauer FJM, Wolff K-D, Nobis C-P, Kesting MR. Sandwich flaps as a feasible solution for the management of huge mandibular composite tissue defects. *J Cranio-Maxillofacial Surg*. 2015;43(9):1769-1775. doi:10.1016/j.jcms.2015.07.038.
57. Babu N. Unicystic Ameloblastoma of Mandible Treated with an Innovative Approach: A Clinical Case Report. *J Clin Diagnostic Res*. 2015;9(7):11-13. doi:10.7860/JCDR/2015/13908.6177.
58. Knoll W-D, Gaida A, Maurer P. Analysis of mechanical stress in reconstruction plates for bridging mandibular angle defects. *J Cranio-Maxillofacial Surg*. 2006;34(4):201-209. doi:10.1016/j.jcms.2006.01.004.
59. Yamaguchi S, Nagasawa H, Suzuki T, et al. Sarcomas of the oral and maxillofacial region: a review of 32 cases in 25 years. *Clin Oral Investig*. 2004;8(2):52-55. doi:10.1007/s00784-003-0233-4.
60. Hawrot A, Alam M, Ratner D. Squamous cell carcinoma. *Curr Probl Dermatol*. 2003;15(3):91-133. doi:10.1016/S1040-0486(03)00039-5.
61. Wong KC, Kumta SM, Sze KY, Wong CM. Use of a patient-specific CAD/CAM surgical jig in extremity bone tumor resection and custom prosthetic reconstruction. *Comput Aided Surg*. 2012;17(6):284-293. doi:10.3109/10929088.2012.725771.
62. Markiewicz MR, Bell RB, Bui TG, et al. Survival of microvascular free flaps in mandibular reconstruction: A systematic review and meta-analysis. *Microsurgery*. 2015;30(3):242-248. doi:10.1002/micr.
63. Mazzoni S, Bianchi A, Schiariti G, Badiali G, Marchetti C. Computer-Aided Design and Computer-Aided Manufacturing Cutting Guides and Customized Titanium Plates Are Useful in Upper Maxilla Waferless Repositioning. *J Oral Maxillofac Surg*. 2015;73(4):701-707. doi:10.1016/j.joms.2014.10.028.
64. Tarsitano A, Ciocca L, Ciprani R, Scotti R MC. Mandibular reconstruction using fibula free flap harvested using a customised cutting guide : how we do it. *Clin Tech Technol*. 2015;35:198-201.
65. Liu Y, Xu L, Zhu H, Liu SS-Y. Technical procedures for template-guided surgery for mandibular reconstruction based on digital design and manufacturing. *Biomed Eng Online*. 2014;13(1):63. doi:10.1186/1475-925X-13-63.
66. Zheng G Sen, Su YX, Liao GQ, Liu HC, Zhang SE, Liang LZ. Mandibular reconstruction assisted by preoperative simulation and accurate transferring templates: Preliminary report of clinical application. *J Oral Maxillofac Surg*. 2013;71(9):1613-1618. doi:10.1016/j.joms.2013.02.018.
67. Sternheim A, Daly M, Qiu J, et al. Navigated Pelvic Osteotomy and Tumor Resection. *J Bone Jt Surg*. 2015;97:40-46.
68. Gouin F, Paul L, Odri GA, Cartiaux O. Computer-Assisted Planning and Patient-Specific Instruments for Bone Tumor Resection within the Pelvis: A Series of 11 Patients. *Sarcoma*. 2014;2014:842709. doi:10.1155/2014/842709.
69. Weijs W, Coppen C. Research subject. 2016.
70. NextDent B.V. NextDent SG (Surgical Guide). <http://nextdent.com/products/sg-surgical-guide/>.

Published 2016.

71. Vertex Dental. NextDent 3D printing materials. 2014;23:1-6. <http://nextdent.com/wp-content/uploads/2014/10/Safety-Data-Sheet-NextDent-Materials.pdf>.
72. Martin GmbH & Co. KG. Septumelevatorium Roger. <http://www.klsmartin.com/catalog/de/article/37/Periostelevatorien/>. Published 2015.
73. Matros E, Santamaria E, Cordeiro PG, Cam CAD. Standardized Templates for Shaping the Fibula Free Flap in Mandible Reconstruction. 2013.
74. Olayemi AB. Assessment and determination of human mandibular and dental arch profiles in subjects with lower third molar impaction in Port Harcourt, Nigeria. *Ann Maxillofac Surg*. 2011;1(2):126-130. doi:10.4103/2231-0746.92775.
75. Tie Y, Wang DM, Ji T, Wang CT, Zhang CP. Three-dimensional finite-element analysis investigating the biomechanical effects of human mandibular reconstruction with autogenous bone grafts. *J Cranio-Maxillofacial Surg*. 2006;34(5):290-298. doi:10.1016/j.jcms.2006.03.004.
76. Ma L, Zhou Y, Zhang Y, et al. Biomechanical Effects of Masticatory Muscles on Human Mandible After Reconstructed Mandibulectomy Tumor. *J Craniofac Surg*. 2015;1563-3732. doi:10.1097/SCS.0000000000000840.
77. Ji T, Tie Y, Wang D, Zhang C. Three-dimensional finite element analysis of the mandible reconstruction with fibula. *West China J Stomatol*. 2009;27(2):7-10.
78. Mertens C, Decker C, Engel M, Sander A, Hoffmann J, Freier K. Early bone resorption of free microvascular reanastomized bone grafts for mandibular reconstruction - A comparison of iliac crest and fibula grafts. *J Cranio-Maxillofacial Surg*. 2014;42(5):217-223. doi:10.1016/j.jcms.2013.08.010.
79. Makiguchi T, Yokoo S, Hashikawa K, Miyazaki H, Terashi H. Evaluation of bone height of the free fibula flap in mandible reconstruction. *J Craniofac Surg*. 2015;26(3):673-676. doi:10.1097/SCS.0000000000001509.
80. Elsevier, Netter FH. Teeth: Surfaces of a Tooth. Elsevier. <https://www.netterimages.com/teeth-surfaces-of-a-tooth-labeled-norton-1e-dentistry-dental-hygiene-frank-kip-11813.html>. Published 2016.
81. Ural Ç, Bereket C, Şener I, Aktan AM, Akpınar YZ. Bone height measurement of maxillary and mandibular bones in panoramic radiographs of edentulous patients. *J Clin Exp Dent*. 2011;3(1):5-9. doi:10.4317/jced.3.e5.
82. Klatzky RL, Lederman S, Reed C. Haptic Integration of Object Properties : Texture , Hardness , and Planar Contour. 1989;15:45-57.
83. Bholat OS, Haluck RS, Murray WB, Gorman PJ, Krummel TM. Tactile feedback is present during minimally invasive surgery. *J Am Coll Surg*. 1999;189(4):349-355. doi:10.1016/S1072-7515(99)00184-2.
84. Pinzon D, Byrns S, Zheng B. Prevailing Trends in Haptic Feedback Simulation for Minimally Invasive Surgery. *Surg Innov*. 2016. doi:10.1177/1553350616628680.
85. Maxim integrated products inc. Sterilization Methods and Their Impact on Medical Devices Containing Electronics. <https://www.maximintegrated.com/en/app-notes/index.mvp/id/5068>. Published 2011.
86. Patel M. *MEDICAL STERILIZATION METHODS*; 2003. <https://www.digikey.com/WebExport/SupplierContent/lemo-1124/pdf/lemo-rf-medical-steril.pdf?redirected=1>.

87. Wang K. The use of titanium for medical applications in the USA. *Mater Sci Eng A*. 1996;213(1-2):134-137. doi:10.1016/0921-5093(96)10243-4.
88. Pacific Research Laboratories. Sawbones. [http://www.sawbones.com/Catalog/Biomechanical/Biomechanical Test Materials](http://www.sawbones.com/Catalog/Biomechanical/Biomechanical%20Test%20Materials). Published 2013.
89. Sawbones. Catalogue biomechanical testmaterials. In: Pacific Research Laboratories, Inc; 2014. http://www.sawbones.com/UserFiles/Docs/biomechanical_catalog.pdf.
90. De Waard O, Baan F, Verhamme L, Breuning H, Kuijpers-Jagtman AM, Maal T. A novel method for fusion of intra-oral scans and cone-beam computed tomography scans for orthognathic surgery planning. *J Cranio-Maxillofacial Surg*. 2016;44(2):160-166. doi:10.1016/j.jcms.2015.11.017.
91. Field A, Hole G. *How to Design and Report Experiments*. London: SAGE Publications; 2003.
92. Spinelli G, Lazzeri D, Conti M, Agostini T, Mannelli G. Comparison of piezosurgery and traditional saw in bimaxillary orthognathic surgery. *J Cranio-Maxillofacial Surg*. 2014;42(7):1211-1220. doi:10.1016/j.jcms.2014.02.011.
93. Baek K, Deibel W, Marinov D, et al. A comparative investigation of bone surface after cutting with mechanical tools and Er:YAG laser. *Lasers Surg Med*. 2015;432(February):n/a-n/a. doi:10.1002/lsm.22352.